

การพัฒนาเรซินกลุ่มเบนซอกซาซีนสำหรับใช้ทำวัสดุประกอบแต่งทดแทนไม้



นางสาว จันจิรา จัปศิลป์

สถาบันวิทยบริการ
จุฬาลงกรณ์มหาวิทยาลัย

วิทยานิพนธ์นี้เป็นส่วนหนึ่งของการศึกษาตามหลักสูตรปริญญาวิศวกรรมศาสตรดุษฎีบัณฑิต

สาขาวิชาวิศวกรรมเคมี ภาควิชาวิศวกรรมเคมี

คณะวิศวกรรมศาสตร์ จุฬาลงกรณ์มหาวิทยาลัย

ปีการศึกษา 2550

ลิขสิทธิ์ของจุฬาลงกรณ์มหาวิทยาลัย

DEVELOPMENT OF BENZOXAZINE-BASED RESINS FOR
WOOD COMPOSITE APPLICATION



Miss Chanchira Jubsilp

สถาบันวิทยบริการ
มหาวิทยาลัยเทคโนโลยีพระจอมเกล้าธนบุรี

A Dissertation Submitted in Partial Fulfillment of the Requirements
for the Degree of Doctor of Engineering Program in Chemical Engineering

Department of Chemical Engineering

Faculty of Engineering

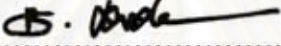
Chulalongkorn University

Academic Year 2007

Copyright of Chulalongkorn University


Thesis Title DEVELOPMENT OF BENZOXAZINE-BASED RESINS FOR
WOOD COMPOSITE APPLICATION
By Miss Chanchira Jubsilp
Field of Study Chemical Engineering
Thesis Advisor Associate Professor Sarawut Rimdusit, Ph.D.
Thesis Co-advisor Professor Tsutomu Takeichi, Ph.D.


Accepted by the Faculty of Engineering, Chulalongkorn University in
Partial Fulfillment of the Requirements for the Doctoral Degree



.....Dean of the Faculty of Engineering
(Associate Professor Boonsom Lerdhirunwong, Dr.Ing.)

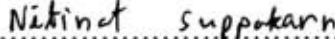
THESIS COMMITTEE



.....Chairman
(Associate Professor Chirakarn Muangnapoh, Dr.Ing.)


.....Thesis Advisor
(Associate Professor Sarawut Rimdusit, Ph.D.)


.....Thesis Co-advisor
(Professor Tsutomu Takeichi, Ph.D.)


.....Member
(Associate Professor Siriporn Damrongsakkul, Ph.D.)


.....Member
(Assistant Professor Nitinat Suppakarn, Ph.D.)


.....Member
(Assistant Professor Watanachai Smittakorn, Ph.D.)

จันจิรา จับศิลป์ : การพัฒนาเรซินกลุ่มเบนซอกซาซีนสำหรับใช้ทำวัสดุประกอบแต่งทดแทนไม้
(DEVELOPMENT OF BENZOXAZINE-BASED RESINS FOR WOOD
COMPOSITE APPLICATION) อ.ที่ปรึกษา : รศ.ดร. ศราวุธ วิมดุสิต, อ.ที่ปรึกษาร่วม :
ศ.ดร. สีสโหม ทาเคอิชิ, 127 หน้า.

งานวิจัยได้ทำการศึกษาปฏิกิริยาการบ่มของเบนซอกซาซีนเรซิน สมบัติของพอลิเมอร์ผสมของ
พอลิเบนซอกซาซีน และสมบัติของวัสดุประกอบแต่งไม้ที่ใช้เมทริกซ์อัลลอยระหว่างเบนซอกซาซีนและอีพอกซี
โดยในปฏิกิริยาการบ่มของเบนซอกซาซีนเรซินเมื่อใช้แบบจำลองของ Kissinger, Ozawa, Friedman, และ Flynn-
Wall-Ozawa ในการหาค่าพารามิเตอร์ทางจลนพลศาสตร์ พบว่าเบนซอกซาซีนชนิด BA-a แสดงพฤติกรรม
การบ่มแบบเร่งปฏิกิริยาเองเพียงปฏิกิริยาเดียว ซึ่งมีค่าพลังงานก่อกัมมันต์โดยเฉลี่ยเท่ากับ 81-85 กิโลจูลต่อโมล
ในขณะที่ปฏิกิริยาการบ่มของเบนซอกซาซีนชนิด BA-35x แสดงพฤติกรรมโดยแบ่งเป็นการบ่มแบบเร่ง
ปฏิกิริยาเองที่อุณหภูมิต่ำและแบบ n/h -order ที่อุณหภูมิสูง โดยมีค่าพลังงานก่อกัมมันต์โดยเฉลี่ยเท่ากับ 81-
87 และ 111-113 กิโลจูลต่อโมล ตามลำดับ สำหรับวิธีการดัดแปรสมบัติของพอลิเบนซอกซาซีนชนิด BA-a
ด้วยตัวทำเจือจางชนิดมอนอฟังก์ชันนอลเบนซอกซาซีนเรซินชนิด Ph-a พบว่า การเติม Ph-a เรซิน 10
เปอร์เซ็นต์โดยน้ำหนักในเรซินผสมระหว่าง BA-a และ Ph-a ส่งผลให้ความหนืดของ BA-a เรซินมีค่าลดลง
เหลือหนึ่งในสาม และเมื่อทำการเพิ่มสัดส่วนของตัวทำเจือจางชนิด Ph-a ส่งผลทำให้อุณหภูมิการหลอมเรซิน
ผสม BA-a/Ph-a และอุณหภูมิ ณ. จุดเกิดเจลลดลง นอกจากนี้อุณหภูมิ ณ.จุดเกิดเจลและค่า Relaxation
exponent ซึ่งมีค่าเท่ากับ 0.24-0.55 เป็นค่าที่ขึ้นอยู่กับสัดส่วนของเรซินผสม BA-a และ Ph-a และอุณหภูมิที่ใช้
ในการบ่ม สำหรับพฤติกรรมเกิดเจลของเรซินผสมระหว่าง BA-a และ Ph-a จากความสัมพันธ์ตามสมการ
ของ Arrhenius พบว่าเมื่ออุณหภูมิเพิ่มขึ้น เวลาที่ใช้ในการเริ่มเกิดเจลมีค่าลดลง จากความสัมพันธ์ดังกล่าวจะ
ได้ค่าพลังงานก่อกัมมันต์ของการเกิดเจลเท่ากับ 60.6 ± 1.5 กิโลจูลต่อโมล สำหรับค่าความแข็งแรงภายใต้แรง
ดัดโค้งของพอลิเมอร์ผสม BA-a และ Ph-a มีค่าสูงขึ้นเมื่อสัดส่วน Ph-a เพิ่มขึ้น อย่างไรก็ตามการเพิ่มสัดส่วน
Ph-a ส่งผลให้ความแข็งแรงภายใต้แรงดัดโค้งและอุณหภูมิการเปลี่ยนสถานะคล้ายแก้วมีค่าลดลง สำหรับ
ระบบวัสดุประกอบแต่งไม้ที่ใช้อัลลอยของเบนซอกซาซีนและอีพอกซีเป็นเมทริกซ์ พบว่าการเสริมแรงด้วยผงไม้
ยางพาราในเมทริกซ์อัลลอยของเบนซอกซาซีนและอีพอกซี จะส่งผลต่อค่าความแข็งแรงโดยมีค่าสูงขึ้นเมื่อ
เปรียบเทียบกับเมทริกซ์อัลลอยของเบนซอกซาซีนและอีพอกซี และเมื่อเพิ่มสัดส่วนของพอลิเบนซอกซาซีนใน
เมทริกซ์อัลลอยของเบนซอกซาซีนและอีพอกซี วัสดุประกอบแต่งไม้ที่ได้มีค่าความแข็งแรงและสมบัติทางความ
ร้อน เช่น อุณหภูมิการเปลี่ยนสถานะคล้ายแก้วเพิ่มสูงขึ้น เนื่องจากความสามารถในการเข้ากันได้ระหว่างผง
ไม้และพอลิเบนซอกซาซีน

ภาควิชา..... วิศวกรรมเคมี..... ลายมือชื่อนิสิต..... *จันจิรา จับศิลป์*
สาขาวิชา..... วิศวกรรมเคมี..... ลายมือชื่ออาจารย์ที่ปรึกษา..... *ศราวุธ วิมดุสิต*
ปีการศึกษา..... 2550..... ลายมือชื่ออาจารย์ที่ปรึกษาร่วม..... *ศาสตราจารย์ สีสโหม ทาเคอิชิ*

##4671805221: MAJOR CHEMICAL ENGINEERING
 KEY WORDS: CURE KINETICS/ ACTIVATION ENERGY/ AUTOCATALYTIC
 CURING/ GELATION/ THERMAL PROPERTIES/ MODIFICATION/ CURING OF
 POLYMERS/THERMOSETS/POLYBENZOXAZINE/ ALLOYS/ WOOD
 COMPOSITES

CHANCHIRA JUBSILP: DEVELOPMENT OF BENZOXAZINE-BASED
 RESINS FOR WOOD COMPOSITE APPLICATION. THESIS ADVISOR:
 ASSOC. PROF. SARAWUT RIMDUSIT, Ph.D., THESIS CO-ADVISOR:
 PROF. TSUTOMU TAKEICHI, Ph.D., 127 pp.

The curing reaction of benzoxazine resin, properties of benzoxazine alloys, and characteristics of wood composites used benzoxazine-epoxy alloy matrices were investigated. Kissinger, Ozawa, Friedman, and Flynn–Wall–Ozawa methods were utilized to determine the kinetic parameters of the curing reaction of the arylamine-based polyfunctional benzoxazine resins. BA-a resin shows only one dominant autocatalytic curing process with the average activation energy of 81–85 kJ/mol, whereas BA-35x exhibits two dominant curing processes signified by the clear split of the curing exotherms. The average activation energies of low-temperature curing (reaction (1)) and high-temperature curing (reaction (2)) were found to be 81–87 and 111–113 kJ/mol, respectively. The reaction (1) is found to be autocatalytic in nature, while the reaction (2) exhibits n th-order curing kinetics. To modify polybenzoxazine properties, effects of a monofunctional benzoxazine diluent (Ph-a) on properties of a bifunctional benzoxazine resin (BA-a) have been studied. The BA-a/Ph-a mixtures are miscible in nature rendering the properties highly dependent on their compositions. The viscosity of the BA-a resin can be reduced to one third using only about 10% by weight the Ph-a diluent. The addition of the Ph-a resin into the BA-a resin can also lower the liquefying temperature of the resin mixtures whereas the gel point is marginally decreased. The gel point, which depends on the BA-a/Ph-a mixtures and the cure temperature, was determined by the frequency independence of loss tangent in the vicinity of the sol-gel transition. The relaxation exponent values of the copolymer were found to be 0.24–0.55, which is dependent on the cure temperature. Gel time of the BA-a/Ph-a systems decreases with increasing temperature according to an Arrhenius relation with activation energy of $60.6 \pm 1.5 \text{ kJ mol}^{-1}$. Flexural moduli of the BA-a/Ph-a polymers also increase with the Ph-a mass fraction, however, with the sacrifice of their flexural strength and glass-transition temperature. To systematically investigate the effect of benzoxazine alloy compositions on the interfacial interaction with *Hevea brasiliensis* woodflour filler, wood-substituted composites from highly filled polybenzoxazine-epoxy alloys were investigated. The reinforcing effect of the woodflour shows the enhancement on the stiffness compared to that of the ternary matrices. The outstanding compatibility between woodflour and polybenzoxazine matrix can improve the modulus and thermal curability i.e., glass transition temperature of the wood composites with polybenzoxazine fraction increased.

Department..... Chemical Engineering..... Student's signature..... Chanchira Jubsilp.....
 Field of study..... Chemical Engineering..... Advisor's signature..... [Signature].....
 Academic year..... 2007..... Co-advisor's signature..... [Signature].....

ACKNOWLEDGEMENTS

The present research receives partial financial support from the Thailand Research Fund (TRF-RTA of Professor Dr. Wiwut Tanthapanichaloon) 2002-2005 and the Industry-University Joint Research Fund of Center of Excellence in Particle Technology, Chulalongkorn University. Additional Funding is from the Affair of Commission for Higher Education-CU Graduate Thesis Grant 2005. One of the authors, S.R., also receives additional financial supports from the Research Grant for Mid-Career University Faculty of the Commission on Higher Education and Thailand Research Fund 2005-2007. The Ratchadapisek Fund of Chulalongkorn University is also acknowledged.

The author would like to express sincere gratitude to my advisor, Associate Professor Dr. Sarawut Rimdusit, for his vision, valuable guidance, intelligence and warm encouragement throughout the course of this research. The author also wishes to give my gratitude to Professor Dr. Tsutomu Takeichi, the thesis co-advisor, for his kind guidance and encouragement. In addition, the author would like to thank to Associate Professor Dr. Chirakarn Muangnapoh as the chairman and Associate Professor Dr. Siriporn Damrongsakkul, Assistant Professor Dr. Nitinat Suppakarn, and Assistant Professor Dr. Watanachai Smittakorn as the member of the thesis committee.

Furthermore, the authors also greatly acknowledged the Centre of Research and Technology Development (Professor Dr. Piyasan Praserttham), Mektec Manufacturing Corporation (Thailand) Ltd. and Chulalongkorn University for TGA measurement. Bisphenol A is kindly supported by Thai Polycarbonate Co., Ltd. (TPCC).

Additionally, I wish to thank the members of the Polymer Engineering Research Laboratory, Department of Chemical Engineering, Faculty of Engineering, Chulalongkorn University, for their discussion and friendly encouragement.

Finally, I would like to express my highest gratitude to my parents who always pay attention to me all the times for suggestions and loves.

CONTENTS

	Page
ABSTRACT IN THAI	iv
ABSTRACT IN ENGLISH	v
ACKNOWLEDGEMENTS	vi
CONTENTS	vii
LIST OF TABLES	x
LIST OF FIGURES	xi
CHAPTER I. INTRODUCTION	1
1.1 Objectives.....	4
CHAPTER II. THEORY	5
2.1 Thermosetting resin.....	5
2.2 Kinetics of network formation.....	6
2.2.1 Kinetic analysis.....	6
2.3 Polymer blends/or alloys.....	10
2.3.1 Thermodynamics of blends.....	11
2.3.2 Properties of blends.....	13
2.4 Rheological monitoring of network formation.....	15
2.4.1 Equilibrium mechanical measurements.....	15
2.4.2 Dynamic mechanical measurements.....	17
2.5 Wood composites.....	20
2.5.1 Wood chemistry.....	20
2.5.2 Characterization of woodflour.....	21
2.5.3 Mechanical properties.....	21
2.6 Types of thermosetting polymers.....	23
2.6.1 Benzoxazine resins.....	23
2.6.2 Epoxy resin.....	29
2.6.3 Phenolic resin.....	31
CHAPTER III. LITERATURE REVIEWS	33

	Page
CHAPTER IV. EXPERIMENTAL	37
4.1 Materials.....	37
4.2 Resin preparation.....	37
4.2.1 Benzoxazine resin.....	37
4.2.2 Phenolic novolac resin.....	38
4.3 Preparation of woodflour.....	38
4.4 Processing method.....	38
4.5 Characterizations.....	39
4.5.1 Rheological experiments.....	39
4.5.2 GPC measurement.....	40
4.5.3 Differential scanning calorimetry.....	40
4.5.4 Density measurement.....	41
4.5.5 Thermogravimetric analysis.....	41
4.5.6 Dynamic mechanical analysis.....	41
4.5.7 Bending test.....	41
4.5.8 Scanning electron microscopy.....	42
 CHAPTER V. CURING KINETICS OF ARYLAMINE-BASED POLYFUNCTIONAL BENZOXAZINE RESINS BY DYNAMIC DIFFERENTIAL SCANNING CALORIMETRY	 43
5.1 Results and discussion.....	44
5.1.1 Curing reaction.....	44
5.1.2 Kinetic model.....	45
 CHAPTER VI. EFFECT OF NOVEL BENZOXAZINE REACTIVE DILUENT ON PROCESSABILITY AND THERMOMECHANICAL CHARACTERISTICS OF BI-FUNCTIONAL POLYBENZOXAZINE	 68
6.1 Results and discussion.....	69
6.1.1 Chemorheological properties of BA-a/Ph-a resin mixture.....	69
6.1.2 Investigation of the gel formation.....	72

	Page
6.1.3 Curing reaction study by calorimetry.....	75
6.1.4 Mechanical property of the polymer network.....	76
6.1.5 Thermal degradation behaviors of BA-a/Ph-a polymer.....	78
 CHAPTER VII. HIGH PERFORMANCE WOOD COMPOSITES BASED ON BENZOXAZINE-EPOXY ALLOYS.....	 95
7.1 Results and discussion.....	96
7.1.1 Chemorheological properties.....	96
7.1.2 Evaluation of activation energy for gelation of the BEP resin mixtures.....	96
7.1.3 Effect of epoxy resin content on the resulting BEP matrix specimens.....	97
7.1.4 Investigation of BEP wood composites filled with 70wt% of woodflour.....	99
 CHAPTER VIII. CONCLUSIONS.....	 113
8.1 Curing kinetics of arylamine-based polyfunctional benzoxazine resins by dynamic differential scanning calorimetry.....	113
8.2 Effect of novel benzoxazine reactive diluent on Processability and thermomechanical characteristics of bi-functional polybenzoxazine.....	113
8.3 High performance wood composites based on benzoxazine-epoxy alloys.....	114
 REFERENCES.....	 115
 APPENDIX.....	 125
List of publications.....	126
 VITAE.....	 127

LIST OF TABLES

Table	Page
2.1 Thermal and mechanical properties of the polybenzoxazine.....	28
4.1 Chemical used for sample preparations.....	37
5.1 Average activation energies of BA-a and BA-35x obtained by Kissinger and Ozawa methods.....	50
5.2 The kinetic parameters evaluated for the curing of the BA-a system.....	51
5.3 The kinetic parameters evaluated for the curing of the BA-35x system (reaction1)....	52
5.4 The kinetic parameters evaluated for the curing of the BA-35x system (reaction2)....	53
6.1 Gelation times of BA-a/Ph-a systems at different temperature.....	79
6.2 The apparent activation energy values obtained from the rheological tests for the BA-a/Ph-a systems at various Ph-a resin contents.....	80
7.1 Gelation times of BEP mixtures at various temperatures.....	101
7.2 Flexural properties of BEP alloys.....	102
7.3 Maximum packing density of woodflour-filled BEP composites.....	103


 สถาบันวิทยบริการ
 จุฬาลงกรณ์มหาวิทยาลัย

LIST OF FIGURES

Figure	Page
2.1 Illustration of three types of behavior for the dependence of miscible blend properties on composition.....	14
2.2 Steady-state mechanical properties of a thermoset as a function of reaction time or conversion. Representative properties are the steady shear viscosity for the liquid state and the equilibrium modulus for the solid state.....	16
2.3 Evolution of the storage modulus, G' , loss modulus, G'' , and loss factor, $\tan \delta$, during the reaction of pure diglycidyl ether of bisphenol A (DGEBA) with poly(oxypropylene) diamine (PPO).....	18
2.4 Decrease in the loss factor ($\tan \delta$) during cure, for the same epoxy-diamine system as that represented in Figure 2.3, at different frequencies of the dynamic measurement, $T_i = 70^\circ\text{C}$	19
2.5 Synthesis of phenol based benzoxazine monomer.....	24
2.6 Ring-opening polymerization of the phenol based benzoxazine monomer.....	24
2.7 Synthesis of phenol-aniline type benzoxazine monomer.....	25
2.8 Synthesis of bisphenol A and aniline based benzoxazine (BA-a) monomer.....	26
2.9 Arylamine-based benzoxazine monomers.....	27
2.10 Network structure of the arylamine-based polybenzoxazines.....	28
2.11 Oxirane ring found in common epoxy resins.....	29
2.12 Epoxy prepolymer formed from bisphenol A and epichlorohydrin.....	30
2.13 Preparation and molecular structure of phenolic novolac resin.....	31
5.1 DSC thermograms of BA-a resin at different heating rates: (○) $1^\circ\text{C}/\text{min}$, (□) $2^\circ\text{C}/\text{min}$, (◇) $5^\circ\text{C}/\text{min}$, (Δ) $10^\circ\text{C}/\text{min}$, (▽) $20^\circ\text{C}/\text{min}$	54
5.2 DSC thermograms of BA-35x resin at different heating rates: (○) $1^\circ\text{C}/\text{min}$, (□) $2^\circ\text{C}/\text{min}$, (◇) $5^\circ\text{C}/\text{min}$, (Δ) $10^\circ\text{C}/\text{min}$, (▽) $20^\circ\text{C}/\text{min}$	55
5.3 DSC thermograms of two types of benzoxazine resins at $10^\circ\text{C}/\text{min}$: (○) BA-a resin, (□) BA-35x resin.....	56
5.4 DSC thermograms of BA-35x resin using $10^\circ\text{C}/\text{min}$ heating rate after isothermal curing of 160°C at different curing time in oven: (○) uncured BA-35x monomer, (□) 5 min, (◇) 10 min, (Δ) 15 min, (▽) 60 min, (●) 120 min.....	57

Figure	Page
5.5 DSC thermogram of BA-35x resin recorded at 10°C/min: the DSC thermogram (solid line), calculated the DSC thermogram (dash line), (●) reaction 1, (○) reaction 2.....	58
5.6 (●) Kissinger method and (■) Ozawa method plots for averaged activation energy determination of the BA-a resin.....	59
5.7 Flynn-Wall- Ozawa plots at various degree of curing of the BA-a resin: (○) $\alpha = 0.05$, (□) $\alpha = 0.10$, (◇) $\alpha = 0.20$, (Δ) $\alpha = 0.30$, (▽) $\alpha = 0.40$, (●) $\alpha = 0.60$, (■) $\alpha = 0.80$, (◆) $\alpha = 0.90$, (▲) $\alpha = 0.95$	60
5.8 Friedman plots at various degree of curing of the BA-a resin: (○) $\alpha = 0.05$, (□) $\alpha = 0.10$, (◇) $\alpha = 0.20$, (Δ) $\alpha = 0.30$, (▽) $\alpha = 0.40$, (●) $\alpha = 0.60$, (■) $\alpha = 0.80$, (◆) $\alpha = 0.90$, (▲) $\alpha = 0.95$	61
5.9 Values of the apparent activation energy obtained from Flynn-Wall- Ozawa plots at different degree of curing: (-○-) BA-a resin, (-□-) BA-35x reaction 1, (-■-) BA-35x reaction 2.....	62
5.10 Values of the apparent activation energy obtained from Friedman plots at different degree of curing: (-○-) BA-a resin, (-□-) BA-35x reaction 1, (-■-) BA-35x reaction 2.....	63
5.11 Plots of $\ln[Af(\alpha)]$, vs $\ln(1-\alpha)$ of BA-35x resin using the heating rate of 10°C/min. and using the average activation energy from Kissinger method: (○) reaction 1, (●) reaction 2.....	64
5.12 Experimental (symbols) and calculated (solid lines) DSC peaks corresponding to the curing process of BA-a resin: (○) 1°C/min, (□) 2°C/min, (◇) 5°C/min, (Δ) 10°C/min, (▽) 20°C/min.....	65
5.13 Experimental (symbols) and calculated (solid lines) DSC peaks corresponding to the first curing process (reaction 1) of BA-35x resin: (○) 1°C/min, (□) 2°C/min, (◇) 5°C/min, (Δ) 10°C/min, (▽) 20°C/min.....	66
5.14 Experimental (symbols) and calculated (solid lines) DSC peaks corresponding to the second curing process (reaction 2) of BA-35x resin: (○) 1°C/min, (□) 2°C/min, (◇) 5°C/min, (Δ) 10°C/min.....	67

Figure	Page
6.1 Processing window of the BA-a/Ph-a resin mixtures at various Ph-a resin using a heating rate of 2°C/min: (●) BA-a resin, (■) BP91, (◆) BP82, (▲) BP73, (▼) BP64, (○) BP55, (□) Ph-a resin.....	81
6.2 Dynamic viscosity at 90°C of the BA-a/Ph-a resin mixtures at various Ph-a mole fractions: Experimental data (symbol), Predicted data with the Grunberg-Nissan equation (solid line).....	82
6.3 Stress sweep experiment at the gel points of BP systems: (●) BP91, (■) BP73, (◆) BP55.....	83
6.4 Loss tangent at various frequencies as a function of time for BP91 at 140°C: (●) 10 rad/s, (■) 31 rad/s, (◆) 100 rad/s.....	84
6.5 The relaxation exponent, n, from gel point as a function of cure temperature at different Ph-a resin content: (●) BP91, (■) BP73, (◆) BP55.....	85
6.6 Plots of gel times as a function of 1/T based on rheology data at various Ph-a mass fractions: (●) BP91, (■) BP73, (◆) BP55.....	86
6.7 DSC thermograms of the BA-a/Ph-a resin mixtures at different Ph-a resin contents: (●) BA-a resin, (■) BP82, (◆) BP55, (▲) BP28, (▼) Ph-a resin.....	87
6.8 Conversion-time curve of thermally cured the BA-a/Ph-a mixtures at 180°C: (●) BA-a resin, (■) BP82, (◆) BP55, (▲) BP28, (▼) Ph-a resin.....	88
6.9 Storage modulus of the BA-a/Ph-a polymer as a function of temperature at different Ph-a contents: (●) poly(BA-a), (■) BP91, (◆) BP82, (▲) BP73, (▼) BP64, (○) BP55, (□) poly(Ph-a).....	89
6.10 Loss modulus of the BA-a/Ph-a polymer as a function of temperature at different Ph-a contents: (●) poly(BA-a), (■) BP91, (◆) BP82, (▲) BP73, (▼) BP64, (○) BP55, (□) poly(Ph-a).....	90
6.11 Tanδ of the BA-a/Ph-a polymers as a function of temperature at different Ph-a contents: (●) poly(BA-a), (■) BP91, (◆) BP82, (▲) BP73, (▼) BP64, (○) BP55, (□) poly(Ph-a).....	91
6.12 Flexural modulus of the BA-a/Ph-a polymers as a function of Ph-a compositions.....	92
6.13 Flexural strength of the BA-a/Ph-a polymers as a function of Ph-a compositions.....	93

Figure	Page
6.14 TGA thermograms of the BA-a/Ph-a polymers at different Ph-a mass fractions: (●) poly(BA-a), (■) BP91, (◆) BP82, (▲) BP73, (▼) BP64, (○) BP55, (□) Poly(Ph-a).....	94
7.1 Relationship between dynamic viscosity and temperature of BEP mixtures: (○) BEP811, (□) BEP721, (◇) BEP631, (△) BEP541, (▽) BEP451.....	104
7.2 Relationship between gel time and temperature based on rheological data as BEP compositions: (●) BEP721, (■) BEP631, (◆) BEP541.....	105
7.3 Storage and loss modulus of the BEP alloys as function of temperature: (●) BEP811, (■) BEP721, (◆) BEP631, (▲) BEP541, (▼) BEP451.....	106
7.4 Flexural stress and strain relationship of BEP alloys at various compositions: (●) BEP811, (■) BEP721, (◆) BEP631, (▲) BEP541, (▼) BEP451.....	107
7.5 TGA thermograms of BEP alloys at different compositions: (●) BEP811, (■) BEP721, (◆) BEP631, (▲) BEP541, (▼) BEP451.....	108
7.6 Storage and loss modulus of the BEP composites made with 70wt% woodflour as function of temperature: (●) BEP811, (■) BEP721, (◆) BEP631, (▲) BEP541, (▼) BEP451.....	109
7.7 Flexural strength and modulus of the BEP composites made with different values epoxy content having 70wt% woodflour. (●) Flexural strength, (■) Flexural modulus.....	110
7.8 TGA thermograms of the BEP composites made with 70wt% woodflour as function of temperature: (●) BEP811, (■) BEP721, (◆) BEP631, (▲) BEP541, (▼) BEP451.....	111
7.9 SEM micrographs of an interface between woodflour and BEP721 matrix of the woodflour-filled BEP721 fracture surface.....	112

CHAPTER I

INTRODUCTION

Many of the advances in material performance over the last decade can be attributed to developments in multicomponent polymer systems and, specifically, to multiphase materials such as incompatible polymer blends and filler-reinforced composites [1]. In recent years, thermosetting polymer has received strong attention from the automotive, aerospace and construction industries because of the great potential of these materials. Polybenzoxazines are a new class of phenolic polymers being developed as an alternative to traditional high performance thermosetting polymer, having a wide range of interesting features and the capability to overcome several shortcomings of conventional novolac and resole type phenolic resins. These materials exhibit low a-stage viscosity, near-zero volumetric change upon polymerization in which no strong acid catalysts was required and no toxic by-product was released. Moreover, polybenzoxazines possess several outstanding properties such as high stiffness, relatively high glass transition temperature even though it has relatively low cross-linking density, high char yield, and low water absorption [2]. In addition, they can be tailored to have a range of properties that covers advanced epoxies and phenolic resins to bismaleimides and polyimides [3].

Because of the advantage characteristics of the polybenzoxazine [2,4], their cure reactions, blends/alloys and composite systems were investigated in this research. In order to make on optimum use of the benzoxazine resins, it is important to understand the nature of their curing process, the structure of the cured material, and how its kinetic parameters can be influenced by temperature, etc. The processing of these materials is complicated because of the involvement of chemical reactions. Furthermore, the availability of reliable methods for cure monitoring also plays a crucial role in process control and optimization of the polymer network processing [5]. As previous study, the curing reactions of the bisphenol A-aniline based benzoxazine resin (BA-a) were studied [6,7]. The curing of the resin is an autocatalysed reaction until vitrification is reached, and diffusion begins to control the curing process afterwards. The average activation energy of the bisphenol A-aniline type polybenzoxazine (BA-a) was found to be 77 kJ/mol. Therefore, the different mechanism of curing reaction of other benzoxazine types was observed as reported in this research. In addition, the reduction of viscosity of

polybenzoxazine to achieve easier handling, increase filler loading was employed. As previously reported by Rimdusit and Ishida [8], the effect of epoxy used as a reactive diluent on the viscosity of benzoxazine-epoxy resin mixtures was investigated. They found that using an epoxy as a diluent, the viscosity of the resin mixture can be significantly reduced with increasing epoxy content. Ishida and Allen [9] reported that the addition of liquid epoxy (EPON825) to the polybenzoxazine network greatly increased the crosslink density of the thermosetting matrix and strongly influenced its mechanical properties besides its obvious ability to lower the liquefying temperature of the resin mixtures. To obtain the lower viscosity of polybenzoxazine (BA-a), in this work, the effect of a monofunctional benzoxazine diluent (Ph-a) on properties of a bifunctional benzoxazine resin (BA-a) has been investigated. Due to the Ph-a is a reactive diluent that actually undergoes chemical reaction with the resin and becomes part of the polymeric structure and do not release the volatile organic compounds as a nonreactive diuent.

Recently, in filler-reinforced polymer composite system, the multicomponent of polymer alloys based on benzoxazine resin to act as a matrix for the composites was studied. Rimdusit et al. [10] had to develop the wood-substituted composites from highly filled polybenzoxazine-phenolic novolac alloys. They found that phenolic novolac resin can significantly reduce the curing temperature of the neat benzoxazine, thereby minimizing the degradation of woodflour filler during processing. In addition, the rate of burning decreased as the phenolic novolac fraction in the resin mixtures increased as well as the resulting wood composites showed the outstanding mechanical properties i.e. flexural modulus and strength. Moreover, the ternary systems based on benzoxazine, epoxy and phenolic novolac resins was of particular interest as reported by Rimdusit et al. [11]. The authors reported that phenolic novolac resin acts mainly as an initiator for the ternary systems while low melt viscosity, flexibility and improved crosslink density of the materials are attributed to the epoxy fraction. Polybenzoxazine imparts thermal curability, mechanical properties as well as low water uptake to the ternary systems. Therefore, the materials exhibit promising characteristics suitable for application as highly filled systems.

This dissertation was divided to seven chapters starting with this introductory chapter. The second chapter involves the knowledge of curing reaction and gelation behavior of polymer systems, as well as composite characteristics of polymer reinforced with woodflour. The literature review as accentuated the study concerning the kinetic of benzoxazine curing, the effect of reactive diluent on the rheological properties of

polybenzoxazine alloy systems and their properties as well as the utilization of benzoxazine resin and benzoxazine-phenolic novolac alloys as a wood composite matrix. The experimental procedure as well as the instrument and technique used for characterizing the resulting of polybenzoxazine's curing reaction, novel benzoxazine reactive diluent blended with bi-functional polybenzoxazine system, and wood composite based on polybenzoxazine-epoxy alloys were described in the chapter IV.

In Chapter V, to the best knowledge, the effect of alkyl-substituted arylamines in the curing characteristics of the polyfunctional benzoxazine resins has been investigated. The polyfunctional benzoxazine resins based on arylamine, i.e. aniline and 3,5 xylydine. The curing kinetics of the systems were examined by non-isothermal differential scanning calorimetry (DSC) at different heating rates in order to understand the reaction kinetics of both systems and be the way of achieving successful processing.

A relatively low a-stage viscosity, one of the most useful properties of benzoxazine resins results in an ability of the resins to accommodate relatively large quantity of filler while still maintaining their good processability. In Chapter VI, the Ph-a benzoxazine resin will be examined as a novel reactive diluent of a bifunctional benzoxazine resin i.e BA-a resin. Since the molecule structure of the Ph-a resin resembles the BA-a resin chemically, a miscible mixture of the Ph-a and the BA-a resins should also be expected. The processability, thermal, and mechanical properties of the resulting polymer hybrids will also be examined. Furthermore, improvements of polybenzoxazine properties to be excellent candidates for high-performance materials such as high thermal stability, high char yield, and high glass transition temperature, are becoming more and more attractive in many methods.

In Chapter VII, the mixture of benzoxazine, epoxy, and phenolic novolac resins to form the ternary systems is believed that to provide a great variety of resin properties suitable for wide applications, particularly in the highly filled systems. Therefore, the objective of this chapter is to examine the matrix systems that are the modification of thermally curable benzoxazine resin by partial incorporation of epoxy resin on the interfacial interaction with rubberwood flour including the mechanical and thermal performance of their wood composites will be presented. Finally, conclusions of this work were provided in Chapter VIII.

1.1 Objectives

- 1.1.1 To study the effect of types of arylamine-based benzoxazine resins on curing characteristics.
- 1.1.2 To examine the addition of a novel reactive diluent on themomechanical characteristics of bi-functional polybenzoxazine
- 1.1.3 To systematically investigate the effect of benzoxazine-epoxy alloy compositions on the interfacial interaction with *Hevea brasiliensis* woodflour as a filler.



สถาบันวิทยบริการ
จุฬาลงกรณ์มหาวิทยาลัย

CHAPTER II

THEORY

2.1 Thermosetting resin

Thermoset is the term used to describe those polymers produced by polymerization of relatively low-molecular-weight precursors either within a mould cavity or in some other *in situ* situation. Thus, the part shape is set by chemical reaction within the mould cavity and this distinguished thermosets from thermoplastics for which shape is set by the cooling of a melt. Most polymers processed as thermosets are cross-linked and therefore undergo an irreversible liquid to solid transition unlike thermoplastics, which show a reversible liquid to solid transition. Consequently, thermoplastics may, in principle, be reprocessed.

During the curing or polymerization of a cross-linked polymer, two phenomenological steps occur – gelation and vitrification. Gelation occurs when conversion of the reaction groups on resin/monomer has proceeded to such an extent that the amount of branching ensuing is sufficient to generate a ‘global’ network of essentially infinite molecular weight. As conversion proceeds, the glass transition temperature of the resin swollen gel increases and, when it corresponds to the temperature at which the resin is polymerizing, vitrification occur, i.e. the swollen gel is hardened to a glass. The significance of the point of vitrification is that, after vitrification, the mobility of the reactive groups within the glass is severely inhibited and the rate of further reaction falls sharply, in the limit to zero. Thus, in moulding thermosets, it is important that the mould temperature or the maximum exotherm temperature be close to the glass transition temperature of the fully cured polymer, i.e. vitrification occurs as late as possible in the conversion process, otherwise under cure will result [12].

Furthermore, alloying/blending of thermosetting polymer systems has been modified to improve their performance [8-11], i.e., processability, thermal stability, stiffness, and strength. Several attempts to model the thermodynamics of modified thermosets have been made [13]. These model are generally based on the Flory-Huggins lattice theory, original developed for linear polymer-solvent systems, but also applied to evolving thermoset networks which are discussed in section 2.3 (polymer blends/alloys). For filler-filled thermosetting systems, the function of the filler in a thermoset can be to

offer material cost reduction, since most fillers are of low cost relative to polymers or to confer property modification. Filler can modify the properties of the cured polymer in a wide variety of ways. Some examples of properties readily modified by incorporation of fillers are mechanical properties such as stiffness, hardness, strength and toughness, and thermal properties such as expansion, conductivity or thermal decomposition. The latter can have a considerable effect on flammability and smoke generation. Fillers are also an important way of varying and enhancing aesthetics. [12].

To develop the new materials, incorporating organic filler into thermoset polymer and modification utilizing thermoset polymer alloy/or blend technology have been investigated to afford improved properties of these materials with even broader range of applications. Therefore, the curing reaction, gelation behavior of polymer alloys, as well as properties of polymer composites based on the thermosetting polymer matrix have been studied.

2.2 Kinetics of network formation

There are several techniques previously used to examine the kinetics of the polybenzoxazine curing, for instance, differential scanning calorimetry (DSC) [6,14-22], Fourier Transform Infrared Spectroscopy (FTIR) [23], and rheokinetic measurements [24]. Among these, differential scanning calorimetry (DSC) has been the most utilized technique for the determination of kinetic parameters and the corresponding rate equation of the polybenzoxazine curing [6,7,15,16,19-21]. In general, the kinetic parameters estimated from DSC dynamic experiments were reported to agree relatively well with those estimated by other methods. The basic assumption for the application of DSC is that the measured of heat flow, dH/dt , is proportional to the reaction rate, $d\alpha/dt$. Without knowing the exact reaction mechanism, it is reasonable to assume that the reaction rate at a given time is only a function of the conversion fraction particularly in the isothermal method [5].

2.2.1 Kinetic analysis

Kinetic analysis of non-isothermal resin-cured system is based on the rate equation [16]

$$\frac{d\alpha}{dt} \equiv \beta \frac{d\alpha}{dT} = k(T)f(\alpha) \quad (2.1)$$

Where $k(T)$ is a temperature-dependent reaction rate constant, $f(\alpha)$ is the differential conversion function depending on the reaction mechanism, and $\beta = dT/dt =$ a constant heating rate. The rate constant, $k(T)$ is temperature dependent according to Arrhenius law shown in Eq.(2.2)

$$k(T) = A \exp\left(-\frac{E_a}{RT}\right) \quad (2.2)$$

Where A is the pre-exponential factor, E_a is the activation energy, and T is the absolute temperature.

Non-isothermal method, a more precise measure to evaluate the curing kinetic parameters, is carried out at different heating rates. This method is very attractive because the kinetic data can be obtained in a relatively short period of time. Nevertheless, there are some complications in the mathematical analysis of the temperature integral which are inherent to the non-isothermal approach. In addition, the isothermal method renders the destabilization of the DSC heat flow at the beginning of the measurement which leads to experimental errors. The two methods also cover different temperature domains as discussed by Sbirrazzuoli et al. [17]. Moreover, considering the shape of curing peak, the number of peaks and/or shoulders in the isothermal and non-isothermal DSC thermograms may be different. Although there is only a single peak in the isothermal DSC thermogram, a peak and a shoulder may appear in the non-isothermal DSC thermogram. Consequently, the kinetic parameters obtained from an isothermal cure study may be not good in predicting the non-isothermal curing behaviors [25]. The non-isothermal method which involves single or multiple dynamic temperature scans, has been applied extensively in the study of the curing reactions of thermosetting polymers [14,26,27]. Four kinetic methods widely used to study dynamic kinetics of thermosetting polymers are Kissinger, Ozawa, Friedman, and Flynn-Wall-Ozawa methods.

2.2.1.1 The Kissinger method

Kissinger method is based on a linear relationship between the logarithm of (β/T_p^2) with the inverse of the peak temperature of the exothermic curing reaction, through the following expression [18,28]:

$$\ln\left(\frac{\beta}{T_p^2}\right) = \ln\left(\frac{Q_p AR}{E_a}\right) - \frac{E_a}{RT_p} \quad (2.3)$$

$$\text{Where } Q_p = - \left[\frac{df(\alpha)}{d\alpha} \right]_{\alpha = \alpha_p}$$

The graphic representation of Eq. (2.3) allows us to examine both the activation energy and the pre-exponential factor of curing kinetics.

2.2.1.2 The Ozawa method

A similar method to Kissinger method is Ozawa method, which relates the logarithm of the heating rate and the inverse of the exothermic peak temperature. Therefore, the curing activation energy can be determined from the resultant slope [29].

$$\ln\beta = \ln\left(\frac{AE_a}{R}\right) - \ln F(\alpha) - 5.331 - 1.052 \left(\frac{E_a}{RT}\right) \quad (2.4)$$

$$F(\alpha) = \int_0^{\alpha} \frac{d\alpha}{f(\alpha)} \quad (2.5)$$

where $F(\alpha)$ is a constant function

2.2.1.3 Isoconversional method

The isoconversional method assumes that both of the activation energy and pre-exponential factor are the functions of the degree of curing. In addition, the isoconversional approach can be used to evaluate both simple and complex chemical reactions. The significance of this technique is that no kinetic rate expression is assumed for the data evaluation [30]. Two different isoconversional methods are as follows.

A. Friedman method

The Friedman method, differential isoconversional method, is used to determine a kinetic model of the curing process. The method is based on Eq. (2.1), (2.2) that leads to:

$$\ln \frac{d\alpha}{dt} = \ln \beta \frac{d\alpha}{dT} = \ln [Af(\alpha)] - \frac{E_a}{RT} \quad (2.6)$$

In case of the n th-order reaction: $f(\alpha) = (1-\alpha)^n$ (2.7)

From Eq. (2.1), (2.2) and (2.7)

$$\ln [Af(\alpha)] = \ln \left[\frac{d\alpha}{dt} \right] + \frac{E_a}{RT} = \ln A + n \ln(1-\alpha) \quad (2.8)$$

The value of $\ln [Af(\alpha)]$ can be obtained from the known values of $\ln [d\alpha/dt]$ and E_a/RT . Therefore, the plot of $\ln [Af(\alpha)]$ and $\ln(1-\alpha)$ yields a straight line which the slope providing the reaction order. The intercept is the natural logarithm of the frequency factor if the reaction mechanism of the n th-order kinetics. The rate, da/dt , at each temperature can be determined from

$$\frac{d\alpha}{dt} = \frac{\varphi}{\Delta H} \quad (2.9)$$

where ΔH is the enthalpy of the curing reaction and φ is the measured heat flow normalized with the sample mass.

B. Fynn-Wall-Ozawa method

The isoconversional integral method was also proposed independently by Flynn, Wall and Ozawa [18] using Doyle's approximation of the temperature integral. This method is based on Eq. (2.10) and Eq. (2.11).

$$\ln \beta = \ln \left(\frac{AE_a}{R} \right) - \ln g(\alpha) - 5.331 - 1.052 \left(\frac{E_a}{RT} \right) \quad (2.10)$$

$$g(\alpha) = \int_0^\alpha \frac{d\alpha}{f(\alpha)} \quad (2.11)$$

where $g(\alpha)$ is the integral conversion function.

Thus, for a constant α , the plot of $(\ln \beta)$ vs. $(1/T)$ obtained from DSC thermograms using various heating rates, should render a straight line where the slope allows the determination of the apparent activation energy. The apparent activation energy received from the Flynn-Wall-Ozawa analysis is reported to be more reliable than that from the Friedman analysis. Moreover, the Flynn-Wall-Ozawa method, owing to its integrating character, exhibits less sensitivity to noise than the Friedman method. The latter; however, provides a better visual separation of more reaction steps as well as information concerning the existence of an autocatalytically activated process [31]. The advantage of these four kinetic methods over other non-isothermal methods is that they do not require prior knowledge of the reaction mechanism in order to quantify kinetic parameters [5].

2.3 Polymer blends/or alloys

Polymer blends are a key component of current polymer research and technology, because of their ease of production of new materials by mixing and the diversity of properties that result. From scientific standpoint, however, an increasing set of characterization techniques have also led to an increased understanding of the mechanisms involved in the polymer mixing, their fundamental interactions, and how these interactions affect their final properties. This link between molecular interactions and physical and engineering properties continues to be an important challenge for both scientific and industrial viewpoints, due to the increasing economical impact of polymer blends and alloys in many domains affecting our everyday life.

At equilibrium, a mixture of two amorphous polymers may exist as a single phase of intimately mixed segments of the two macromolecular components or separate into two distinct phases consisting primarily of the individual components. Which of these occurs is dictated by the same principles of solution thermodynamics governing the phase behavior of mixtures of low molecular weight liquids, with some quantitative differences arising from the higher molar masses in the case of polymers. It is important to note that amorphous polymers form glasses upon sufficient cooling and that a homogeneous, or miscible, polymer blend exhibits a single, composition-dependent glass-transition temperature, T_g , whereas an immiscible blend has separate glass transitions associated with each phase [32].

2.3.1 Thermodynamics of blends

Whether a particular polymer blend will be homogeneous or phase-separated will depend upon many factors, such as the kinetics of the mixing process, the processing temperature, and the presence of solvent or other additives; however, the primary consideration for determining miscibility of two polymers is a thermodynamic issue that is governed by the same (Gibbs) free-energy considerations. The relationship between the change in Gibbs free energy due to mixing (ΔG_m) and the enthalpy (ΔH_m) and entropy (ΔS_m) of mixing for a reversible system was given as

$$\Delta G_m = \Delta H_m - T\Delta S_m \quad (2.12)$$

If (ΔG_m) is positive over the entire composition range at a given temperature, the two polymers in the blend will separate into phases that are pure in either component, providing that a state of thermodynamic equilibrium has been reached. For complete miscibility, two conditions are necessary: ΔG_m must be negative and the second derivative of ΔG_m with respect to the volume fraction of component 2 (ϕ_2) must be greater the zero

$$\left(\frac{\partial^2 \Delta G_m}{\partial \phi_2^2} \right)_{T,p} > 0 \quad (2.13)$$

over the entire composition range [33].

The thermodynamic equilibrium of a system at constant pressure is described as above mentioned by the Gibbs free energy of mixing, which was derived by Flory and Huggins for linear polymer solvent mixtures using a lattice model [13]. When n_1 moles of polymer are mixed with n_2 moles of solvent, the free energy of mixing, ΔG_m , is:

$$\Delta G_m = RT(n_1 \ln \phi_1 + n_2 \ln \phi_2 + n_2 \phi_1 \chi'_{12}) \quad (2.14)$$

where T is the temperature expressed in Kelvin, R is the perfect gas constant, ϕ_1 and ϕ_2 are the volume fractions of components 1 and 2 (polymer and solvent), and χ'_{12} is the

interaction parameter expressing the interaction enthalpy between two different molecules. Equation 2.14 expresses the energy in terms of extensive parameters. Dividing by the overall volume, the free energy change per unit volume of solution ΔG_v can be expressed as a function of intensive parameters:

$$\Delta G_v = RT \left(\frac{\phi_1}{V_1} \ln \phi_1 + \frac{\phi_2}{V_2} \ln \phi_2 + \phi_1 \phi_2 \chi_{12} \right) \quad (2.15)$$

where V_1 and V_2 are the molar volumes of the two components. The free energy of mixing can be expressed as the contribution of the interaction enthalpy ΔH_v , and the entropy of mixing, ΔS_v , which following Eq. (2.16) and Eq. (2.17) are:

$$\Delta S_v = RT \left(\frac{\phi_1}{V_1} \ln \phi_1 + \frac{\phi_2}{V_2} \ln \phi_2 \right) \quad (2.16)$$

$$\Delta H_v = RT \phi_1 \phi_2 \chi_{12} \quad (2.17)$$

The term χ_{12} corresponds to $(\chi'_{12})/(V_1)_0$ where $(V_1)_0$ is the lattice site molar volume. In polymer-solvent blend, $(V_1)_0$ is normally attributed to the solvent or to the monomer unit molar volume. χ_{12} can be expressed as a function of the solubility parameters:

$$\chi_{12} = \left[(\delta_{1h} - \delta_{2h})^2 + (\delta_{1p} - \delta_{2p})^2 + (\delta_{1d} - \delta_{2d})^2 \right] / RT \quad (2.18)$$

in which the subscripts designate the hydrogen (h), polar (p) and dispersive (d) components of the solubility parameters of components 1 and 2.

In polymer-polymer systems, the entropic contribution to Eq. (2.15) is relatively low because of the relatively large molar volumes of both components. In the case of macromolecular components, the solubility parameters of each polymer will refer to their repetitive unit cell. At a fixed concentration in unreactive thermoplastic polymer blends, changes in Eq. (2.14) and Eq. (2.15) are induced only by temperature variation and are limited to the entropic contribution, while the enthalpy is unaffected, as shown by Eq. (2.15) and Eq. (2.18). In thermoset polymer blends, the Gibbs free energy of mixing is also controlled by the conversion due to the evolution of molecular structure. Conversion

thus affects the entropy of mixing since the molecular weight increases, resulting in a decrease of the entropy of mixing.

2.3.2 Properties of blends [32,34]

Sine the driving force for development of polymer blends is generally some combination of economics and blend performance or properties, knowledge of the rules of mixtures for blend properties is of critical interest. These rules will again depend on the state of miscibility of the blend. The properties of miscible blends will follow relationships that are functions of composition and to some extent the degree of interaction between the blend components whereas immiscible blend properties will depend on the phase morphology and phase interaction as well as composition.

Properties of miscible polymer blends may be intermediate between those of the individual components (i.e., additive behavior), as is typically the case for glass transition temperature (T_g). In the other cases, blend properties may exhibit either positive or negative deviation from additivity. The compositional variations of properties typically encountered for miscible binary mixture of amorphous materials can take the form

$$M = \omega_1 M_1 + \omega_2 M_2 + \omega_1 \omega_2 \Delta M^E \quad (2.19)$$

as a first approximation. In Eq. (2.19), M is the blend property, M_i that of the pure component i , ω_i the fraction of component i in the blend, and ΔM^E a measure of the deviation from additivity, $\Delta M^E > 0$, or minimum deviations from additivity, $\Delta M^E < 0$, depending on the direction of the property with changes in temperature or free volume as illustrated by Figure 2.1. For example, both modulus and tensile strength of miscible polymer blends exhibits a small maximum at some intermediate blend composition, while impact strength and permeability will normally go through a broad minimum. This latter behavior has been attributed to a loss in free volume corresponding to a negative volume change of mixing (ΔV_m) due to favorable interactions between blend polymers.

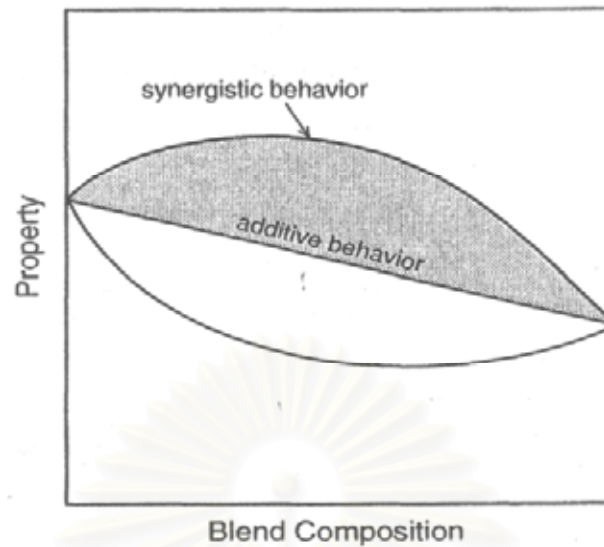


Figure 2.1 Illustration of three types of behavior for the dependence of miscible blend properties on composition.

As above mentioned, miscibility results in the formation of a single amorphous phase that has a single, composition-dependent, glass transition temperature (T_g). For miscible blend T_g versus composition is not a universally similar relationship for all systems. In fact, each of the three types of generalized curves in Figure 2.1 are possible and have been reported in various systems. The most usual situation is the lower curve, which is approximated by

$$\frac{1}{T_g} = \frac{\omega_1}{T_{g1}} + \frac{\omega_2}{T_{g2}} \quad (2.20)$$

However, it is interesting to note that several examples similar to the upper curve in Figure 2.1 have been observed, and it has been postulated that such behavior results from the existence of very strong intermolecular interactions such as hydrogen bonding. The T_g is a parameter of practical significance since it determines in part the maximum use temperature, or heat distortion temperature of product.

2.4 Rheological monitoring of network formation [35]

Two main transformations can be take place during the formation of a polymer network: gelation and vitrification. Gelation corresponds to the incipient formation of an infinite network, while vitrification involves the transformation from a liquid of rubbery state to a glassy state.

Gelation is characterized by the divergence of the mass-average molar mass, M_w , and the radius of gyration, and by the formation of an insoluble gel. Vitrification occurs when the increasing glass transition temperature, T_g , becomes equal to the reaction temperature. Below $T_{g,gel}$, the temperature at which the time to gel is the same as the time to gel is the same as the time to vitrify, the reactive system vitrifies in an ungelled (liquid) state. Although conversion may increase at a very slow rate during storage, the polymer can be processed as long as it remains in the ungelled state. The thermosetting polymer will not vitrify during an isothermal cure at a reaction temperature higher than $T_{g\infty}$, the glass transition temperature of the fully cured material.

The experimental determination of gelation and vitrification is very important for the design of cure cycles and to control the morphology of inhomogeneous polymer networks and modified-thermosetting polymers that undergo a phase-separation process during cure [36].

2.4.1 Equilibrium mechanical measurements

A typical evolution of equilibrium mechanical properties during reaction is shown in Figure 2.2. The initial reactive system has a steady shear viscosity that grows with reaction time as the mass-average molar mass, M_w , increases and it reaches to infinity at the gel point. Elastic properties, characterized by nonzero values of the equilibrium modulus, appear beyond the gel point. These quantities describe only either the liquid (pregel) or the solid (postgel) state of the material. Determination of the gel point requires extrapolation of viscosity to infinity or of the equilibrium modulus to zero.

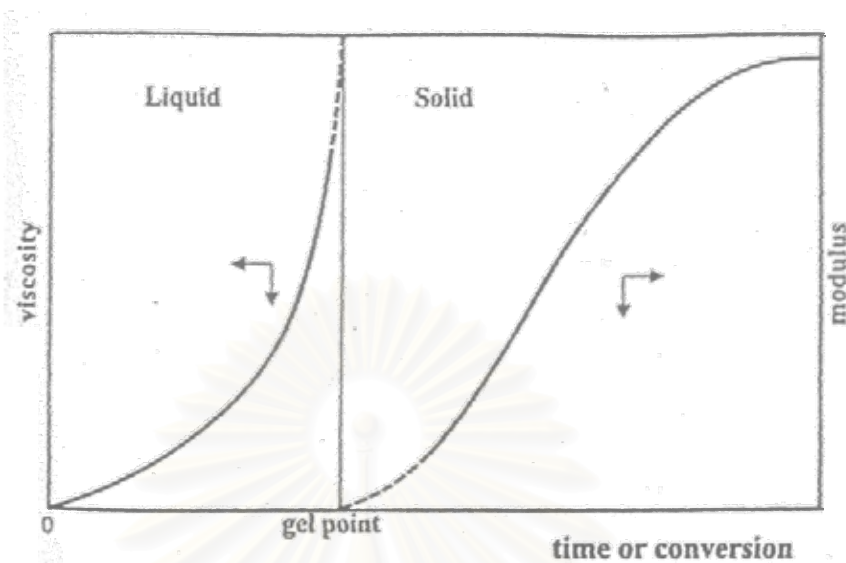


Figure 2.2 Steady-state mechanical properties of a thermoset as a function of reaction time or conversion. Representative properties are the steady shear viscosity for the liquid state and the equilibrium modulus for the solid state.

Accurate measurement of the equilibrium modulus is extremely difficult because its value remains below the detection limit for a considerable time and, theoretically, and infinite time is required to perform the measurement.

Steady shear viscosity measurements are very simple and are often used in practice. Very often a viscosity of 10^3 Pa.s is arbitrarily identified with the gel point. But the determined gelation time, T_{gel} , depends on the shear rate, and extrapolation to zero shear rate meets the following difficulties:

- (a) T_{gel} may depend on the shear rate due to shear thinning at high rates.
- (b) The network structure near the gel point is very fragile and can be taken by the shear flow experiment.
- (c) Infinite viscosity is not an unambiguous indicator of gelation: it can equally be caused by vitrification. This means that complementary methods, such as sol fraction measurements, are necessary to distinguish between both phenomena.

For all these reasons, steady-state mechanical measurements, even if they are very simple and very often used in practice, lead to an apparent gel point.

2.4.2 Dynamic mechanical measurements

2.4.2.1 Criterion for gelation

The evolution of the dynamic viscosity $\eta^*(\omega, x)$ or of the dynamic shear complex modulus $G^*(\omega, x)$ as a function of conversion, x , can be followed by dynamic mechanical measurement using oscillatory shear deformation between two parallel plates at constant angular frequency, $\omega = 2\pi f$ (f = frequency in Hz). In addition, the frequency sweep at certain time intervals during a slow reaction ($x \sim \text{constant}$) allows determination of the frequency dependence of elastic quantities at the particular conversion. During such experiments, storage $G'(\omega)$, and loss $G''(\omega)$ shear modulus and their ratio, the loss factor $\tan\delta(\omega)$, are obtained:

$$G^*(\omega) = G'(\omega) + iG''(\omega) \quad (2.21)$$

$$\tan \delta = G''/G' \quad (2.22)$$

Typical rheological curves obtained during a diepoxy-diamine reaction are shown in Figure 2.3. The cure temperature ($T_i = 90^\circ\text{C}$) is well above the glass transition temperature of the fully cured network ($T_{g\infty} = 35^\circ\text{C}$) which means that only gelation occurs. Three typical regions are observed during cure.

- (a) The pregel region is characterized by an increase in the loss modulus, G'' , corresponding to the increase of the real part of dynamic viscosity $\eta' = (G')\omega$, due to the increasing molar mass of the thermosetting polymer. The storage modulus, G' , is very low and tends to zero at low frequencies. In this region the loss modulus, G'' , is higher than the elastic modulus (G'), and the loss factor, $\tan \delta > 1$
- (b) The “critical region” begins with a sudden increase in the storage modulus (G') by several orders of magnitude. At the intersection of the $G'(t)$ and $G''(t)$ curves, $\tan \delta = 1$. After the intersection point. G' becomes higher and $\tan \delta$ becomes less than 1

The viscous properties are dominant in the liquid state, i.e., $G'' > G'$ and $\tan \delta > 1$, While the elastic properties predominate in the solid state, where $G' > G''$ and $\tan \delta < 1$. For this reason, the G' - G'' crossover ($\tan \delta = 1$) was firstly identified as the gel point [37]. The problem is that when a reaction like the one represented in Figure 2.3 is followed at

different angular frequencies, it is found that the reaction time to reach $\tan \delta = 1$ increases with angular frequency. As the gel point is a material constant and should not depend on experimental conditions, the crossover point between $G'(t)$ and $G''(t)$ cannot correspond to gelation.

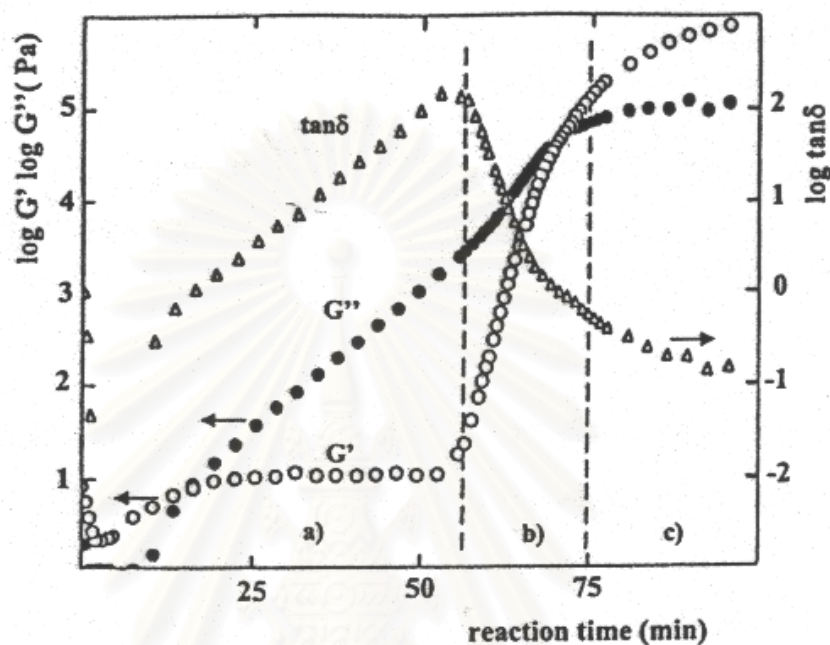


Figure 2.3 Evolution of the storage modulus, G' , loss modulus, G'' , and loss factor, $\tan \delta$, during the reaction of pure diglycidyl ether of bisphenol A (DGEBA) with poly(oxypropylene) diamine (PPO) [35].

The value of $\tan \delta$ decreases in the (b) region and the rate of this decreased depends on the angular frequency, ω shown in Figure 2.4. As a rough approximation:

- (1) As $G' \sim \omega^2$ and $G'' \sim \omega$, $\tan \delta \sim 1/\omega$ in the Newtonian liquid state.
- (2) In the solid state $G' \sim \text{constant}$ and $G'' \sim \omega$, thus, $\tan \delta \sim \omega$.

Therefore, the drop of $\tan \delta$ during the reaction is steeper at low angular frequencies. Figure 2.4 reveals that for a particular $\tan \delta$ value higher than 1 ($\tan \delta \sim 2$ in the case of Figure 2.4), the time to reach the value is independent of frequencies in the 0.1-50 Hz range. This crossover of the $\tan \delta$ curves at various frequencies can be used as a criterium for the identification of the gel point.

- (c) Finally, in the postgel region, a slow increase in G' , that levels off in the final stages of the reaction is observed; $\tan \delta < 1$ for the fully cured rubbery network

($T_i > T_{g\infty}$). Additional experiments show that the stoichiometric mixture has the highest final modulus and the lowest final loss factor ($\tan \delta$) because it forms the most perfect network, with the highest crosslink density.

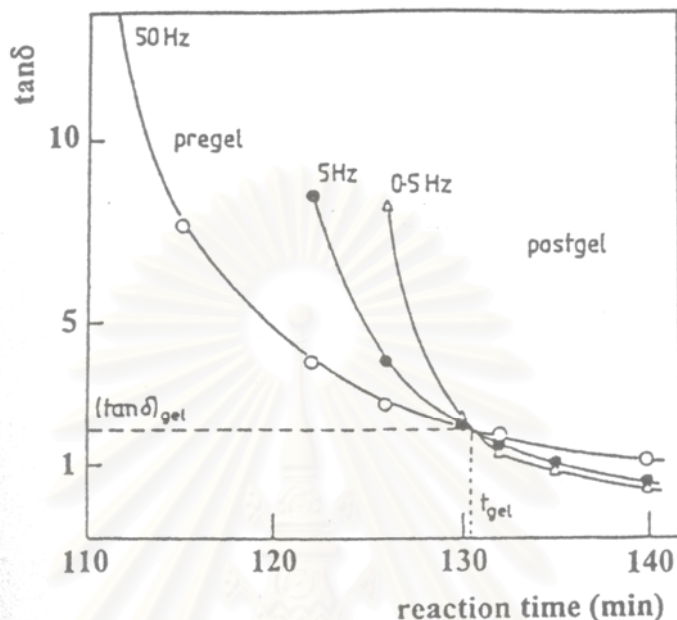


Figure 2.4 Decrease in the loss factor ($\tan \delta$) during cure, for the same epoxy-diamine system as that represented in Figure 2.3, at different frequencies of the dynamic measurement, $T_i = 70^\circ\text{C}$ [35].

2.4.2.2 Singular power laws at the gel point

The frequency dependence of dynamic mechanical results is of primary importance for the interpretation of data. The dependence of G' and G'' versus ω can be evaluated from experiments. Chambon and Winter [38] first revealed that the $G'(\omega)$ and $G''(\omega)$ curves, in logarithmic scales, were parallel over a wide range of angular frequencies at the gel point. The validity of a power law

$$G'(\omega) \sim G''(\omega) \sim \omega^n \quad (2.23)$$

As a consequence, $\tan \delta = G'/G'' = \tan(n\pi/2)$ is frequency independent. By knowing the value of $\tan \delta$ at the gel point, the viscoelastic exponent or the relaxation exponent, n , can also be directly determined. The values of n lie mainly in the range of

0.4-0.8 and were found to be dependent on thermal history and concentration of the sol fraction.

2.5 Wood composites

A composite material can be defined as a macroscopic combination of two or more distinct materials, having a recognizable interface between them and the combination brings about new desirable properties, have many advantages over synthetic polymers and copolymers such as less density, reinforcement of the resin resulting in increased mechanical properties and size stability [39]. The term wood-plastic composites usually consist of polymer matrix, reinforcing material, and additives. For the polymer matrix, thermosetting polymers i.e., phenolic and epoxy resins are widely used because of their good heat resistance, low flammability and low smoke generation. Recently, filler particles i.e. woodflour are often incorporated into a polymer to modify properties to meet performance requirement. Woodflour has several advantages compared to inorganic filler, including low cost per volume basis, low density, high specific strength, high specific modulus, nonabrasiveness that shows flexibility during the processing with no harm to the equipment, renewable nature and the utilization of waste materials [40].

2.5.1 Wood chemistry [41]

The chemical components of wood strongly influence the characteristics, properties and opportunities for use of this complex natural composite. The major components of natural fibres are cellulose, hemicellulose, and lignin. Cellulose is the chief component of the cell wall in plants and some protists; an insoluble complex carbohydrate formed of microfibrils of linear chains of glucose molecules (a common six-carbon sugar; $C_6H_{12}O_6$) which are the most common monosaccharide attached end to end in most organisms. Cellulose contributes its high tensile strength to the complex of wood structure. Generally, the fibers contain 60 to 80% of cellulose. Hemicellulose, that the mass fraction is of the order 5 to 20%, is a polysaccharide of branched chains of various sugars, more soluble and less ordered than cellulose; found particularly in cell walls and lignin is one of the most important constituents of the secondary wall of vascular plants, although not all secondary walls contain lignin; after cellulose, lignin called the cementing agent that binds individual cell together is the most abundant plant polymer. Their chief monomer units are various ring-substituted phenylpropanes linked together in

ways. The lignin is thermally stable but is responsible for the UV degradation. Composition of lignin in wood contains about of 2 to 15%.

2.5.2 Characterization of woodflour [42]

Woodflour is finely divided ground wood having a flour-like appearance. Bulk density of woodflour is typically around 0.1-0.3 g/cm³. Aspect ratio of woodflour (length to thickness of fibers) is typically between 3:1 and 5:1. Specific gravity (density) of wood is about 1.3-1.4 g/cm³. When ashed (commonly at temperatures between 525 and 575°C), wood often leaves 0.25-0.50% of mineral residues. For example, ashing of Trex boards, containing reportedly 50% of woodflour, produced 0.55±0.02% of ash. In addition, woodflour and sawdust do not melt but rather decompose above 190°C. This is, again, due to a more susceptible to temperature lignin and hemicellulosics, and because pure cellulose decomposed above 240°C.

2.5.3 Mechanical properties [33]

While many different mechanical properties may be measured for polymer composites, the description of the mechanical behavior is afforded by the Young's modulus, E , and yield stress, σ_y . The mechanical properties of composites are strongly influenced by the size, type, concentration, and dispersion of filler, as well as the extent of interfacial adhesion between the filler and matrix (i.e., continuous phase) and the properties of the matrix. The interrelationships between these variables are complex and only basic principles relating these parameters to the mechanical properties and ultimate performance of particular and fiber-reinforced composites are developed.

2.5.3.1 Modulus

The principal function of reinforcing fillers is to increase the modulus of the composite. This is typically accompanied by an increase in the heat-distortion temperature. The modulus of a glassy-polymer composite containing a rigid particulate filler may be estimated by use of the use of the modified *Halpin-Tsai* equation given as

$$\frac{M}{M_m} = \frac{1 + AB\phi_f}{1 - B\psi\phi_f} \quad (2.24)$$

where M is the modulus (tensile, shear, or bulk) of the composite, M_m is the corresponding modulus of the unreinforced matrix polymer, A is a constant that depends on the filler geometry and the Poisson's ratio of the matrix, ϕ_f is the volume fraction of filler, ψ depends upon the maximum packing volume fraction of the filler (0.601 for random loose packing of spheres), and B is a function of A and the relative moduli of the filler (M_f) and matrix as

$$B = \frac{(M_f/M_m) - 1}{(M_f/M_m) + A} \quad (2.25)$$

If the particulate filler is uniformly dispersed, the mechanical properties of a particulate-filled composite are independent of the testing direction (i.e., isotropic). By comparison, the properties of fiber-reinforced composites are dependent upon the direction of measurement—they are *anisotropic*. This is because fibers are usually uniaxially oriented or oriented randomly in a plane during the fabrication of the composite.

2.5.3.2 Strength

In general, composite strength, and ultimate property, depends upon many factors, such as the adhesive strength of the matrix-filler interphase, and therefore, is not as easily modeled as is modulus. Interfacial strength may be reduced by the presence of water adsorbed on the filler surface or by thermal stresses resulting from a mismatch between the thermal coefficients of linear expansion for the filler and matrix polymer. Polymers have relatively high linear-expansion coefficients (60 to 80×10^{-6} per °C for polystyrene) compared to fillers such as silica glass (0.6×10^{-6} per °C) or graphite (7.8×10^{-6} per °C).

Several relationships have been proposed to relate the ultimate strength of a particulate-filled composite (σ_u) to the ultimate strength of the unfilled matrix (σ_m). One such equation proposed by Schrage [43] is given as

$$\sigma_u = \sigma_m \exp(-r\phi_f) \quad (2.26)$$

where r is an interfacial factor (typically 2.66 for many composites). This provides a maximum value for strength (up to 35 to 40vol% filler) and assumes good adhesion

between the dispersed filler and matrix. Strength of the composite will decrease with decreasing interfacial strength.

2.6 Types of thermosetting polymers

During the past decades, thermosetting polymers are well established in areas where thermoplastics cannot compete because of either properties or costs. For example, phenolics constitute a first option when fire resistance is required because they are self-extinguishing and exhibit low smoke emission. Urea-formaldehyde polymers for wood agglomerates and melamine-formaldehyde for furniture coatings give products of good quality at low costs. Unsaturated polyesters are extensively used to produce structural part with a glass-fiber reinforcement. In addition, epoxies, cyanate, esters, and polyimide are employed for aeronautical and electronic applications where their excellent properties cannot be matched by thermoplastics. In recent years, a newly developed thermosetting resin with interesting properties, polybenzoxazine, was investigated [1,6-11].

2.6.1 Benzoxazine resins

A new type of addition-cure phenolic system, polybenzoxazine, has recently been developed. They have gained immense interest because they have the capability to exhibit the thermal and flame retardance properties of phenolics along with mechanical performance and molecular design flexibility. Although benzoxazines were first synthesized by Cope and Holy in 1940s [44], the potential of polybenzoxazines has been recognized only recently [45]. The molecular structure of polybenzoxazines offers enormous design flexibility, which allows the properties of the cured material to be tailored for a wide range of applications. These newly developed resins possess unique features, namely (i) near-zero volumetric change upon curing, (ii) low water absorption, (iii) for some polybenzoxazine based materials T_g much higher than cure temperature, (iv) high char yield, (v) no strong acid catalysts required for curing, and (vi) release of no by-products (even non-toxic) during curing [2,46].

2.6.1.1 Chemical methodologies for synthesis of benzoxazine monomers

Benzoxazine monomers are typically synthesized using phenol, formaldehyde and amine (aliphatic or aromatic) as starting materials either by employing solution or solventless methods. Various types of benzoxazine monomer can be synthesized using

various phenols and amines with different substitution groups attached. These substituting groups can provide additional polymerizable sites and also affect the curing process. Consequently, polymeric materials with desired properties may be obtained by tailoring the benzoxazine monomer.

A. Mono-functional benzoxazine monomers

Holly and Cope [44] first reported the condensation reaction of primary amines with formaldehyde and substituted phenols for the synthesis of well defined benzoxazine monomers. According to the reported procedure, this reaction was performed in a solvent in two-steps. Later, Burke et al. found that the benzoxazine ring reacts preferentially with the free *ortho* positions of a phenolic compound and forms a Mannich bridge [47]. The synthetic procedure of the Mannich condensation for benzoxazine synthesis in a solvent proceeds by first addition of amine to formaldehyde at lower temperatures to form an *N,N*-dihydroxymethylamine derivative, which then reacts with the labile hydrogen of the hydroxyl group and *ortho* position of the phenol at the elevated temperature to form the oxazine ring [48] as shown in Figure 2.5 and Figure 2.6

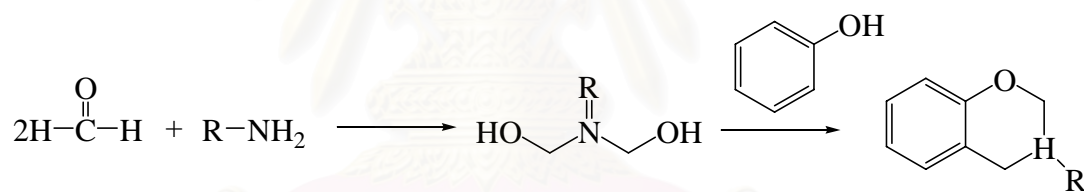


Figure 2.5 Synthesis of phenol based benzoxazine monomer.

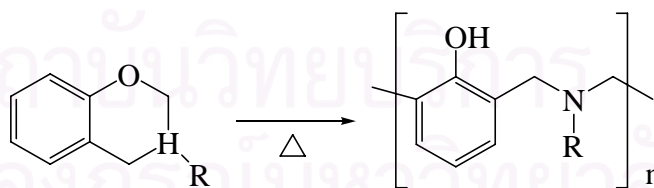


Figure 2.6 Ring-opening polymerization of the phenol based benzoxazine monomer.

The mono-functional benzoxazine monomers are liquid at room temperature and can potentially be developed into high-performance polybenzoxazines, which are of interest for some applications, such as coatings and highly filled compounds. In previous research on polybenzoxazine composites for electronic packaging applications, the addition of a low-

viscosity reactive diluent other than the solid benzoxazine matrix was helpful to balance the steep increase of the viscosity as the filler loading was increased [49]. With considerable molecular mobility, liquid benzoxazines can possibly be polymerized faster than their solid counterparts with the help of appropriate initiators/catalysts. The mono-functional benzoxazine monomer was used in this research shown in below

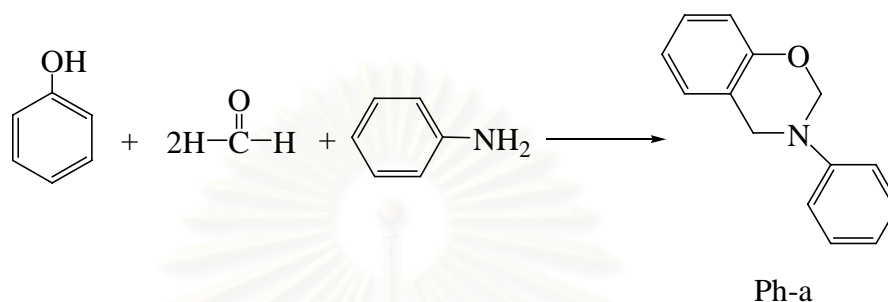


Figure 2.7 Synthesis of phenol-aniline type benzoxazine monomer.

B. Di-functional and multifunctional benzoxazine monomers

Curing of mono-functional benzoxazines with resulted in the formation of only oligomeric structures. Thus, no materials could be made from this approach since the thermal dissociation of the monomer competed with chain propagation reaction so that high-molecular weight linear structures were unobtainable. Actually, there is no convincing evidence reported for the thermal dissociation theory. Moreover, Hemvichian et al. [50] have reported that the reduction of reactivity is due to hydrogen bonding formation. Such a phenomenon was observed in the temperature range below that for which reverse Mannich reaction occurs in benzoxazine chemistry. To overcome this limitation, in recent years, Ishida et al. [51] have developed a new class of difunctional or multifunctional benzoxazine monomers, and their curing into phenolic materials with the ring opening reactions being initiated by dimers and higher oligomers in the resin composition. A series of difunctional benzoxazine monomer based upon alkyl-substituted arylamines with useful mechanical and thermal properties were investigated. These benzoxazine monomers were synthesized from bisphenol-A, paraformaldehyde, and a series of aromatic amines such as aniline, m-toluidine, and 3,5-xylidine with a solventless method [4]. The structure of bisphenol A-aniline type of difunctional benzoxazine monomer was shown in Figure 2.8

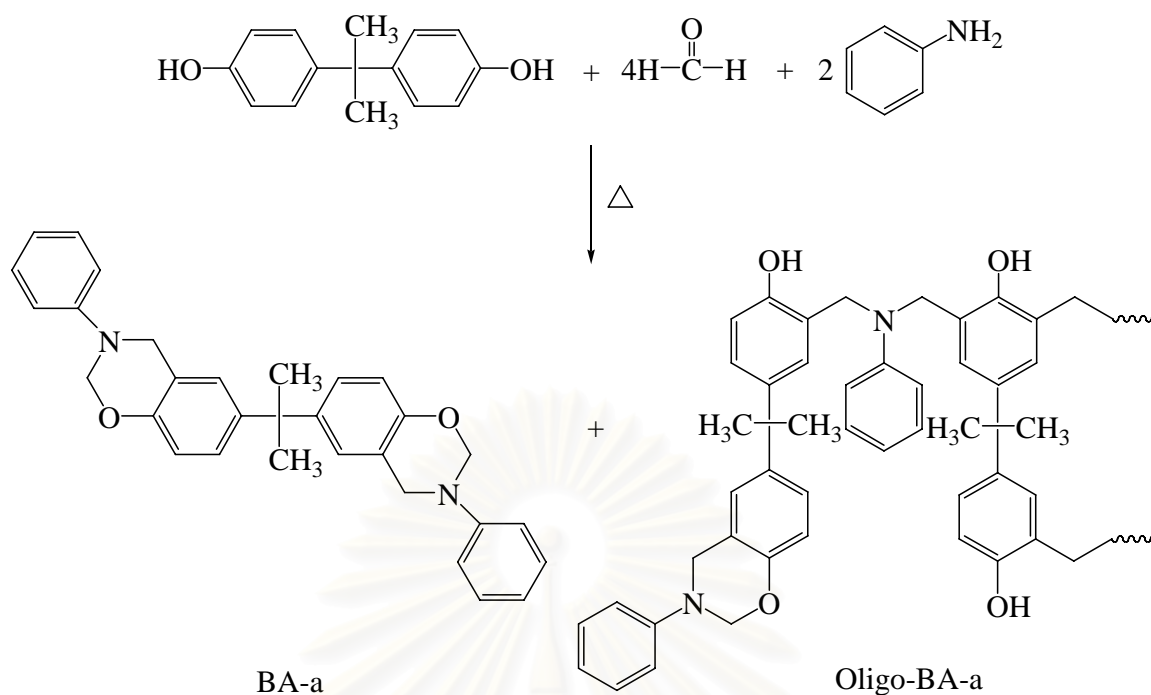
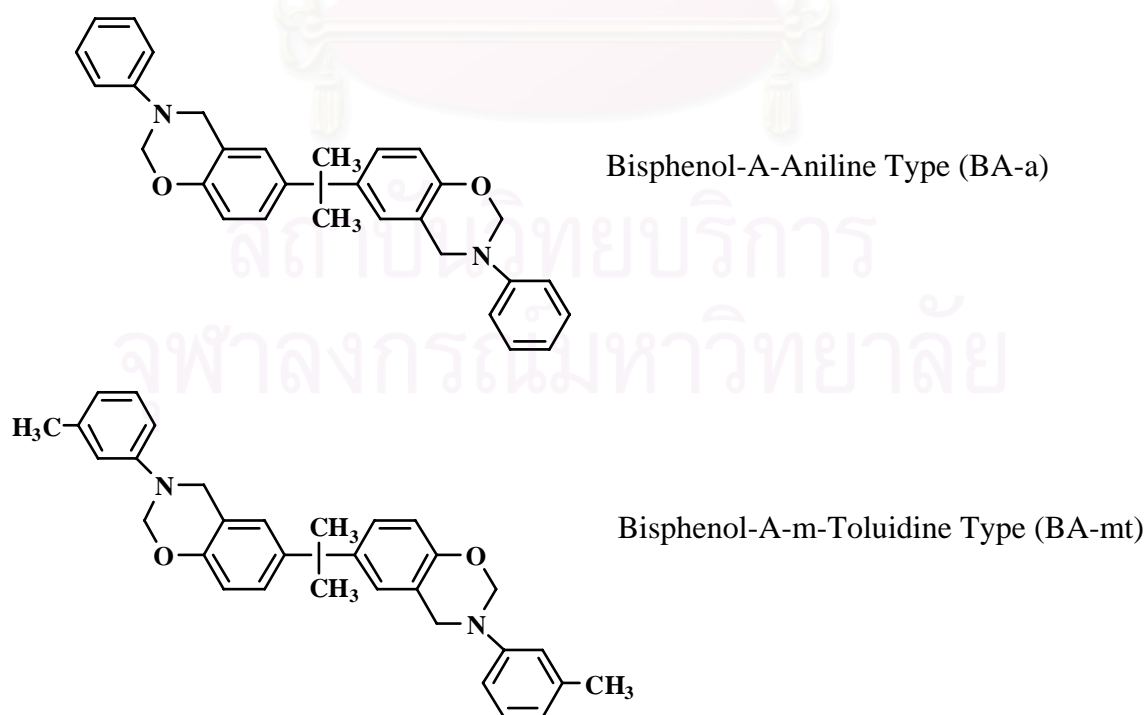


Figure 2.8 Synthesis of bisphenol A and aniline based benzoxazine (BA-a) monomer.

C. Structures of benzoxazine monomers

A series of difunctional benzoxazine monomer based upon alkyl-substituted arylamines were developed [51] as shown in Figure 2.9



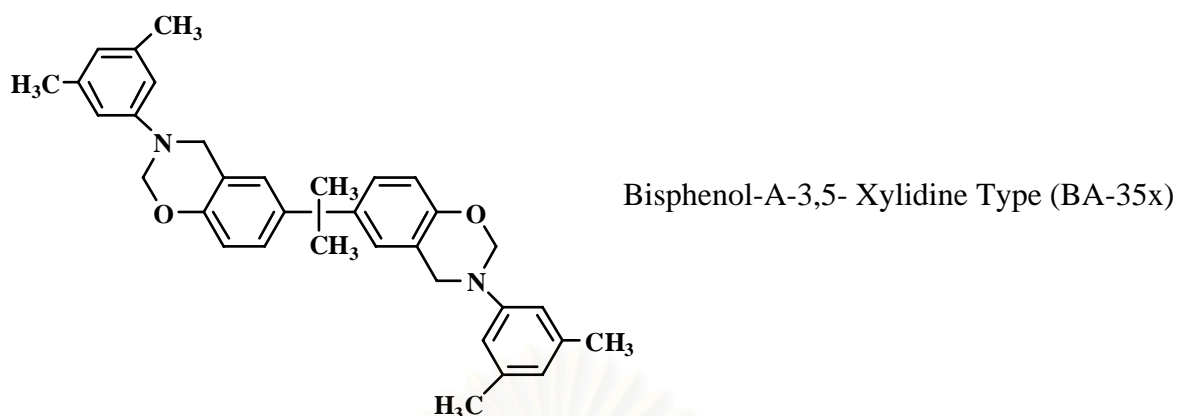
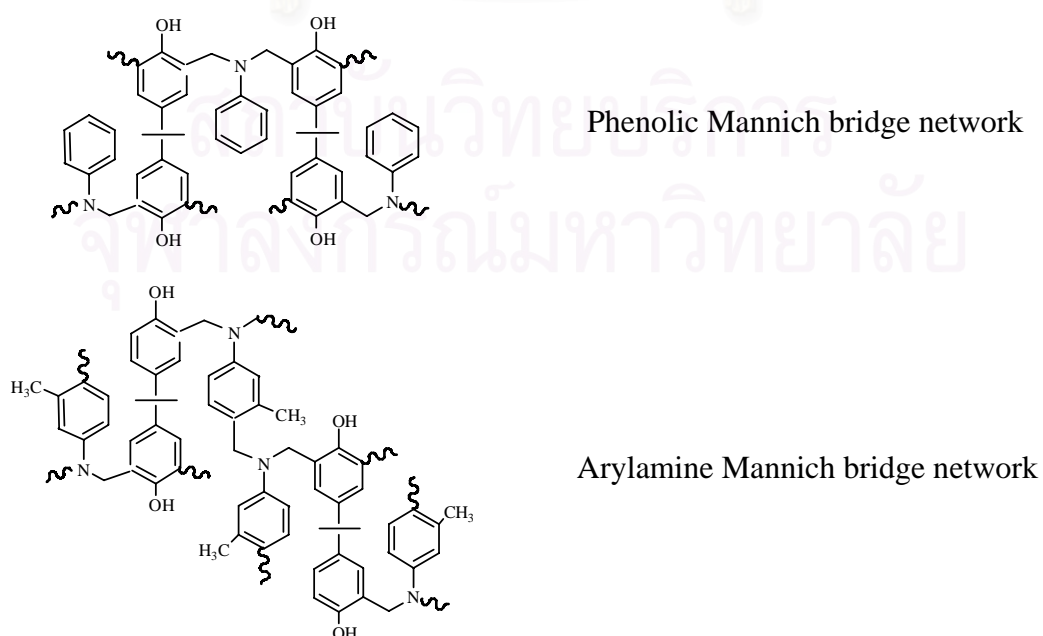
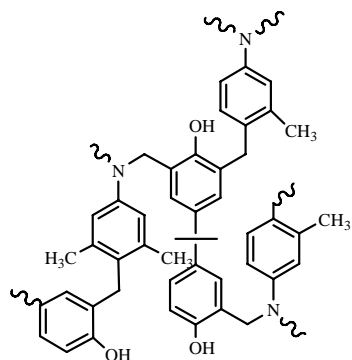


Figure 2.9 Arylamine-based benzoxazine monomers.

D. Properties of polybenzoxazines

As mentioned above, polybenzoxazine has been developed as a new class of phenolic resins with a wide range of mechanical and physical properties that can be tailored to various needs. Several works have examined what the crosslinked structure of polybenzoxazine may be more study is needed to fully understand the crosslinking mechanism of the aromatic amine-based polybenzoxazine. In addition, the effect of the various types and amounts of crosslinking on the thermal and mechanical properties of the polymerized networks has been reported [52]. From the results, different network structures of crosslink, i.e. phenolic Mannich bridges, arylamine Mannich bridges, and methylene bridges as shown in Figure 2.10 have effect on thermal property.





Arylamine Methylene bridge network

Figure 2.10 Network structure of the arylamine-based polybenzoxazines.

The results have been reported that the thermal stability (as determined by the 5% weight loss temperature) shown by BA-mt and BA-35x is the highest thermal stability achieved from neat benzoxazine chemistry based on Bisphenol-A and unfunctionalized aniline derivatives due to arylamine Mannich bridge and methylene linked structure could form. The aromatic carbon-nitrogen bond being significantly stiffened by resonance and the absence of one of the methylene hinges in the Mannich bridge; therefore: this arylamine Mannich bridge should be significantly more rigid, resulting in a higher glass transition temperature at the same extent of conversion. The properties of the polybenzoxazines have been reported as shown in Table 2.1

Table 2.1 Thermal and mechanical properties of the polybenzoxazines

Properties	BA-a	BA-mt	BA-35x
Tg (°C)	168	209	238
Char yield (% at 800 °C)	30	31	28
Temperature-1% weight loss (°C)	276	300	318
Temperature-5% weight loss (°C)	315	350	350
Storage modulus at 28 (GPa)	1.39	1.78	1.63
Loss modulus at 28 (MPa)	15.7	35.8	25.9
Storage modulus at rubbery plateau (MPa)	4.4 at 225 °C	11.9 at 265 °C	13.6 at 285 °C
Molecular weight between crosslinks (rubber elasticity)	1300	500	430
Crosslink density (mol/cm ³)*10 ⁻³ (Nielsen's equation)	1.1	1.9	2.6
Density @ 27.5 (g/cm ³)	1.33	1.32	1.26

2.6.2 Epoxy resin [32,53]

Epoxy resins are characterized by a three-membered ring known as the epoxy, epoxide, oxirane, or ethoxyline group.

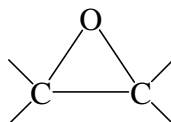


Figure 2.11 Oxirane ring found in common epoxy resins.

Commercial epoxy resins contain aliphatic, cycloaliphatic, or aromatic backbones. The capability of the epoxy ring to react with a variety of substrates imparts versatility to the resins. Treatment with curing agents gives insoluble and intractable thermoset polymers. In order to facilitate processing and modify cured properties, other constituents may be included in the compositions: fillers, solvents, diluents, plasticizers, and accelerators.

A. Chemistry of preparation and curing

The epoxy resin used most widely is made by condensing epichlorohydrin with bisphenol A, diphenylol propane. An excess of epichlorohydrin is used, to leave epoxy groups on each end of the low molecular-weight polymer. Depending on molecular weight, the epoxy resin is a viscous liquid or a brittle high-melting solid. The formation of the crude diglycidyl ether of bisphenol shown in Figure 2.12. From the reaction, DGEBA is obtained by reacting epichlorohydrin with bisphenol A in the presence of sodium hydroxide. The reaction takes place in two steps; they are the formation of a chlorohydrin intermediate and the dehydrohalogenation of the intermediate to the diglycidyl ether, respectively. Each molecule of the diglycidyl ether will react with that of the bisphenol A at the epoxide group, forming eventually the higher molecular weight DGEBPA.

and strength with outstanding adhesive properties to various types of surface. In addition, epoxy resin has wide range of curing temperature, low shrinkage, outstanding corrosion resistance, and relatively low water absorption; however, they are rather flammable materials and possess rather low thermal stability compared to phenolic resin.

2.6.3 Phenolic resin [12]

A. Reactions of phenol and formaldehyde

Phenols react with aldehydes to give condensation products of there are free positions on the benzene ring ortho and para to the hydroxyl group. Formaldehyde is by far the most reactive aldehyde and is used almost exclusively in commercial production. The reaction is always catalyzed, either by acids or by bases. The nature of the product is greatly dependent on the type of catalyst and the mole ratio of the reactants.

The two most common types of phenolic resins are resols and novolacs. The reaction mechanism to form the prepolymers is controlled by the pH and the reactant ratio of phenol to formaldehyde. In strongly acidic conditions with an excess of phenol, novolacs are formed; whereas, in basic conditions with an excess of formaldehyde, resols are formed. Phenolic novolacs are soluble and fusible, and require an external curing agent, such as hexamethylenetetramine (HMTA), to form the phenolic network. On the other hand, resols will crosslink with heat to form insoluble, infusible networks [54]. In this study, the phenolic novolac resin is used to form polymer alloys with the benzoxazine resin. The resin contains no reactive methylol groups in its molecule. Therefore, it is, upon heating, unable to be cured by itself to form a crosslinked resin. In order to cure phenolic novolac, a curing agent must be added. The molecular structure of the phenolic novolac is shown in Figure 2.13

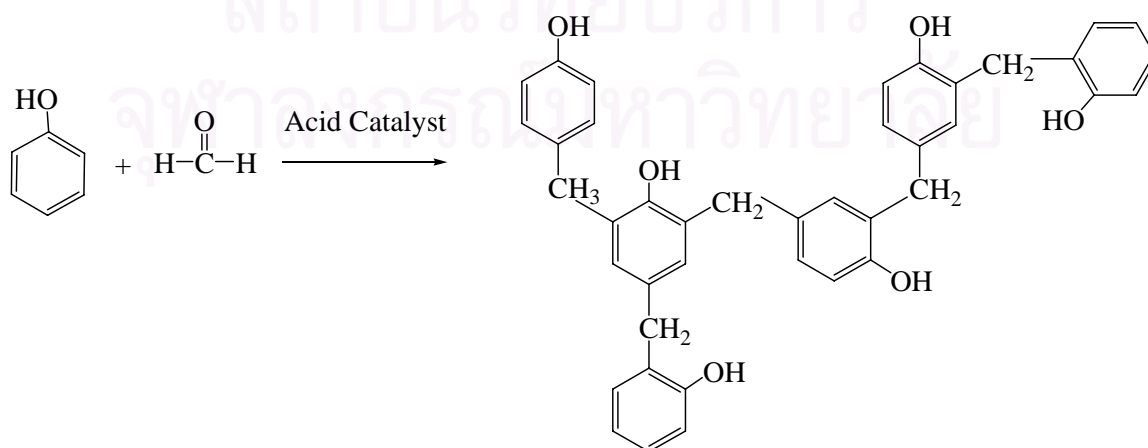


Figure 2.13 Preparation and molecular structure of phenolic novolac resin.

C. Properties and applications

Phenolic resins, both novolacs and resoles, are widely used commercially due to their excellent flame retardant, high char yield, dimensional stability, high temperature resistance, and low cost. Phenolics have a broad range of applications varying from construction to electronics and aerospace. Commercial novolac resins are normally cured with curing agent to form networks with relatively high crosslink densities and very brittle behavior. In addition, phenolic moulding compounds are invariably filled with reinforcing fillers such as woodflour, wollastonite, mica, mineral wool flour and glass fiber. Curing phenolic resins with curing agent; however, produces volatile by-products, which commonly lead to voids in the materials. This makes negative feature in forming phenolic matrix composites because the high void content results in brittle components. In addition, void, itself, can act as a stress concentrator to the specimen and form a weak point in the material. Therefore, current commercial novolacs are limited to applications where high strength is not a requirement. The advantages of using phenolic novolac resin as wood binder are their known high compatibility with wood, high char yield, no toxic by products from burning, and its low cost. The addition of phenolic resin can sometimes significantly enhance fire resistant properties of the base polymers it is with incorporated.

CHAPTER III

LITERATURE REVIEWS

As aforementioned in chapter I, a class of thermosetting polybenzoxazine materials has been developed that overcomes many of the deficiencies commonly associated with novolac and resole-type phenolic resins, while retaining their beneficial thermal, flame retardant, and dielectric characteristics. These new polybenzoxazines have shown a mechanical and thermal performance that exceeds many epoxy resins, as well as conventional phenolics. In addition to excellent water absorption and dielectric characteristics, these novel phenolic resins appear to polymerize with almost no volumetric shrinkage [55].

As with any new resin, many parameters must be established before the material may be properly processed. The understanding of thermosetting resins, such as the polybenzoxazines, is complicated by the fact that they are reactive systems with continuously changing properties. Ishida and Rodriguez [6] studied the curing reactions of benzoxazine precursors based on bisphenol A and aniline (BA-a). This new type of phenolic material cures via a ring-opening mechanism that does not produce any condensation or other reaction by-products. According to differential scanning calorimetry (DSC), the benzoxazine precursor is an autocatalytic-type curing mechanism. The Kissinger and Ozawa models proposed for the curing reaction is valid for the early stages of cure, prior to diffusion control. The activation energy is between 102 and 116 kJ/mol with an overall order of reaction of approximately 2. In addition, the curing of the benzoxazine precursors with catalysts can effectively decrease the induction time for curing and increase the reaction rate. The activation energy values were reported to be 99-107 kJ/mol [7]. The phenol moiety of the ring-opened benzoxazine monomers was reported to have a catalytic effect on the curing reaction, i.e. reducing a reaction induction time and increasing reaction rate. Weak acids such as adipic acid and sebacic acid can also be effectively used as catalysts for benzoxazine resin. The kinetic analysis of other systems of benzoxazine resins such as random co-polybenzoxazine of BA-a type and P-a type benzoxazines has also been reported [55]. The isothermal curing process of the co-polybenzoxazine precursor involves an autocatalytic-type curing mechanism. In the dynamic DSC experiments, the activation energy was found to be 72 kJ/mol based on the Kissinger method and 84 kJ/mol using the Flynn–Wall–Ozawa

method. Furthermore, in the isothermal experiments, the activation energy was reported to be 50 kJ/mol based on the Kamal method, whereas the total order of reaction is between 2.66 and 3.03, depending on the isothermal curing temperature.

Moreover, benzoxazine has been reported capability to be alloyed with various existing resin systems. As some types of bifunctional benzoxazine resins are solid at room temperature. Some studies had been done to utilize a reactive diluent to lower the liquefying temperature as well as to further reduce the melt viscosity of the as-synthesized benzoxazine resins for processability purposes. Rimdusit and Ishida [8] investigated the gelation behaviors of low melt viscosity ternary systems of benzoxazine, epoxy, and phenolic resins and analyzed by Fourier transform mechanical spectroscopy technique in order to study the effect of epoxy diluent on the rheological property. They found that epoxy diluent can be added in the ternary systems to reduce the liquefying temperature of the uncured resins, besides its major function as a diluent in the molten state of the mixture. The blend renders homogeneous and void-free cured specimens with an outstanding characteristic. Low melt viscosity with suitable period of time was achieved e.g. 0.3 Pa.s constant up to 1000 seconds at 100°C. The gel time at 140°C ranges from 5 min to 30 min and less than 5 min at 180°C which is suitable to the “B-stage” time. The gelation process of these systems shows single activation energy up to their ultimate glass transition temperature signifying single thermal event involved. Furthermore, it will prolong the gel time of the ternary systems without changing their activation energy.

As alloy ability of polybenzoxazine, Ishida and Allen [9] reported that the addition of liquid epoxy (EPON825) to the polybenzoxazine network greatly increased the crosslink density of the thermosetting matrix and strongly influenced its mechanical properties besides its obvious ability to lower the liquefying temperature of the resin mixtures. Copolymerization leads to a significant increase in the glass transition temperature. Reaction of DGEBA with bisphenol A-aniline based benzoxazine (BA-a) increased the glass transition temperature (T_g) of the latter from about 143 to about 153°C for an epoxy content of 35% by weight. Further increase in epoxy decreases T_g to below that of pure polybenzoxazine. The copolymer also showed improvement in flexural strain at break and flexural strength. The flexural strength increased from 125 to 170 MPa on enhancing the epoxy content to 50% by weight. Kimura et al. [56] reported the similar binary systems. The curing reaction

proceeded without any accelerator. Molding compound showed good thermal stability under 150°C, this corresponds to the injection molding temperature. Above 150°C, the curing reaction proceeded rapidly. The cured epoxy resin showed good heat resistance, water resistance, electrical insulation, and mechanical properties compared with the epoxy resin cured by the bisphenol-A type novolac. Moreover, Rimdusit et al. [57] showed that the toughness of the alloys of rigid polybenzoxazine and flexible epoxy diluent (EPO732) systematically increased with the amount of the epoxy due to the addition of more flexible molecular segments in the polymer hybrids. Although a significant reduction in viscosity and liquefying point was expectedly obtained using the epoxy, the resulting benzoxazine-epoxy resin mixtures required higher curing temperatures than that of the neat benzoxazine resin. The addition of a small fraction of phenolic novolac resin as an initiator into the benzoxazine-epoxy mixtures was reported to be necessary to help lowering their curing temperature [10,47]

Recently, Rimdusit and Ishida [58] observed the synergism in the T_g of ternary systems based on benzoxazine, epoxy, and phenolic resins. The systems showed the maximum T_g up to about 180°C in mass ratio of benzoxazine 50%, epoxy 40%, and phenolic resin 10%. The addition of amount of a small fraction of phenolic resin enhanced the crosslink density and, therefore, the T_g in the copolymers of benzoxazine and epoxy resins. To obtain the ultimate T_g in the ternary systems, 6-10% by weight of phenolic resin is needed. The molecular rigidity from benzoxazine and the improved crosslink density from epoxy contribute to the synergistic behavior. In addition, the ternary mixtures were found to have a wide range of desirable properties. The benzoxazine imparts to a combination of good thermal curability, high mechanical properties, and low water uptake. The epoxy reactant provides improved crosslink density, low melt viscosity, flexibility, and possibly enhanced adhesion to polar substrates. The phenolic provides a lower polymerization temperature for the benzoxazine monomer and improved thermal stability for the epoxy component. The fully cured polymer mixtures show a glass transition temperature as high as 170°C, relatively high degradation temperature, reported at 5% weight loss, i.e. up to 370°C. The char yield of the ternary systems increase significantly compared with the pure epoxy resin. That is due to the fact that both polybenzoxazine and phenolic novolac are known to give higher char yield compared with epoxy resin. The tendency for benzoxazines and phenolic resins not to support

flame propagation makes the ternary blend a desirable material in applications where flammability is to be avoided such as interior parts [10].

High performance composite properties are attributed to the ability of the low viscosity benzoxazine resin (BA-a) to accommodate very high filler loading. Highly filled wood composites made from polybenzoxazine and woodflour were developed [59]. The relatively low melt viscosity of the resin enabled the incorporation of a large amount of woodflour up to 75% by weight at its maximum packing. The outstanding compatibility between the woodflour filler and the polybenzoxazine matrix was evidenced by a increase in the glass transition temperature when compared with that of neat polybenzoxazine, a substantial reduction in water uptake as the amount of the matrix increased, and substantial interfacial interactions as revealed by scanning electron micrographs. Moreover, a relatively high flexural modulus of 7.3 GPa and flexural strength as high as 75 MPa were achieved in these highly filled system. In addition, the utilization of benzoxazine-phenolic novolac alloys as a wood composite matrix is investigated [60]. The results showed that the incorporation of phenolic novolac into benzoxazine resin can reduce the curing temperature of benzoxazine resin and enhancing the fire resistant characteristics of the resulting alloys. The limiting oxygen indices (LOIs) of all desirable content of the benzoxazine-phenolic novolac alloys were above the self-extinguishable limit i.e. > 26 . In addition, the LOI values were found to moderately increase whereas the rate of burning decreased with increasing the phenolic novolac and high woodflour content at 70% by weight can be incorporated into the alloy to yield good processing ability and high performance wood composite systems with relatively high flame retardant characteristics.

CHAPTER IV

EXPERIMENTAL

4.1 Materials

The lists of chemicals used in this research are shown in Table 4.1

Table 4.1 Chemicals used for sample preparation

Chemicals	Grade	Supplier
Bisphenol-A	used to produce PC	Thai Polycarbonate Co., Ltd.
Phenol		Fluka Chemicals Co.
Formaldehyde		Merck Company
Aniline	99%	Fluka Chemicals Co.
3,5-xylydine	98%	Fluka Chemicals Co.

4.2 Resin preparation

4.2.1 Benzoxazine resin

Monofunctional benzoxazine resin used is phenol-aniline type (Ph-a). The resin was synthesized by a solventless procedure [4]. The phenol-aniline-based benzoxazine synthesis is as follows. Phenol, paraformaldehyde, and aniline at a molar ratio of 1:2:1. The as-synthesized Ph-a resin is a clear yellowish liquid at room temperature while bifunctional benzoxazine resins also synthesized by a solventless method, the resins are bisphenol-A-aniline type (BA-a), and bisphenol-A-3,5-xylydine type (BA-35x). The molar ratio of bisphenol-A, para-formaldehyde, and derivative amine was 1:4:2. The benzoxazine resin is solid at the room temperature. It was ground into fine powder and kept in a refrigerator. The resins were obtained as a light yellow powder.

4.2.2 Phenolic novolac resin

Phenolic novolac resin is based on phenol and formaldehyde. In the synthesis process, a phenol 0.1 mol, 37% aqueous formaldehyde 0.084 mol, and oxalic acid 0.001 mol as a catalyst were taken in a container and were then stirred mechanically under constant stirring for 1 hr followed by heating at 100°C for 2 hr and vacuum dried at 100°C. The obtained product is light yellow to orange solid at room temperature.

4.3 Preparation of woodflour

The woodflour from rubberwood (*Hevea brasiliensis*) was selected for this work because of its availability and this wood is widely calciticated in Thailand. The true density of the woodflour determined by a gas pycnometer is 1.49 g/cm³. The particles that pass through a sieve of less than 149 micron were used. The over size wood particle was crushed using ball mill apparatus in order to reduce its particle size. All woodflour was dried at 105°C for 24h in a vacuum oven and was kept in a desiccator.

4.4 Processing method

4.4.1 Curing kinetics of arylamine-based polyfunctional benzoxazine resins by dynamic differential scanning calorimetry

A differential scanning calorimeter (DSC) was employed to study the exothermic curing reactions of arylamine-based polyfunctional benzoxazine resins (BA-a and BA-35x) were investigated using a. The resin mass of about 5 mg was sealed in a nonhermetic aluminum pan with lid. The five different heating rates used were 1, 2, 5, 10, and 20°C/min under a constant flow of nitrogen at 50 ml/min.

4.4.2 Effect of novel benzoxazine reactive diluent on processability and thermo-mechanical characteristics of bi-functional polybenzoxazine

The BA-a/Ph-a polybenzoxazine specimen was prepared by weighing the desired amount of the resin mixture into an aluminum container. The binary systems to be investigated are BP91, BP82, BP73, BP64, BP55, and BP28. In the nomenclature of the

specimens, B stands for the bifunctional BA-a resin whereas P is the monofunctional Ph-a resin. The numbers after the letters are the mass ratio of the two monomers in the respective order. The mixture was mixed mechanically at 80°C for about 15 minutes to obtain a homogeneous mixture and was then poured onto a metal mold. All specimens were cured in an air-circulating oven using the step heating profile to ensure fully cured condition as follows: 100°C for 45 min, 120°C for 45 min, 160°C for 90 min, and 200°C for 120 min.

4.4.3 High performance wood composites based on benzoxazine-epoxy alloys

A. Preparation of benzoxazine-epoxy-phenolic ternary mixtures

Ternary mixtures of benzoxazine, epoxy and phenolic novolac resins (BEP alloys) were prepared by melt-mixing the three resins at temperature about 80°C. The weight ratios of the benzoxazine (B), epoxy (E) and phenolic novolac (P) in the ternary mixtures were 80/10/10 (BEP811), 70/20/10 (BEP721), 60/30/10 (BEP631), 50/40/10 (BEP541), and 40/50/10 (BEP451), respectively.

B. Preparation of wood-BEP alloy composites

Hevea brasiliensis woodflour with particle sizes in the range of 50-150 micron was used in this investigation. The woodflour was dried at 105°C for 24h in a vacuum oven and was then kept in a desiccator at room temperature.

The BEP alloys were compounded with the woodflour content at 70% by weight. The alloy and the woodflour were mixed in an aluminium container at 80°C for at least 15 min to ensure good resin-wood flour wetting. The molding compound was placed in a preheated 3-mm-thick stainless steel mold and compressed at 170°C for 210 min under a hydraulic pressure of 35 MPa. The sample was left to cool to room temperature. The density of each specimen was measured to evaluate the packing of the woodflour with each of the above contents.

4.5 Characterizations

4.5.1 Rheological experiments

Dynamic shear viscosity measurements were performed on a parallel plate rheometer using HAAKE RheoStress model RS600. Disposable aluminum plates having

20mm in diameter were preheated for 30 min with the gap zeroed at the testing temperature. The void-free monomer mixture, which was liquefied at 80°C, was then poured onto the lower plate and the gap was set to 0.5 mm. The temperature was immediately equilibrated at the set point for about 180 s and the test was then started.

Processing window of the resin mixture was determined under an oscillatory shear mode. The sample waveform was obtained by the superposition of mechanical waves with three different frequencies i.e. 1, 3, and 10 rad/s. The testing strain amplitude is maintained at 2.5% for each frequency. The testing temperature program was ramped from room temperature at a heating rate of 2°C/min to a temperature beyond the gel point of each resin and the dynamic viscosity was recorded.

Gel time based on frequency independent of $\tan\delta$ of each mixture was examined. The superposition of mechanical waves was five different frequencies ranging from 1 to 100 rad/s at constant stress of 50 Pa. The gel time is obtained from the point where the loss tangent of different frequencies intersects each other

4.5.2 GPC measurement

Gel permeation chromatography (GPC) analysis was performed at 40°C on a Waters 600 using three Waters Styragel[®] HT columns (Styragel[®] HT 0.5, Styragel[®] HT 1, and Styragel[®] HT 4). Molecular weights are relative to monodisperse polystyrene standards. Samples were prepared by dissolving the resin in tetrahydrofuran (THF) mobile phase at 40°C in order to reach the final concentration of 0.25% (w/v). The detector was Waters 2414 refractive index (RID).

4.5.3 Differential scanning calorimetry

The curing behaviors and thermal transitions of the specimens were measured using a differential scanning calorimeter (DSC) model DSC 2910 from TA Instruments. Specimen mass of about 5-10 mg was sealed in a non-hermetic aluminum pan with lid. The heating rate used was 10°C/min from 30-300°C. The experiment was performed under nitrogen purging.

4.5.4 Density measurement

A density of each specimen was determined by a water displacement method according to ASTM D792-91 (Method A). All specimens were prepared in a rectangular shape (52×25×3 mm³). The average value from at least three specimens was calculated. The density was calculated by the following equation:

$$\rho = \left(\frac{A}{A - B} \right) \times \rho_0$$

where ρ = Density of the specimen (g/cm³)

ρ_0 = Density of the liquid at the given temperature (g/cm³)

A = Weight of the specimen in air (g)

B = Weight of the specimen in liquid (g)

4.5.5 Thermogravimetric analysis

Thermal decomposition characteristic of each specimen was determined using a thermogravimetric analyzer from Perkin Elmer (Diamond TG/DTA). The experiment was performed under nitrogen purging with a constant flow of 100 ml/min. Sample mass of 15-20 mg was heated at a linear heating rate of 20°C/min from room temperature to 800°C.

4.5.6 Dynamic mechanical analysis

Dynamic mechanical properties of the specimens were obtained using a dynamic viscoelastic analyzer model DMA 242 C from Netzsch Inc. The test was done under a three point bending mode. The strain amplitude used was 30 μ m at the frequency of 1 Hz. The specimen was heated at a rate of 2°C/min from 30 to 300°C. The specimen was 52×10×2.5 mm³. The storage modulus (G'), loss modulus (G''), and damping curve ($\tan \delta$) were determined. Glass transition temperature was taken from the temperature at the maximum point on the loss modulus curve.

4.5.7 Bending test

The flexural behaviors of the cured copolymers were determined using a universal testing machine (Instron Instrument, model 5567) at room temperature. The specimens were

tested according to ASTM D790-00 (Method I). A crosshead speed of 1.2 mm/min was used. Three specimens from each copolymer composition were tested and the average values were reported.

4.5.8 Scanning electron microscopy (SEM)

Interfacial bonding of a composite specimen was investigated using a scanning electron microscope (JEOL Ltd., model ISM-5800LV) at an acceleration voltage of 15 kV. Fractured samples were coated with a thin film of gold using an ion sputtering device (Balzers, model SCD040) for 4 min to obtain a film thickness of about 30 nm, and micrographs of the fractured surfaces were taken.



CHAPTER V

CURING KINETICS OF ARYLAMINE-BASED POLYFUNCTIONAL BENZOXAZINE RESINS BY DYNAMIC DIFFERENTIAL SCANNING CALORIMETRY

Polyfunctional benzoxazine resins which can be modified by changing the amine group on the ring structure, were reported to provide self-polymerizable crosslink-system with high thermal and mechanical integrity [6,55,61]. The polymers undergo ring-polymerization upon heating without the aid of a curing agent (strong acid and alkaline); therefore, no condensation by-products are released during a fabrication process as well as no corrosion of processing equipments. Moreover, polybenzoxazines possess several outstanding properties such as near-zero shrinkage after curing, low water absorption, and relatively high glass transition temperature even though it has relatively low cross-linking density [10,55]. In recent years, Ishida and Sander [51,52,62] disclosed improving thermal and mechanical properties of polybenzoxazines based on alkyl-substituted aromatic amines (e.g. BA-35x type benzoxazine). A series of benzoxazine resins have been synthesized that, upon polymerization produced a varying amount of phenolic Mannich bridges, arylamine Mannich bridges, and methylene linkages. For the 3,5-xylidine based benzoxazine, its thermal degradation temperature at 5% weight loss was reported to be 350°C which is higher than that of BA-a type benzoxazine i.e. about 315°C. In theory, polybenzoxazines with additional amounts of arylamine Mannich bridges, and methylene linkages showed improved mechanical and thermal properties as a result of greater crosslink densities. Correlations between the observed mechanical properties and network structures of polybenzoxazines were reported [49]. Consequently, the polybenzoxazine and its alloys were investigated as a high performance matrix of composite materials such as in electronic packaging applications [63-67]. In order to make on optimum use of the benzoxazine resins, it is important to understand the nature of their curing process, the structure of the cured material, and how its kinetic parameters can be influenced by temperature, etc. The curing reaction is a very complex process because many reactive processes sometimes occur simultaneously. The final properties of the crosslinked benzoxazine resins depend significantly on the kinetics of the curing

reaction concerned with extent of curing, the curing conditions, etc. [6,7]. Therefore, the study of the curing kinetics contributes to both a better knowledge of process development and an improvement of the quality of final products related to the structures of the polymer network [14,26]. In addition, the availability of reliable methods for cure monitoring also plays a crucial role in process control and optimization of the polymer network processing [5].

To our best knowledge, the effect of alkyl-substituted arylamines in the curing kinetics of the polyfunctional benzoxazine resins has not been explored. It is; therefore, of interest to investigate that of the polyfunctional benzoxazine resins based on arylamine, i.e. aniline and 3,5 xylidine. The curing kinetics of the systems were examined by non-isothermal differential scanning calorimetry (DSC) at different heating rates in order to understand the reaction kinetics of both systems and be the way of achieving successful processing.

5.1 Results and discussion

5.1.1 Curing reaction

The heat flow of BA-a and BA-35x from the conventional DSC mode are shown in Figure 5.1 and 5.2, respectively. From these figures, information about the nature of the curing reaction such as initial curing temperature, peak temperature and the curing range of both resins at different scan rates, could be derived. It can be observed that the exothermic peak shifts to a higher temperature with higher heating rate. In our systems, the heating rates show no effect on the total exothermic reaction heat estimated from the area under the exothermic peak of BA-a and BA-35x. The average total exothermic reaction heat of BA-a and BA-35x is 341 and 299 J/g, respectively. It is noticed that the curing reaction of BA-a has more amount of heat released than that of BA-35x. This suggests that BA-a would be more sensitive to accelerate the curing than BA-35x. Moreover, the step changes of the thermograms of both resins at the temperature range of 45 to 60°C are the glass transition temperatures of the benzoxazine monomers or T_g zero (T_{g0}). From Figure 5.3, one can observe that BA-a benzoxazine shows only one exothermic peak of the non-isothermal DSC traces while BA-35x type benzoxazine shows overlapped exothermic peaks or a small shoulder beside the main peak. Thus, it is suggested that the curing reaction of BA-35x type benzoxazine has at least two cure

stages; the curing reaction at lower temperature, was caused by reaction 1 and the one occurred at higher temperature was caused by reaction 2. The individual reaction may be calculated by a combination of programmed and isothermal techniques. To verify the two curing reactions of BA-35x, further experiments on isothermal curing of partially cured samples (5-120 min) at 160°C are depicted in Figure 5.4. It can be noticed that the thermogram of partially cured BA-35x resin at 5 min shows no significant change of the exothermal peak temperature (200°C) and still indicates the overlapped exothermic peaks, i.e. the effect of the second reaction to the first peak is small. However, when the sample is cured to 10 min, the peak temperature is shifted to 210°C, revealing stronger effect of the second reaction on the first peak. When the sample is cured to 15 min, the first peak almost disappears as the second peak is obviously observed. The partially cured BA-35x resin to 120 min clearly shows only one exothermic peak at higher temperature, implying that the effect of the first reaction to the second peak temperature could be neglected. The results in Figure 5.4 ensure that there are two reaction phases in the hypothetical product.

The kinetics of the DSC curves for BA-35x at the heating rates of 1 to 20°C/min were analysed using PeakFit v4.12. In order to separate two exothermic peaks, and to analyse the distinct characterization of each, Pearson VII distribution was used as shown in Figure 5.5. The DSC thermograms recorded for the curing reaction of the BA-35x sample at 10°C/min (solid line) and calculated data from Peakfit v4.12 (dash line) with two distinct peaks (peak I-black circles and peak II-white circles)

5.1.2 Kinetic model

As the multiple heating rate methods for non-isothermal analysis proposed by Kissinger and Ozawa can be used as an alternative way of calculating the activation energy without assuming any model of kinetic parameters and without integrating the exothermic peak, the logarithm plots of heating rate vs. the reciprocal of the absolute peak temperature of BA-a resin are given in Figure 5.6. They are shown that a good linear relationship between the heating rate and the reversal of the exothermic peak temperature can be obtained. The average activation energy values of BA-a and BA-35x resins calculated from the slopes of the plots are listed in Table 5.1. BA-a resin shows only one dominant curing kinetic process with the average activation energy of 81-85 kJ/mol whereas BA-35x exhibits two major curing processes. The average activation energies of BA-35x for reaction 1 and 2 were 81-87 and 111-113 kJ/mol, respectively. In addition,

the average activation energy values obtained from Kissinger and Ozawa methods are not significantly different. From the results, the calculated values of the activation energy values of BA-a and BA-35x are different from other reported works [6,7] because the molecular weight distribution of the benzoxazine precursor is different as indicated by GPC results. The precursor obtained is a mixture of monomers, dimers, and other oligomers formed in subsequent reactions during the synthesis, for instance, in case of BA-a, the molecular weight is 431, 498, and 807 g/mol, respectively, while those of BA-35x are 462, 562, and 964 g/mol, respectively. Typically, the molecular weight of purified BA-a and BA-35x type benzoxazine monomers is 463 and 527 g/mol, respectively [9]. Furthermore, considering the system of BA-35x, one can see that the activation energy of reaction 2 is much higher than that of reaction 1. As a result, reaction 1 is more sensitive to the temperature than reaction 2.

From the results, we can observe that the average activation energy value of reaction 1 for BA-35x resin is almost the same as the average activation energy of BA-a resin. This implies that the curing mechanism in the first stage of BA-35x resin is the same as that of BA-a resin. This mechanism is the heterocyclic ring opening polymerization of benzoxazine precursors since the oxazine ring is the reactive site for curing of benzoxazine. The conformation of a mono-oxazine ring containing benzoxazine is a distorted semichair structure, with the nitrogen and the carbon between the oxygen and nitrogen on the oxazine sitting, and is irreversible formation of the methylene bridge, respectively [68]. Whereas the second exothermic peak of the reaction 2, indicated by the high-temperature shoulder, corresponds to the side reactions which generate the bisphenolic methylene linkages and possible reaction to the para position of the arylamine ring called arylamine Mannich bridge and methylene linked structures. In addition, Ishida and Sander [52] have reported different network structure of polybenzoxazine (BA-a, and BA-35x types) investigated by FTIR. They found that the FTIR absorbed peak position of BA-35x after polymerization shows a large band centered at 847 cm^{-1} corresponding to the out-of-plane, in phase hydrogen wagging mode of the 1,2,3,5-tetrasubstituted arylamine ring, but this peak can not be observed for BA-a resin. However, the spectrum of both polybenzoxazine types centered at 878 cm^{-1} . This band agrees with the frequency predicted for the out-of-plane, out-of phase hydrogen wagging node for the 1,2,3,5-tetrasubstituted aromatic ring.

Moreover, a more complete assessment of the apparent activation energy of benzoxazine resins throughout the entire conversion range may be obtained using the

isoconversional methods that are the Flynn-Wall-Ozawa and Friedman methods. If the data fall into a straight line, the slope should then correspond to E_a/R at the particular conversion. For instance, Figure 5.7 and Figure 5.8 are Flynn-Wall-Ozawa and Friedman plots of BA-a resin system for $\alpha = 0.05$ to 0.95 , respectively. A good linear relationship was observed from both Flynn-Wall-Ozawa and Friedman plots. Values of E_a of BA-a, and BA-35x resins obtained in this manner at different degree of curing are shown in Figure 5.9 and Figure 5.10. From the plots, the dependence of the apparent activation energies of both benzoxazine resins as a function of degree of curing was observed. The effect has been known in literatures as a kinetic compensation effect [69]. As there was no significant difference in the calculated activation energy values either using differential or integral kinetic methods, the activation energy obtained from Kissinger method was then selected for further determining the reaction order of our systems as recommended by Sbirrazzuoli et al. [18].

As previously mentioned, the mechanisms of the curing reaction of thermoset resins usually have two general kinetic reactions, a n th-order and an autocatalytic reaction [70]. In this work, the method used to find kinetic model is Friedman method. For n th-order reaction, the average activation energy from Kissinger method is taken as a constant, Eq. (2.8) may be written as:

$$\ln[Af(\alpha)] = \ln A + n \ln(1 - \alpha) \quad (5.1)$$

Friedman suggested that the relationship between $\ln[Af(\alpha)]$ against $\ln(1-\alpha)$ should yield a straight line of which the slope corresponds to the order of n of the reaction. Otherwise, for autocatalytic process, the Friedman plot would show a maximum of $\ln(1-\alpha)$ approximately around -0.51 to -0.22 which is equivalent to α of about $0.2-0.4$. This is due to the autocatalytic nature that shows the maximum reaction rate at $20-40\%$ conversion. The results are in good agreement with several works reported [71-73].

Figure 5.11 shows Friedman plots of reaction 1 and 2 of BA-35x resin, respectively. In case of reaction 1, since $\ln[Af(\alpha)]$ and $\ln(1-\alpha)$ are not linearly related, this implies that the curing reaction is autocatalytic in nature. In contrast, the plot for reaction 2 shows linear relationship indicating n th-order kinetic behavior. Using the same analysis for BA-a (not shown here), only single peak reaction is obtained suggesting the behavior of autocatalytic reaction. According to other works reported, the autocatalytic nature of the reaction kinetics of this resin can be explained by the generation of free phenol groups

while the benzoxazine ring starts to open. These groups can actually accelerate further ring opening [6,7].

For the n th-order model, it is assumed that the reaction obeys Eq. (5.2)

$$\frac{d\alpha}{dt} = A \exp(-E_a/RT) (1-\alpha)^n \quad (5.2)$$

Conversely, the autocatalytic model considers independent reaction orders: m and n , as shown in Eq. (5.3)

$$\frac{d\alpha}{dt} = A \exp(-E_a/RT) (1-\alpha)^n \alpha^m \quad (5.3)$$

Theoretically, Eq. (5.2) and Eq. (5.3) could be solved by multiple nonlinear regressions because the curing rate is an exponential function of the reciprocal of the absolute temperature. By taking the logarithm of Eq. (5.4) and Eq. (5.5), a linear expression for the logarithm of curing rate can be obtained.

$$\ln\left(\beta \frac{d\alpha}{dt}\right) = \ln A - \left(\frac{E_a}{RT}\right) + n \ln(1-\alpha) \quad (5.4)$$

$$\ln\left(\beta \frac{d\alpha}{dt}\right) = \ln A - \left(\frac{E_a}{RT}\right) + n \ln(1-\alpha) + m \ln(\alpha) \quad (5.5)$$

Eq. (5.4) and Eq. (5.5) can be solved by multiple linear regression, in which the dependent variable is $\ln(d\alpha/dt)$, and the independent variables are $\ln\alpha$, $\ln(1-\alpha)$, and $1/T$. Therefore, the values of A , m , and n can be obtained using the average activation energy from Kissinger method. The degree of curing is chosen between the beginning of the reaction and the maximum peak of degree of curing ($\alpha = 0.1-0.5$). The results of the multiple linear regressions analysis for all heating rates used of BA-a, and BA-35x (reaction 1 and 2) are listed in Table 5.2, Table 5.3, and Table 5.4, respectively. It can be seen that the variation of A , m , and n with the heating rate for both BA-a, and BA-35x

systems is in the same range as those reported by Ishida and Rodriquez [6,7]. Consequently, we obtain a mathematical model for autocatalytic kinetics of BA-a system as,

$$\frac{d\alpha}{dt} = (5.96 \times 10^6) \exp(-9743/T) (1 - \alpha)^{1.7} \alpha^{0.8} \quad (5.6)$$

Similarly mathematical models for autocatalytic kinetics of BA-35x (reaction 1) and for *n*th-order kinetics of BA-35x (reaction 2), are presented in Eq. (5.7) and Eq. (5.8), respectively.

$$\frac{d\alpha}{dt} = (2.04 \times 10^7) \exp(-9743/T) (1 - \alpha)^{1.7} \alpha^{0.8} \quad (5.7)$$

$$\frac{d\alpha}{dt} = (2.09 \times 10^9) \exp(-13351/T) \alpha^{1.4} \quad (5.8)$$

The experimental results are compared with those predicted from the models for both systems, as shown in Figure 5.12-5.14. It is clearly seen that the calculated data from the model are in good agreement with the experimental results.

Table 5.1 Average activation energies of BA-a and BA-35x obtained by Kissinger and Ozawa methods.

Method	Average Activation Energy (E_a , kJ/mol)		
	BA-a resin	BA-35x resin	
		Reaction 1 (E_{a1})	Reaction 2 (E_{a2})
Kissinger	81	81	111
Ozawa	85	87	113



สถาบันวิทยบริการ
จุฬาลงกรณ์มหาวิทยาลัย

Table 5.2 The kinetic parameters evaluated for the curing of the BA-a system.

Heating Rate (°C/min)	E (kJ/mol)	lnA (s ⁻¹)	Mean	n	Mean	m	Mean
1	81	14.57	15.60	1.7	1.7	0.4	0.8
2		14.99		1.9		0.4	
5		16.12		2.1		1.0	
10		16.28		1.6		1.2	
20		16.05		1.2		1.0	



สถาบันวิทยบริการ
จุฬาลงกรณ์มหาวิทยาลัย

Table 5.3 The kinetic parameters evaluated for the curing of the BA-35x system
(Reaction1).

Heating Rate (°C/min)	E (kJ/mol)	lnA (s ⁻¹)	Mean	n	Mean	m	Mean
1	81	16.37	16.83	1.6	1.7	0.6	0.8
2		16.26		1.3		0.5	
5		17.00		1.8		0.9	
10		17.42		2.0		1.1	
20		17.08		1.7		1.1	



สถาบันวิทยบริการ
จุฬาลงกรณ์มหาวิทยาลัย

Table 5.4 The kinetic parameters evaluated for the curing of the BA-35x system
(Reaction2).

Heating Rate (°C/min)	E (kJ/mol)	lnA (s ⁻¹)	Mean	n	Mean
1	111	21.52	21.46	1.8	1.4
2		21.47		1.4	
5		21.39		1.3	
10		21.45		1.0	
20		-		-	



สถาบันวิทยบริการ
จุฬาลงกรณ์มหาวิทยาลัย

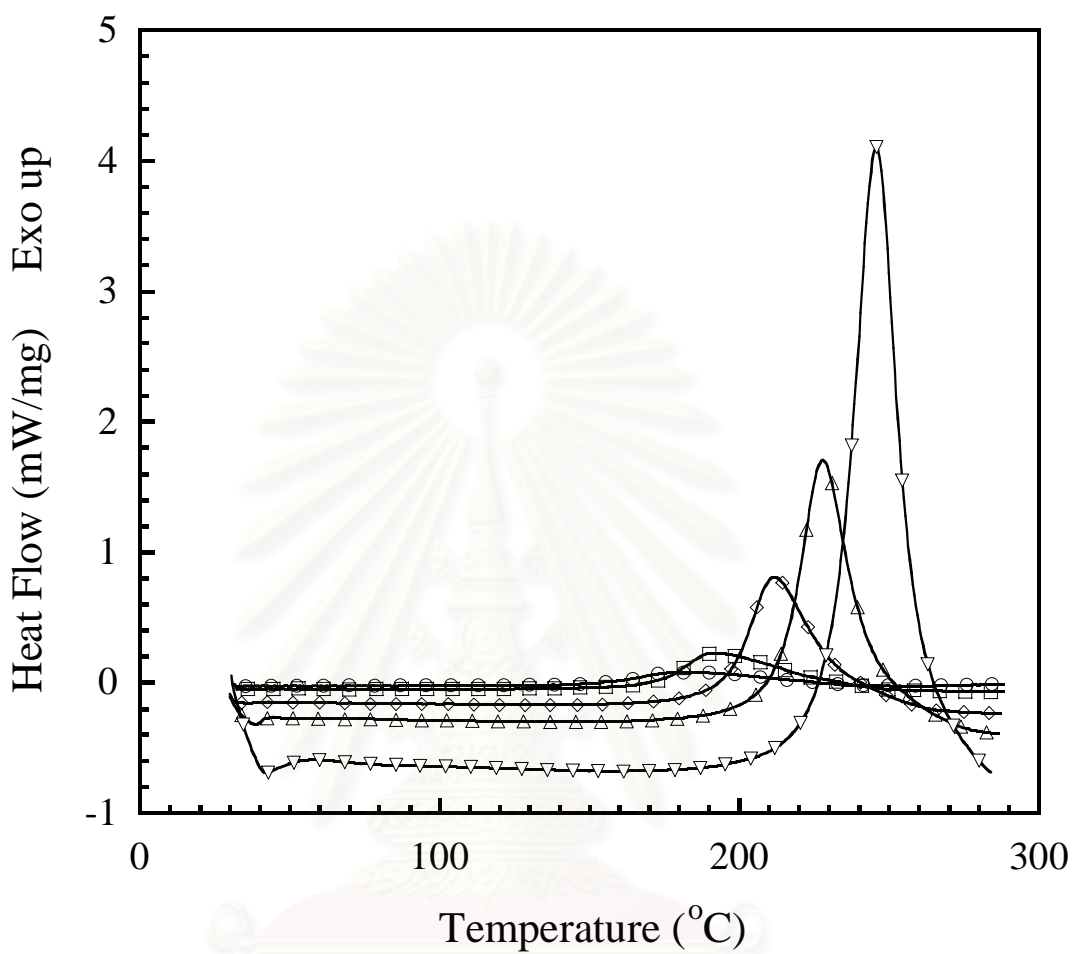


Figure 5.1 DSC thermograms of BA-a resin at different heating rates: (○) 1°C/min, (□) 2°C/min, (◇) 5°C/min, (△) 10°C/min, (▽) 20°C/min.

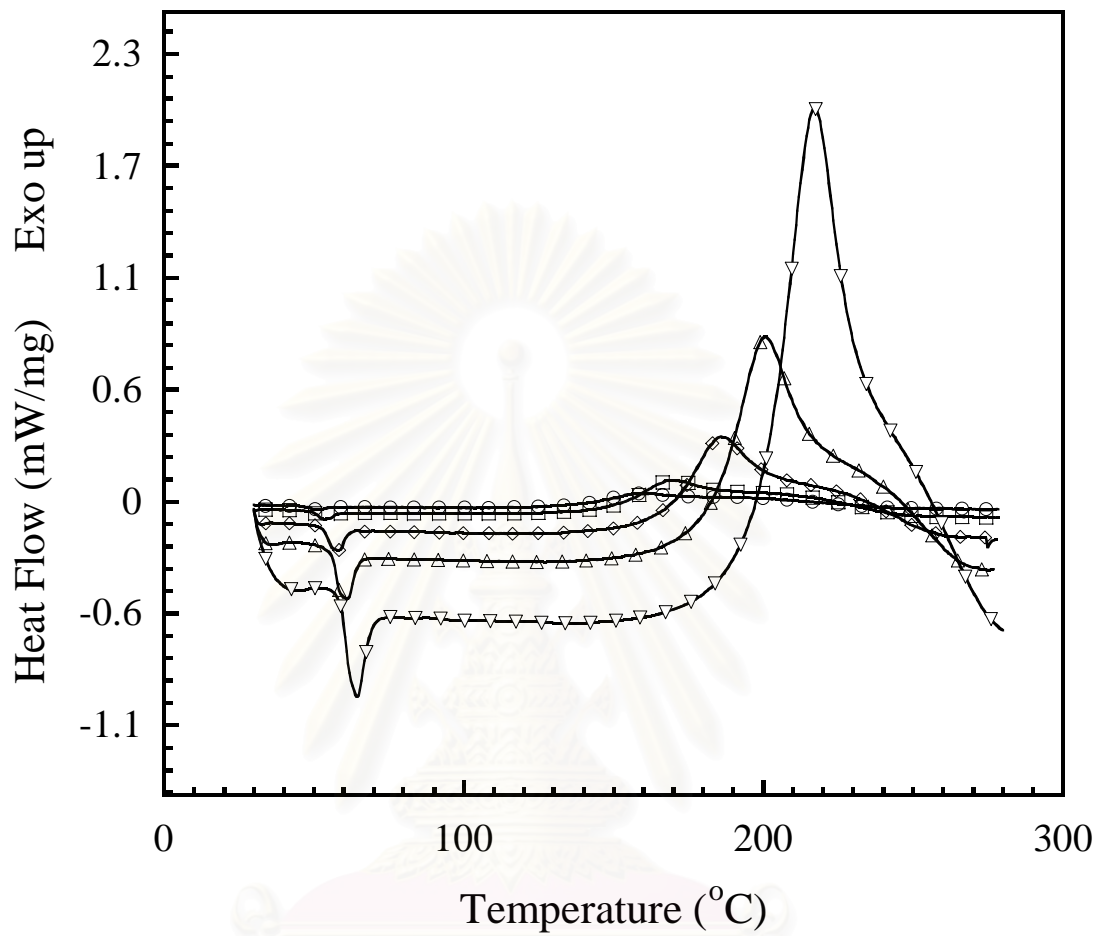


Figure 5.2 DSC thermograms of BA-35x resin at different heating rates: (○) 1°C/min, (□) 2°C/min, (◇) 5°C/min, (△) 10°C/min, (▽) 20°C/min.

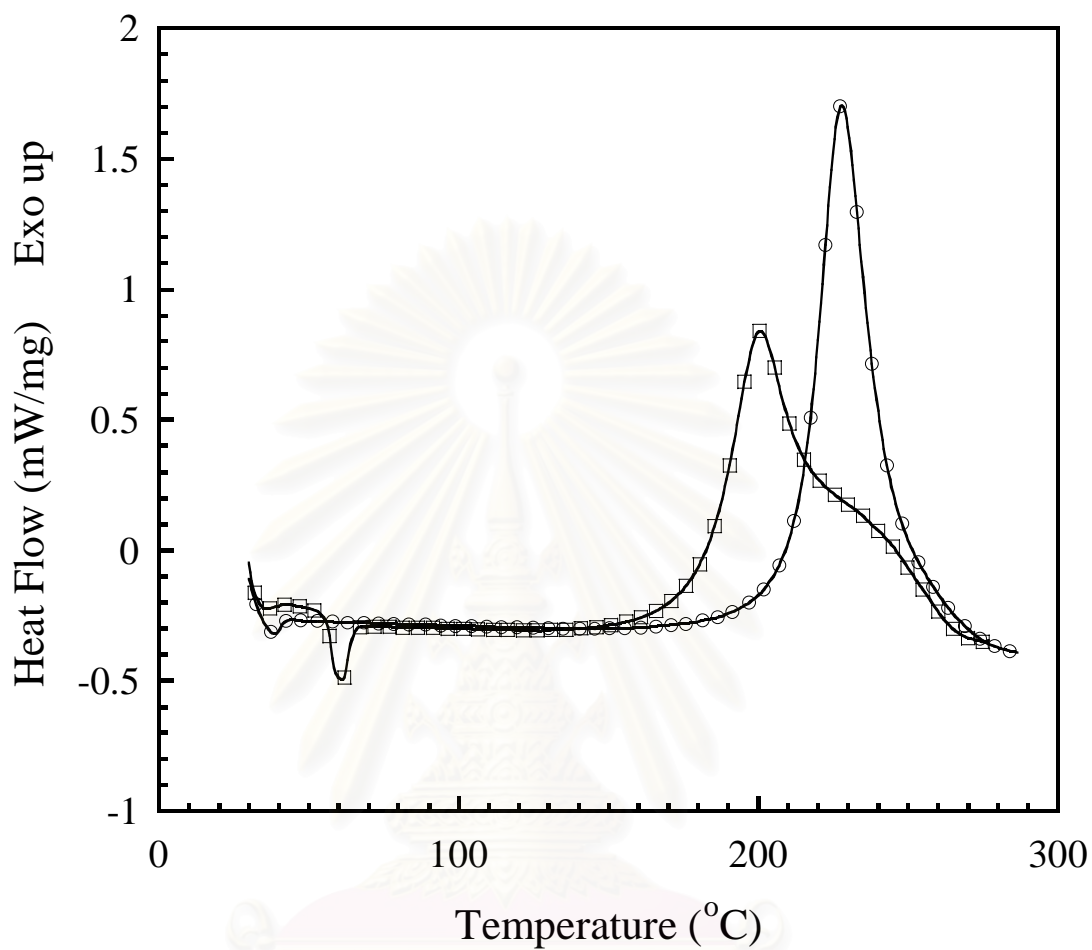


Figure 5.3 DSC thermograms of two types of benzoxazine resins at 10°C/min:

(○) BA-a resin, (□) BA-35x resin.

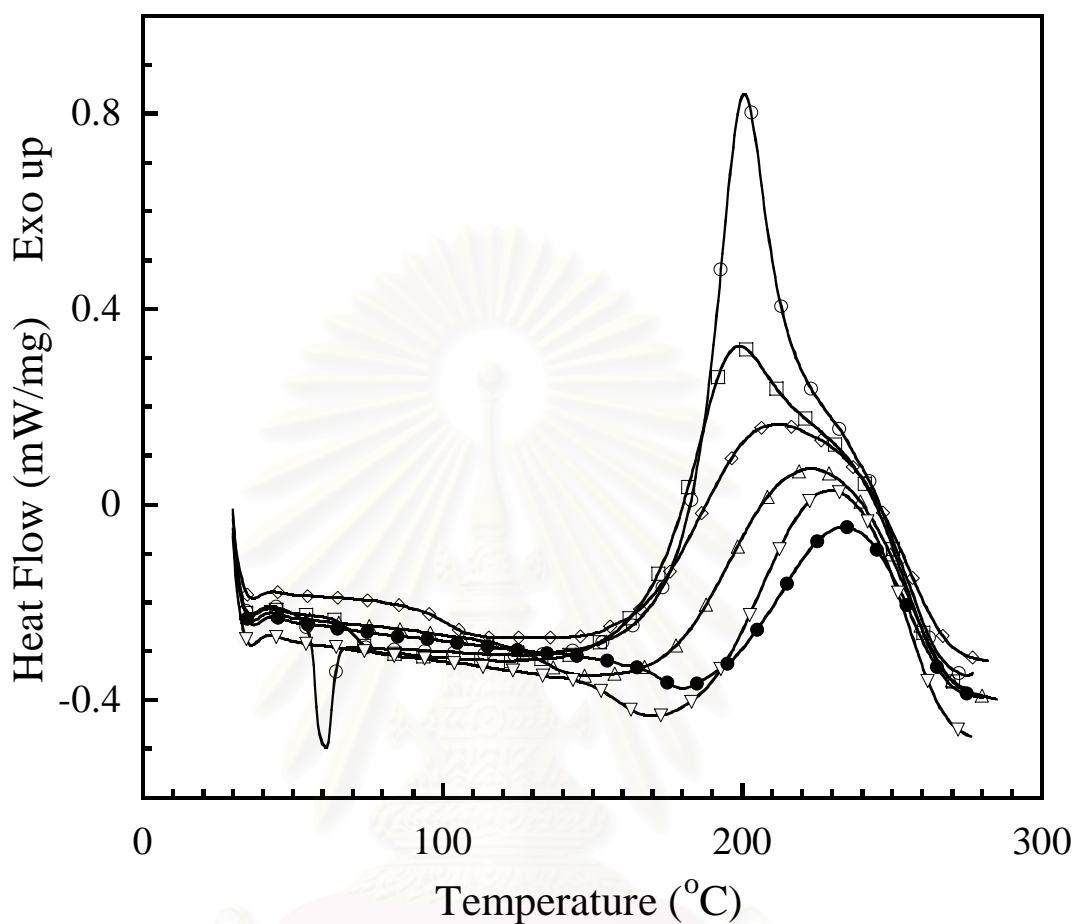


Figure 5.4 DSC thermograms of BA-35x resin using 10°C/min heating rate after isothermal curing of 160°C at different curing time in oven: (○) uncured BA-35x monomer, (□) 5 min, (◇) 10 min, (△) 15 min, (▽) 60 min, (●) 120 min.

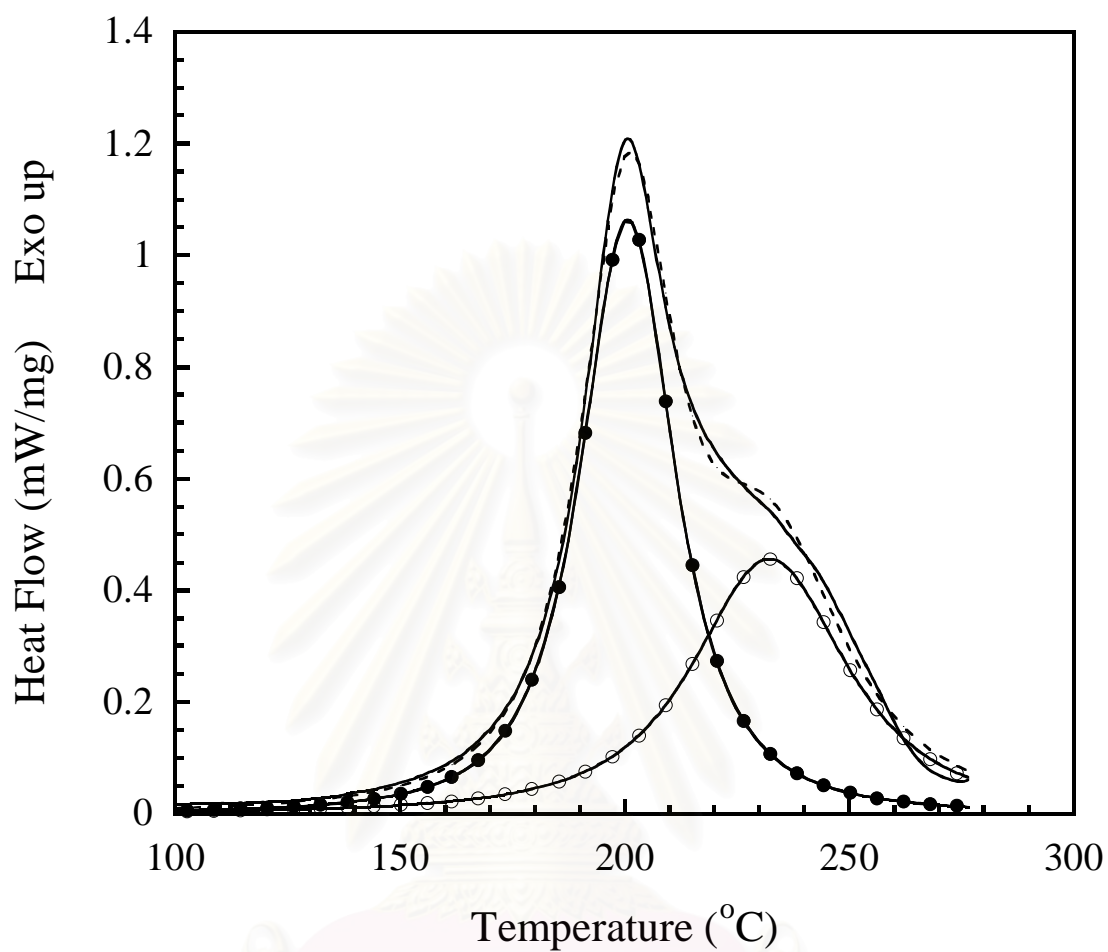


Figure 5.5 DSC thermogram of BA-35x resin recorded at 10°C/min: the DSC thermogram (solid line), calculated the DSC thermogram (dash line), (•) reaction 1, (○) reaction 2.

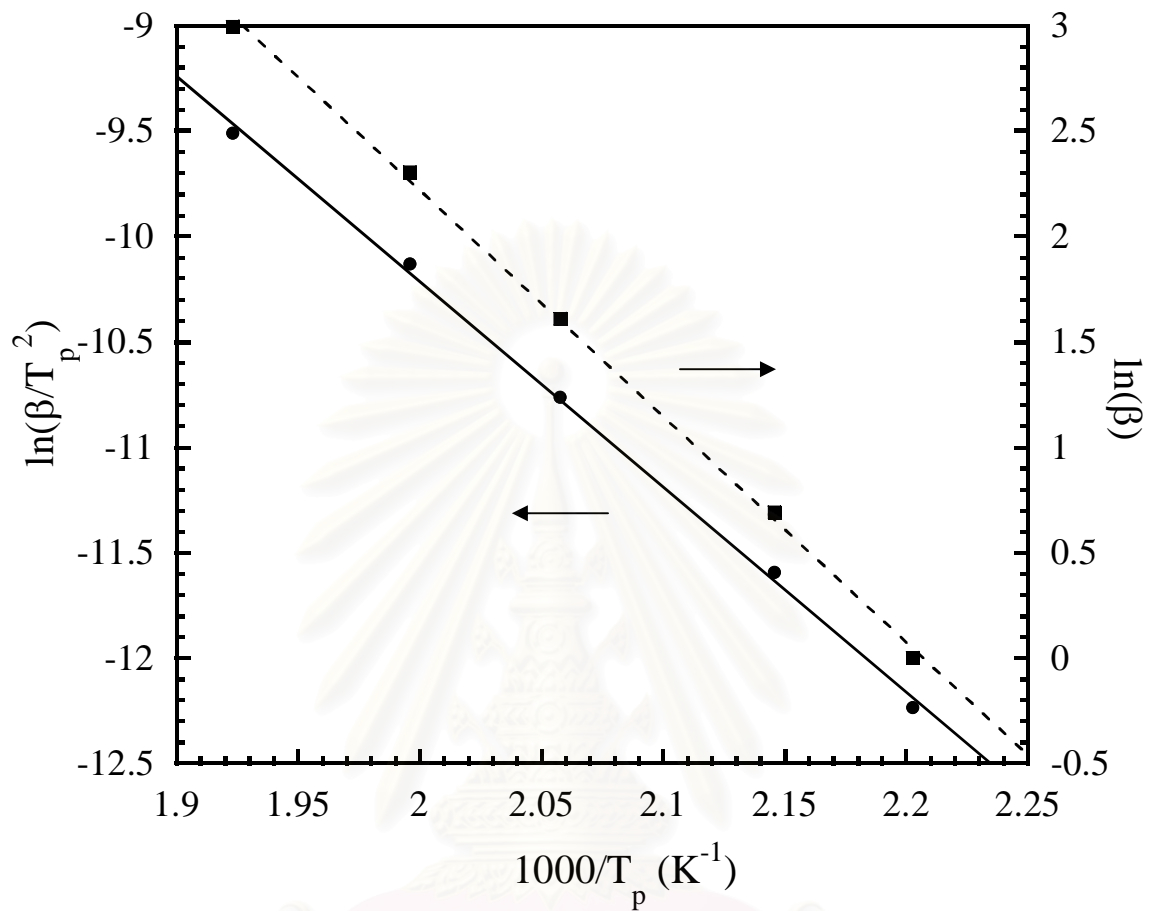


Figure 5.6 (•) Kissinger method and (■) Ozawa method plots for averaged activation energy determination of the BA-a resin.

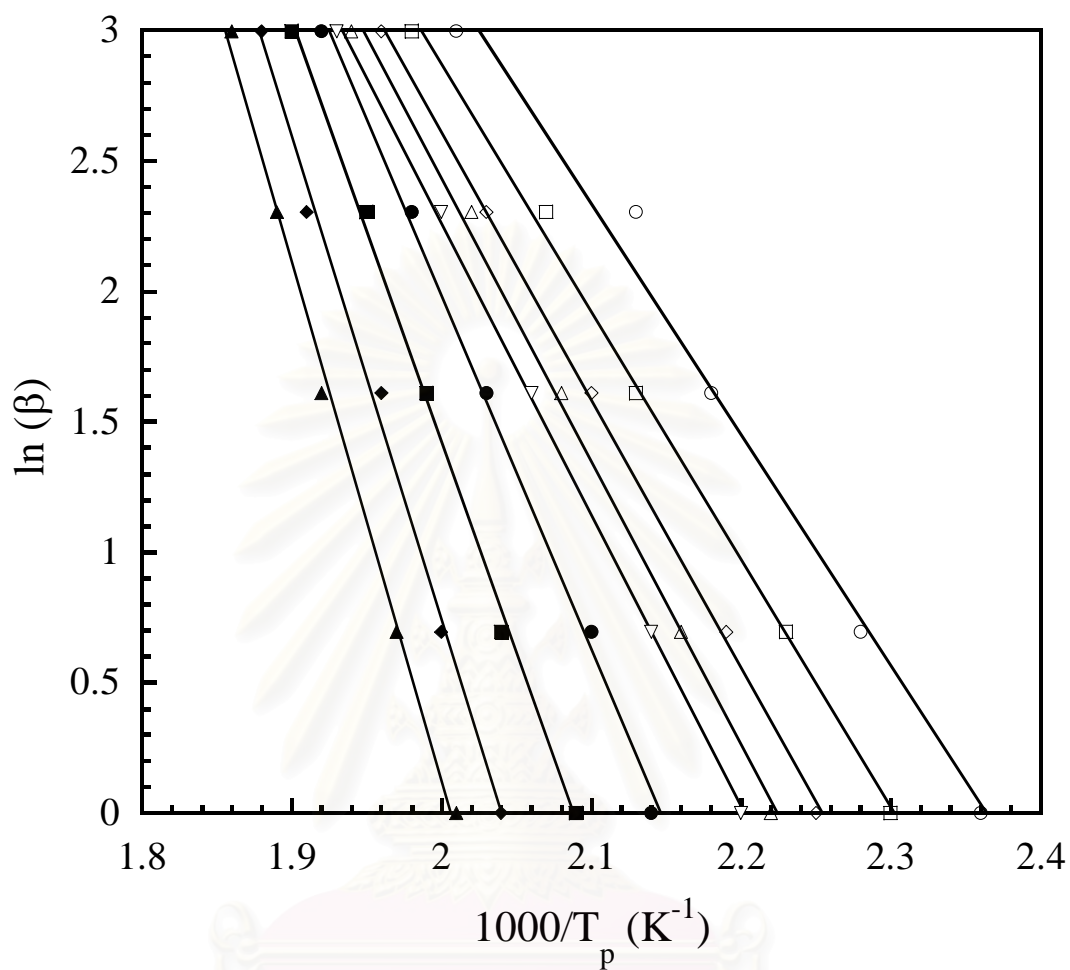


Figure 5.7 Flynn-Wall- Ozawa plots at various degree of curing of the BA-a resin:

(○) $\alpha = 0.05$, (□) $\alpha = 0.10$, (◇) $\alpha = 0.20$, (△) $\alpha = 0.30$, (▽) $\alpha = 0.40$,
 (●) $\alpha = 0.60$, (■) $\alpha = 0.80$, (◆) $\alpha = 0.90$, (▲) $\alpha = 0.95$.

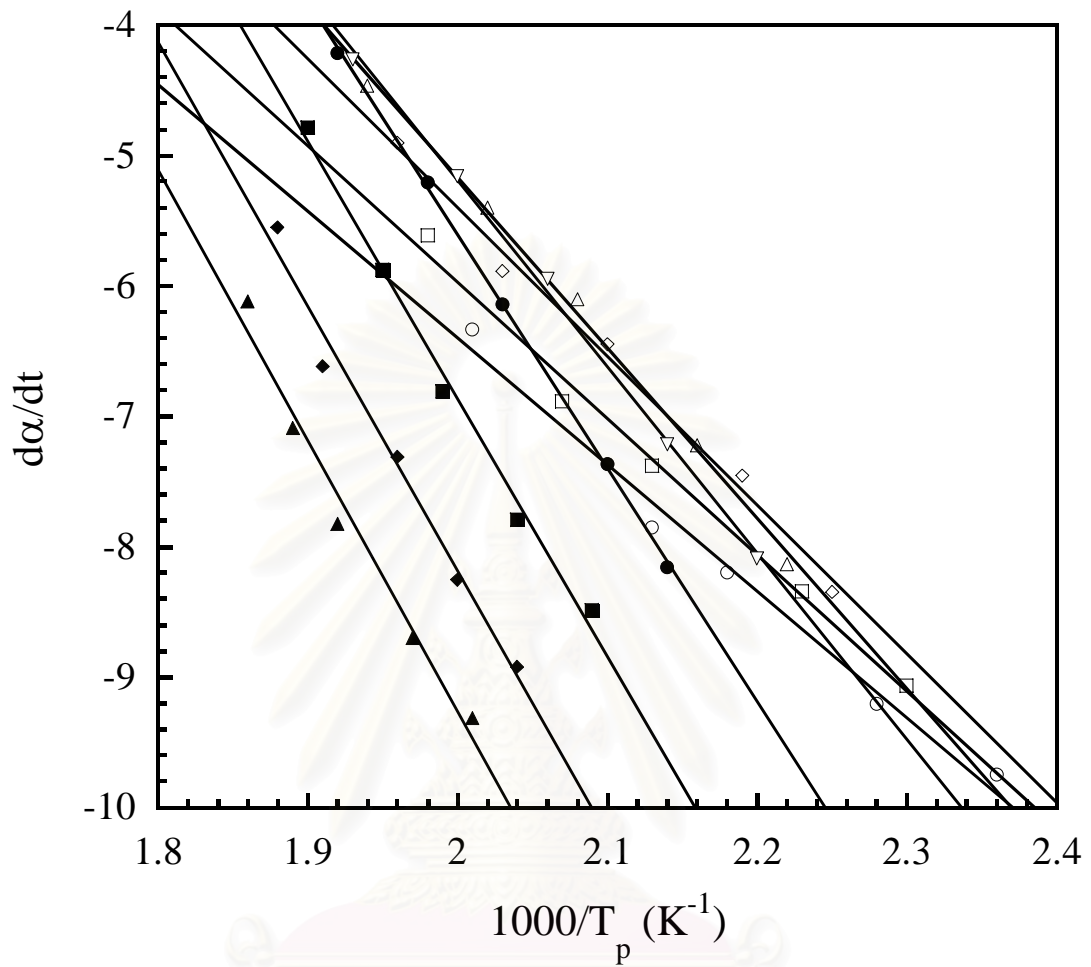


Figure 5.8 Friedman plots at various degree of curing of the BA-a resin: (○) $\alpha = 0.05$,
 (□) $\alpha = 0.10$, (◇) $\alpha = 0.20$, (Δ) $\alpha = 0.30$, (▽) $\alpha = 0.40$, (●) $\alpha = 0.60$,
 (■) $\alpha = 0.80$, (◆) $\alpha = 0.90$, (▲) $\alpha = 0.95$.

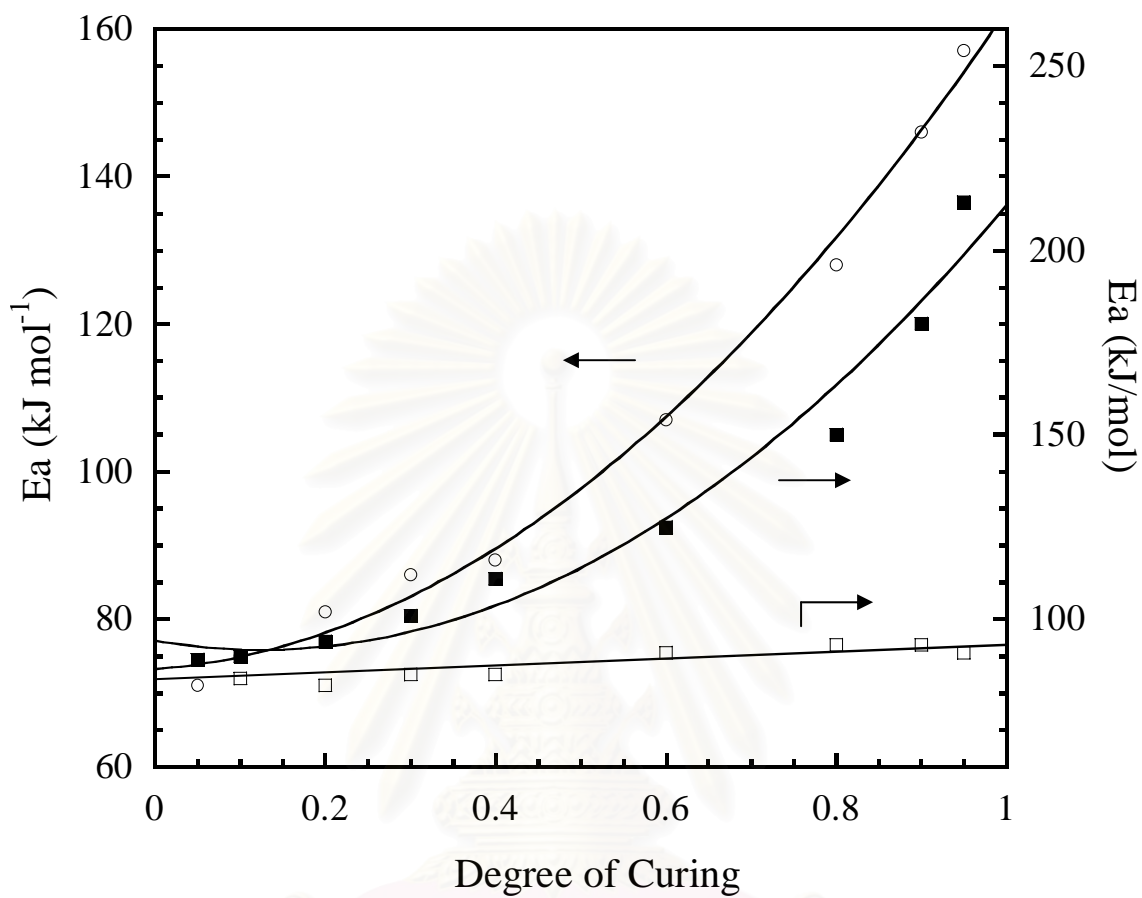


Figure 5.9 Values of the apparent activation energy obtained from Flynn-Wall- Ozawa plots at different degree of curing: (-○-) BA-a resin, (-□-) BA-35x reaction 1, (-■-) BA-35x reaction 2.

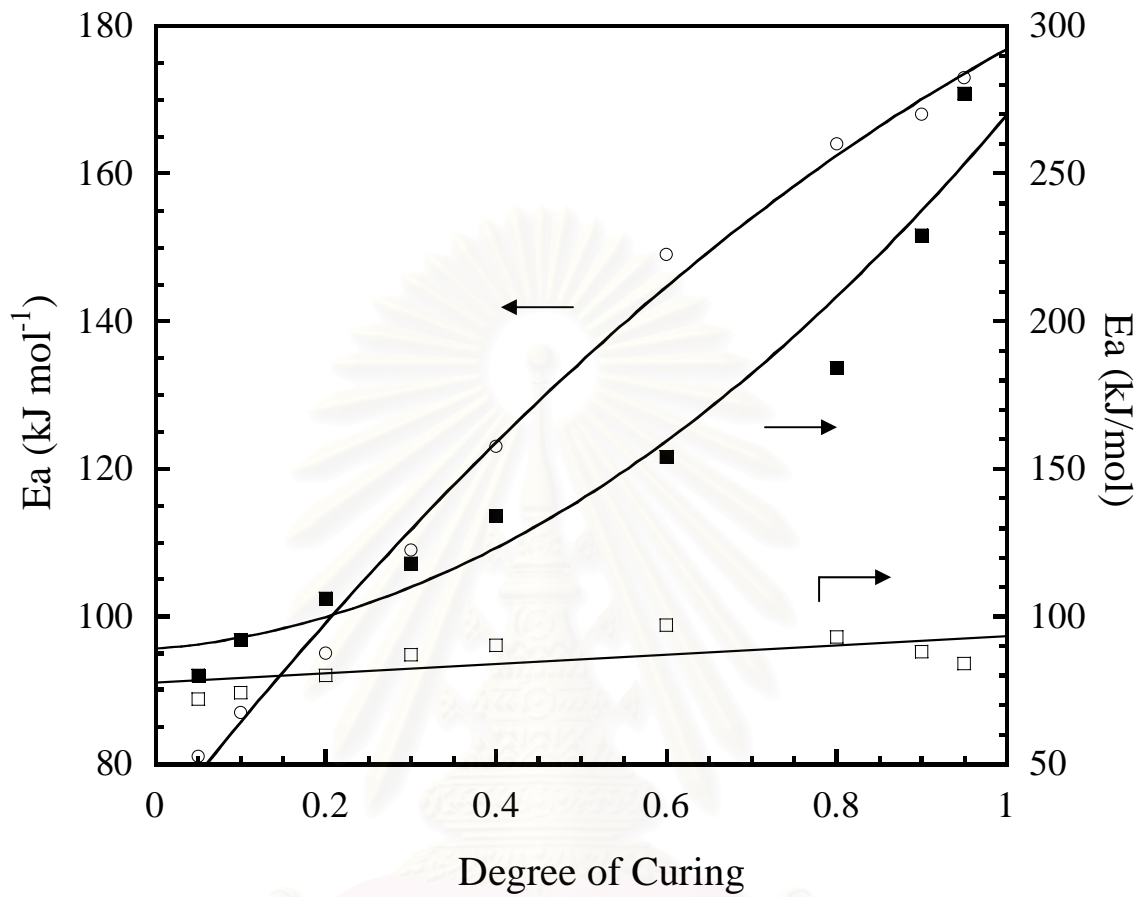


Figure 5.10 Values of the apparent activation energy obtained from Friedman plots at different degree of curing: (-○-) BA-a resin, (-□-) BA-35x reaction 1, (-■-) BA-35x reaction 2.

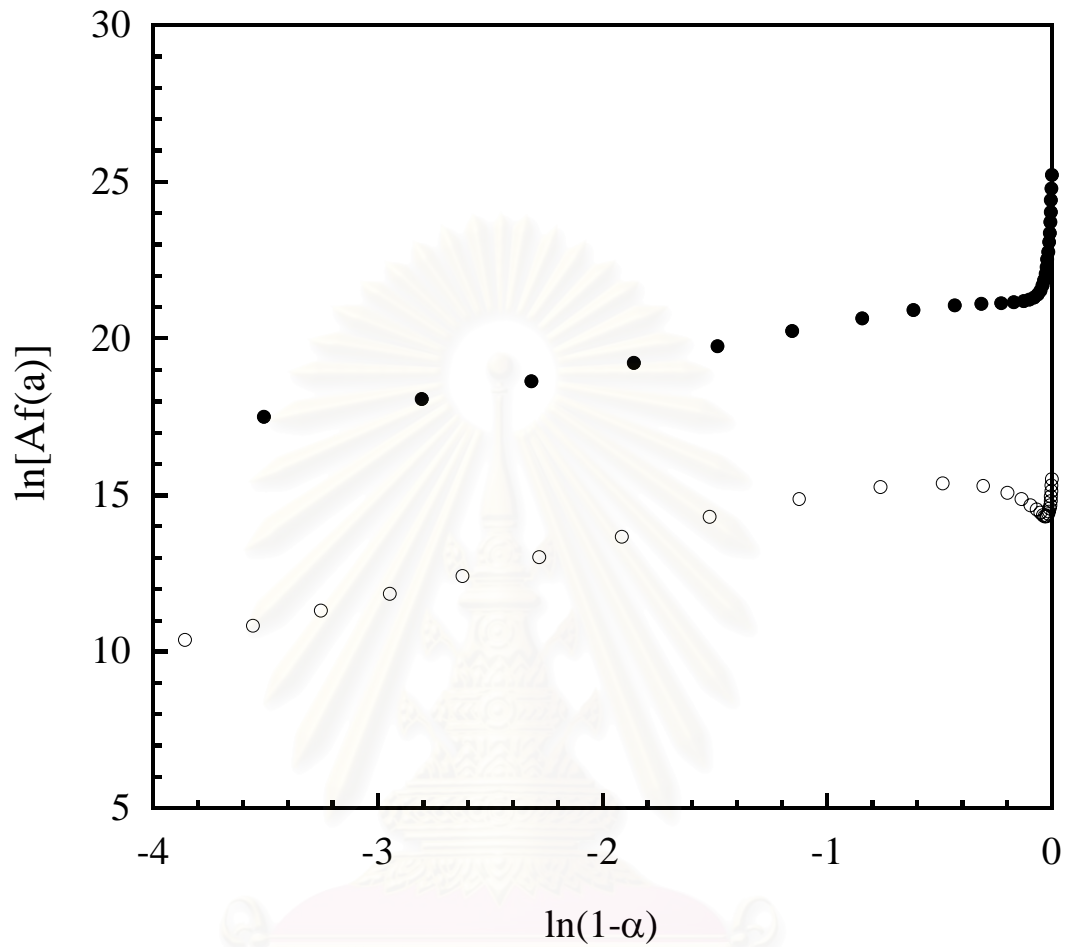


Figure 5.11 Plots of $\ln[Af(\alpha)]$, vs $\ln(1-\alpha)$ of BA-35x resin using the heating rate of $10^\circ\text{C}/\text{min}$. and using the average activation energy from Kissinger method:
 (○) reaction 1, (●) reaction 2.

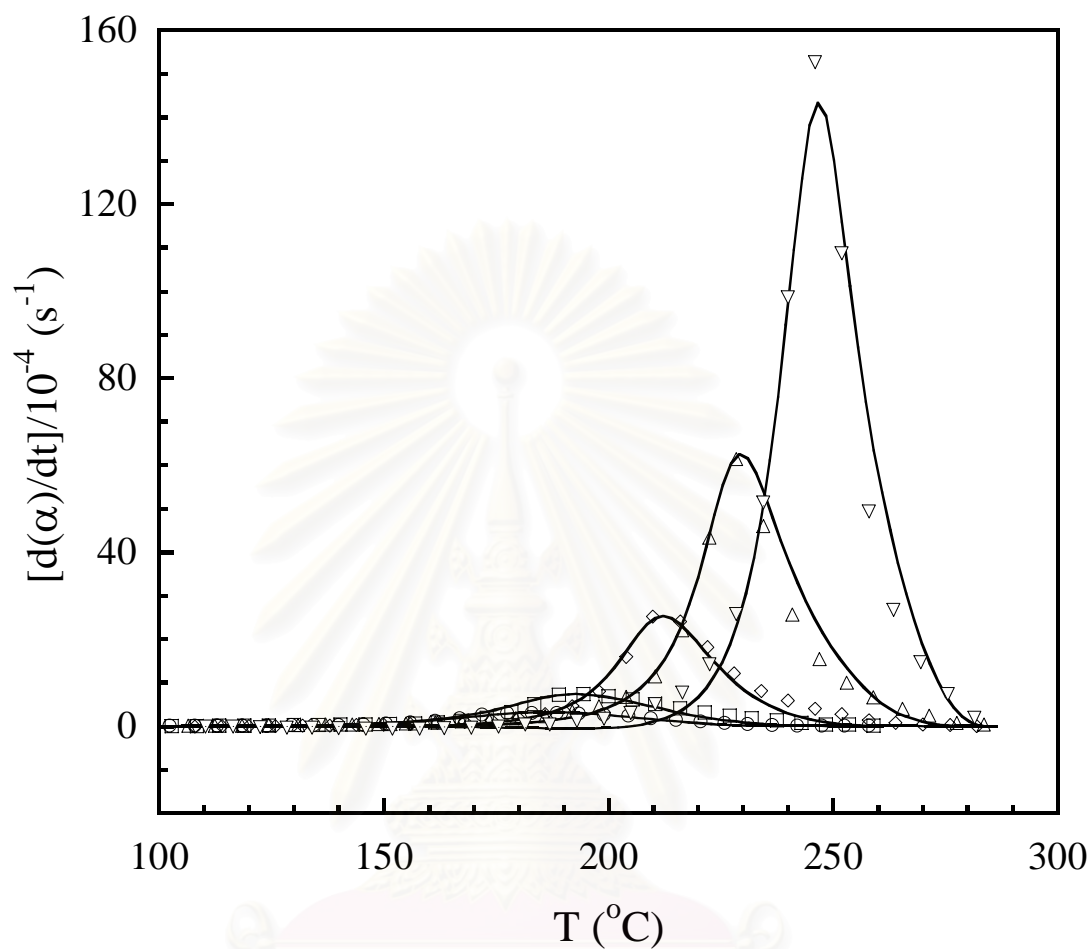


Figure 5.12 Experimental (symbols) and calculated (solid lines) DSC peaks corresponding to the curing process of BA-a resin: (○) 1°C/min, (□) 2°C/min, (◇) 5°C/min, (△) 10°C/min, (▽) 20°C/min.

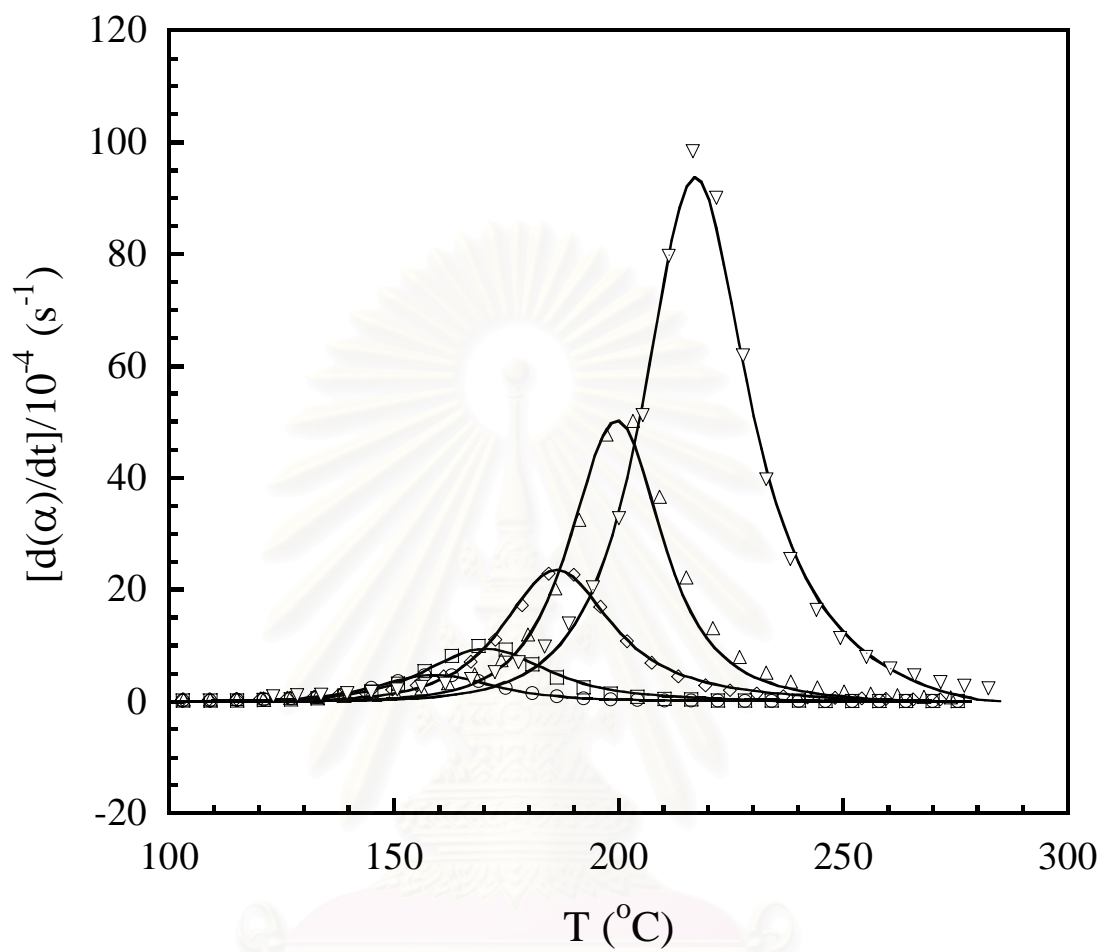


Figure 5.13 Experimental (symbols) and calculated (solid lines) DSC peaks corresponding to the first curing process (reaction 1) of BA-35x resin: (○) 1°C/min, (□) 2°C/min, (◇) 5°C/min, (△) 10°C/min, (▽) 20°C/min.

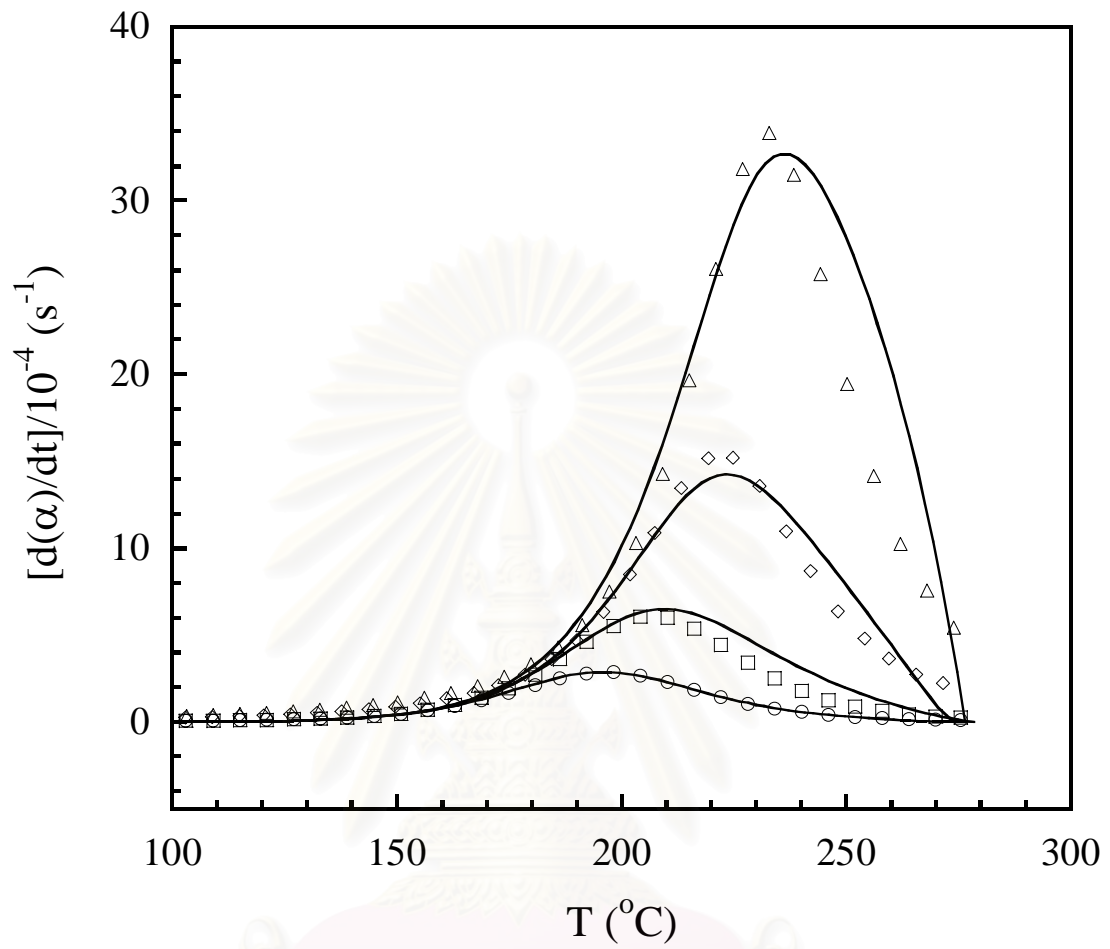


Figure 5.14 Experimental (symbols) and calculated (solid lines) DSC peaks corresponding to the second curing process (reaction 2) of BA-35x resin: (○) 1°C/min, (□) 2°C/min, (◇) 5°C/min, (△) 10°C/min.

CHAPTER VI

EFFECT OF NOVEL BENZOXAZINE REACTIVE DILUENT ON PROCESSABILITY AND THERMO- MECHANICAL CHARACTERISTICS OF BI-FUNCTIONAL POLYBENZOXAZINE

As polymer applications has diversified, the improvement of its properties and development of new polymer products, particularly by modification of the existing polymers, continues to be essential. For example, the reactive diluent has been used in copolymer or blend systems by formulating solvent-free applications in coating, adhesion, composites, and electronic encapsulants [10,49,57]. In the composite fabrication process, the resin viscosity is an important variable, affecting the flow-out properties and the resin wetting characteristic. Furthermore, diluted resins are employed in some formulations in order to achieve easier handling, increase filler loading and reduce costs. In the past, solvents have been used to lower resin viscosity. However, due to recent stricter environmental regulations on the release of volatile organic compounds (VOC), solvent use has become increasingly restrictive [49].

Generally, there are two classes of diluents. A reactive diluent is the ingredient that actually undergoes chemical reaction with the resin and becomes part of the polymeric structure. The other type is a non-reactive diluent which can also lower the viscosity of the base resin but does not take part in the polymer structure formation. The class of resin that most widely used as a reactive diluent is epoxy resin. This type of reactive diluent was reported to provide good properties and enhanced processing characteristics of the base resin [9,10,49,57]. Urethane prepolymer as well as unsaturated polyester had also been investigated as reactive diluents of the major polymer constituents [74,75]. In recent years, a novel class of thermosetting resin based on a benzoxazine structure has gained substantial attraction because of some of its high thermal and mechanical intriguing properties. A relatively low melt viscosity, one of the most useful properties of the benzoxazine resins, results in an ability of the resins to accommodate relatively large quantity of filler while still maintaining their good processability when compared to phenolic resins.

A liquid monofunctional benzoxazine resin had been investigated as a reactive diluent of solid benzoxazine resins. The melt viscosity of a bifunctional benzoxazine resin, a bisphenol-A-aniline type (BA-a), was reported to be substantially reduced by the use of a monofunctional benzoxazine resin i.e. 4-Cumylphenol-aniline type (C-a) [49]. However, the addition of the C-a resin into the solid BA-a resin was reported to decrease the crosslink density of the polymer network and led to the decrease in thermal degradation temperature and char yield of the polymer hybrids. Recently, Wang and Ishida [76] investigated a series of monofunctional benzoxazine resins. In their arylamine-based resins, a monofunctional phenol-aniline type benzoxazine (Ph-a) showed superior processability as well as thermal stability to the phenol-toluidine type (Ph-nt) and the phenol-xylylene type (Ph-35x) resins. At its fully cured stage, Ph-a degradation temperature and its char yield were reported to exhibit the values even greater than its bifunctional counterpart i.e. BA-a polymer. Its maximum $T_{g,DSC}$ of 142°C was the highest among the three monofunctional resins tested though it is lower than that of the bifunctional BA-a polymer i.e. 160°C. The curing kinetic analysis of the benzoxazine resins such as a random copolybenzoxazine of BA-a type and Ph-a type benzoxazines has also been reported to exhibit the activation energy about 50-84 kJ/mol [15]. The activation energy of the copolybenzoxazine is similar to that of the BA-a type benzoxazine ($E = 81$ kJ/mol) obtained from the other reports [6,7,15,77].

In this investigation, the Ph-a benzoxazine resin will be examined as a novel reactive diluent of a bifunctional benzoxazine resin i.e. BA-a resin. Since the molecule structure of the Ph-a resin resembles the BA-a resin chemically, a miscible mixture of the Ph-a and the BA-a resins should also be expected. The processability, thermal, and mechanical properties of the resulting polymer hybrids will also be examined.

6.1 Results and discussion

6.1.1 Chemorheological properties of BA-a/Ph-a resin mixtures

All BA-a/Ph-a resin mixtures are miscible giving homogenous and transparent liquid mixtures. The effect of the Ph-a benzoxazine resin on the chemorheology of the BA-a/Ph-a resin mixture is shown in Figure 6.1. In the thermogram, the temperature of the resin mixture was ramped from about 30°C up to the temperature beyond the gel point of each sample using a heating rate of 2°C/min and the dynamic viscosity was recorded. On the left hand side of Figure 6.1, we can see that the liquefying temperature of the

binary mixture as indicated by the lowest temperature that the viscosity rapidly approaches its minimum value significantly decreases with increasing the Ph-a mass fraction. For consistency, the temperature at the viscosity value of 1,000 Pa.s was used as a liquefying temperature of each resin. Based on this convention, the liquefying temperatures of BA-a resin, BP82 and BP64 resin are 73°C, 58°C and 42°C, respectively. This is due to the fact that the Ph-a resin used is liquid while the BA-a resin is solid at room temperature. The addition of the liquid Ph-a in the solid BA-a resin yielded a softer solid at room temperature ranging from BP91 to BP55. With increasing the Ph-a mass fraction beyond 40% by weight i.e. BP64, the resin mixture became highly viscous liquid with decreasing viscosity at room temperature up to the liquid Ph-a. In practice, lowering the resin liquefying temperature obviously enables the use of lower processing temperature for compounding which is desirable in various composite applications.

On the right hand side of Figure 6.1, gel temperature of each resin mixture can also be determined. Interestingly, the gel temperature of each resin ranging from BA-a, BP91, to BP55 showed less influence by the increase in the Ph-a fraction compared with its effect on the liquefying temperature. In this case, the maximum temperature at which the viscosity was rapidly raised above 1,000 Pa.s was also used as gel temperature of each resin for comparison. The gel temperatures of BA-a, BP82, BP64, and Ph-a were determined to be 190°C, 187°C, 185°C, and 185°C respectively. Therefore, the addition of the Ph-a diluent seemed to marginally affect the gel temperature of the BP resin mixtures with the value of few degrees lower than that of the BA-a resin. In general, the opposite trend i.e. an increase in the gel temperature with an addition of a reactive diluent in various resin mixture, has been reported [8]. The addition of the Ph-a diluent to the BA-a resin was; therefore, found to largely maintain the curing or processing condition of the obtained resin mixtures. Furthermore, all the tested BP resin mixtures could maintain their relatively low viscosity within the temperature range of 80°C to 185°C which provided relatively broad processing window, particularly, for the compounding process of the composite manufacturing.

Dynamic shear viscosity of BA-a/Ph-a resin mixture as a function of Ph-a resin content at 90°C is exhibited in Figure 6.2. From the experiment, the mixture viscosity was found to be significantly reduced from that of the neat BA-a benzoxazine resin with increasing mole fraction of the Ph-a diluent. For instance, BP91 (mole fraction of BA-a = 0.79 and Ph-a = 0.21) possessed its melt viscosity measured at 90°C to be about 9 Pa.s while that of the BA-a resin compared at the same temperature was determined to be

approximately 26 Pa.s. The addition liquid Ph-a resin of only 10% by weight (0.21 mole), therefore, can significantly improve the processability of the BA-a benzoxazine resin in terms of reducing the a-stage viscosity of BA-a benzoxazine resin substantially. In theory, the lower viscosity of the resin mixtures can enhance the ability of the resin to accommodate greater amount of filler and enhance wettability of the resin during the preparation of the molding compound. Furthermore, we can see that viscosity of the BA-a/Ph-a resin mixture with increasing the Ph-a content is non-linear. A viscosity model of liquid mixture based on Grunberg-Nissan equation [78] was used to predict the correlation between viscosity and composition fraction. The Grunberg-Nissan equation was the most suitable equation for determining the viscosity of non-associated liquid mixture as reported by Monnery et al. [79] However, a significant result was obtained for some associated liquid mixture. The calculation of liquid viscosity for a binary mixture using this equation is as follows:

$$\ln \eta_m = \sum_{i=1}^c x_i \ln \eta_i + \frac{1}{2} \sum_{i=1}^c \sum_{j=1}^c x_i x_j G_{i,j} \quad (6.1)$$

where $G_{i,i} = 0$. For example, for a binary mixture ($c = 2$)

$$\ln \eta_m = x_1 \ln \eta_1 + x_2 \ln \eta_2 + x_1 x_2 G_{1,2} \quad (6.2)$$

In Eq.(6.1) and Eq.(6.2), η_m is the mean viscosity of liquid mixture (Pa.s), η the viscosity of pure component i and j (Pa.s), x_i and x_j the mole fractions of the component i and j , $G_{i,j}$ the interaction parameter (Pa.s), c the number of components.

Since chemical structures of BA-a benzoxazine and the Ph-a benzoxazine are quite similar, the components in a mixture should not interact with each other and thus should behave in a similar manner as an individual component. Consequently, it was assumed that the interaction parameter ($G_{1,2}$) in Eq. (6.2) would be small and thus could be neglected. Thus Eq. (6.2) can be written as:

$$\ln \eta_m = x_1 \ln \eta_1 + x_2 \ln \eta_2 \quad (6.3)$$

In Figure 6.2, the calculated viscosity curve by the Grunberg-Nissan equation seems to fit well with the experimental viscosity data thus the present approach is suitable

to predict the liquid viscosities at 90°C of the BA-a/Ph-a resin mixture at the entire composition range.

6.1.2 Investigation of the gel formation

One important aspect of thermosetting polymers is their gelation behavior, especially, the kinetics of gelation as well as gel time. Sol-gel transition, known as the gel point, is one critical phenomenon that is crucial, especially from the material appropriate processing conditions and methods. The linear viscoelastic properties in dynamic experiments are sensitive to the three-dimensional network formation and can be used to precisely examine the gel point. In this study, measurements of the oscillatory shear moduli have frequently been used to monitor continuously the viscoelastic properties in chemically cross-linked networks during the gel evolution. The oscillatory experiment is preferable since minimum deformation is applied to the material particularly the delicate gel materials at the gel point. The frequency independence principle of the loss tangent in vicinity of the gel point in accordance with Winter-Chambon criterion has been widely used to define gel point of cross-linked polymers [8,80-83].

In oscillatory shear mode using a rotational controlled stress rheometer, the range of stress that can be applied to the materials is needed to be verified because different types of gels are able to sustain different levels of stress. Therefore, the gel must exhibit the linear relationship between stress and strain, i.e., modulus is constant in the whole stress range used. In the investigation to find the suitable stress, the gel point is obtained of frequencies, i.e., 1 rad/s with 2.5% strain. The gelation temperature used was 140°C for each composition, i.e. BP91, BP73, and BP55. After reaching the gel point which was defined by the crossover of the storage and loss modulus during an isothermal cure, i.e., at the gel point defined that the storage modulus equals the loss modulus as shown in ASTM D4473 standard procedure, the temperature of each the BA-a/Ph-a resin mixtures was then immediately lowered and equilibrated at 120°C to suppress further the gelation process while maintaining the fluidity of the sol fraction and then the stress sweep experiment at the gel point of three different compositions of the BA-a/Ph-a resin mixtures was performed using frequency of 1 rad/s with the stress ranges from 60 to 250 Pa was shown in Figure 6.3. From the plots, we can observe that all of the BA-a/Ph-a systems show a fairly constant modulus in this stress range. This means that the linear viscoelastic relationship can be obtained in this chemically crosslinked systems in the vicinity of a gel point.

In the rest of our experiments, the minimum constant stress value of 60 Pa will be used for gel point determination to ensure both linear viscoelastic relationship as well as minimum gel network rupturing. The dynamic moduli of a curing system under oscillatory shear follow the power law at the gel point [8, 84-86]. The power law equation at the gel point may be used to examine the gel time and the corresponding value of the relaxation exponent shown in Eq. (6.4)

$$\tan \delta = G''/G' = \tan (n\pi/2) \quad (6.4)$$

when n is the relaxation exponent.

Figure 6.4 show a plot of $\tan \delta$ as a function of time of BP91 for each of the individual frequencies, i.e., 10 rad/s, 31 rad/s, and 100 rad/s, at 140°C. The gel time is obtained from the point where the loss tangent is frequency independent. Experimentally, it is the point where the loss tangent of different frequencies intersects each other. From the plot, the values of $\tan \delta$ intersect at a time = 198 min corresponding to the gel time, t_{gel} . The gel times for the BA-a/Ph-a systems, at different temperatures, were obtained from $\tan \delta$ plots similar to Figure 6.4. The relationship of gel time as a function of temperature of the BA-a/Ph-a systems was presented in Table 6.1. We can see that the gel time of all resin mixture compositions tends to decay behavior of the gel time with increasing temperature. This is due to the fact that increasing the processing temperature increases the rate of cross-linking of BA-a/Ph-a systems. Consequently, at higher temperature, the systems reach their gel points more quickly and the gel times are shorter, i.e., the gel time of BP91 ranges from 198 min at 140°C to about 63 min at 170°C. Moreover, at the same temperature, we can observe that the gel time decreased with increasing the Ph-a content due to their faster cross linking rates. For instance at 140°C, the gel time of BA-a/Ph-a systems are: BP91 = 198 min, BP73 = 185 min, and BP55 = 182 min. This also implies that the curing conversion also increases with the Ph-a resin content compared at the same processing condition.

As mentioned in Eq. (6.4), at the gel point, a power law may be used to examine the corresponding value of the relaxation exponent, n , for each gelling systems. The relaxation exponent is a specific parameter that is related to the growing clusters in a material, which appear as the connectivity increases near the gelation threshold. For the BA-a/Ph-a systems, the relaxation exponents at the gel point were determined from $\tan \delta$

plots and by using Eq. (6.4). Figure 6.5 is a plot of the relaxation exponent as a function of cure temperature of BP91, BP73, and BP55, compared at the same cure temperature, are almost unchanged with the Ph-a content. Moreover, the relaxation exponent tends to decreased with increasing the cure temperature. Recently, the relaxation exponent values of the chemical gel systems have been reported to show a non-universal value and vary with the gelling system. The values of the relaxation exponent of the chemical gels were reported to be 0.2-0.7 in PDMS system [87], 0.5-0.7 in polyurethane system [88], and 0.68-0.72 in BA-m benzoxazine system [85] etc. In this work, the relaxation exponent values of BA-a/Ph-a systems were found to be 0.24-0.55 depending on the cure temperature. This indicates that the cure temperature shows some effect on the structure of the network formed at the gel point for these BA-a/Ph-a systems.

Furthermore, from the gel times calculated at different temperatures, we can then determine apparent activation energies for the BA-a/Ph-a systems. The curing reaction can be represented by a generalized kinetic equation.

$$\frac{dx}{dt} = k(T)f(x) \quad (6.5)$$

where $k(T)$ is the rate constant, t is the time of reaction, $f(x)$ represents an arbitrary functional form for the curing conversion, T corresponds to the temperature of the reaction. The rate constant, $k(T)$, is temperature dependent according to Arrhenius law shown in Eq. (6.6)

$$k(T) = A \exp(-E/RT) \quad (6.6)$$

An integration of Eq. (6.5) from the onset of the cross-linking reaction ($t = 0$, and $x = 0$) to the gel point ($t = t_{gel}$, and $x = x_c$) to obtain

$$\ln(t_{gel}) = \ln\left(\int_0^{x_c} dx/f(x)\right) - \ln(A) + E/RT \quad (6.7)$$

where t_{gel} is the gel time, A is the pre-exponential factor, and E is the activation energy, and T is temperature in Kelvin.

Thus, the activation energies for gelation can be determined from the slope of the plots between $\ln(t_{gel})$ against $1/T$ as depicted in Figure 6.6 and the corresponding activation energies are summarized in Table 6.2. We can notice that the activation energy

values of BP91, BP73, and BP55 are approximately the same. That means the Ph-a reactive diluent does not significantly affect the kinetics of the gelation process of the resin mixtures. The apparent activation energy value averaged from the slopes of the plots was determined to be 60.6 ± 1.5 kJ/mol. The value is in the same range as that of epoxy molding compound, using the same technique to determine the gel point, i.e. $E = 61-73$ kJ/mol [86,89].

6.1.3 Curing reaction study by calorimetry

The DSC thermograms for the curing reaction of the BA-a resin, the Ph-a diluent, and the BA-a/Ph-a mixtures at various compositions, i.e. BP82, BP55, and BP28, are shown in Figure 6.7. From the thermograms, we observed only single dominant exothermic peak of the curing reaction in each resin composition above. The phenomenon suggested that the reaction to form a network structure of these binary mixtures took place simultaneously at about the same temperature. In our previous work, the split of the curing exotherms with an addition of a reactive diluent i.e. in benzoxazine-epoxy resin mixture has been observed. In these resin systems, the newly formed exothermic peak at higher temperature was attributed to the interaction between the benzoxazine monomer and the epoxy diluent whereas the peak at lower temperature was due to the reaction among the benzoxazine monomers [58].

On the contrary, the curing peak temperature observed in our BA-a/Ph-a mixtures in Figure 6.7 was systematically shifted to a slightly lower temperature with increasing the Ph-a diluent. This is due to the fact that the curing peak exotherm of the BA-a resin was determined to be 228°C while that of the Ph-a diluent was found to be 217°C . Our Ph-a diluent thus possessed a slightly low curing temperature comparing with the base BA-a resin. Its addition into the BA-a resin; therefore, rendered a positive effect on curing reaction of the obtained resin mixture by lowering its curing temperature even though only marginally. A relationship between curing conversion with curing time of the BA-a/Ph-a resin mixtures at 180°C was illustrated in Figure 6.8. The trend of each curve is similar with the observed dramatic increase in the degree of conversion at the first 30 minutes of the curing program. The longer curing time beyond 30 minutes could increase the degree of conversion of each resin rather gradually with the maximum achievable conversion depending on the resin composition. From the plot, the curing conversions at 180°C and 120 min of the Ph-a, BP28, BP55, BP82 and BA-a polymers are 98%, 96%, 91%, 83% and 76%, respectively. This result also suggested that our Ph-a reactive diluent

rendered a faster curing than the BA-a. Its present in the BA-a can help lowering the curing temperature of the resulting resin mixtures.

6.1.4 Mechanical property of the polymer hybrids

The effect of the Ph-a composition on the dynamic mechanical properties of the BA-a/Ph-a polymers is depicted in Figure 6.9 to Figure 6.11. The storage modulus in the glassy state region reflecting molecular rigidity of the BA-a/Ph-a polymer networks is shown in Figure 6.9. From this figure, we can clearly see that the storage modulus of the poly(Ph-a) is higher than that of the poly(BA-a). The storage modulus at the room temperature of the poly(Ph-a) exhibits a value of about 6.7 GPa whereas that of the poly(BA-a) is approximately 5.7 GPa. The Ph-a network is thus stiffer molecularly than the BA-a network. Moreover, the storage modulus of the BA-a/Ph-a polymers was found to systematically increase when the Ph-a resin composition increased as a result of the addition of the more rigid molecular segments of the poly(Ph-a) into the network as discussed above. However, the replacement of the poly(BA-a) molecule with the Ph-a resin showed trend to decrease the modulus in the rubbery plateau of. This suggests that the increase in the Ph-a resin composition of the the BA-a/Ph-a polymers results in the reduction the number of the cross-linked density of the polymer hybrids.

The glass transition temperatures (T_g s) of the BA-a and Ph-a polymers as well as their copolymers were determined from the loss modulus peak in the dynamical mechanical thermograms as seen in Figure 6.10. The average $T_{g, DMA}$ of the poly(Ph-a) and poly(BA-a) were reported to be about 115°C and 160°C, respectively [55,57,59,76]. In Figure 10, the T_g s of the BP polymer hybrids were expectedly found to increase with the mass fraction of BA-a polymer. In our study, the T_g s of poly(BA-a), BP82, BP64, and poly (Ph-a) were determined to be 160°C, 142°C, 128°C, and 111°C, respectively. The T_g values of both parent polymers are consistent with those reported elsewhere [55,57,59,76] with the T_g s of their polymer hybrids varied systematically depending on the composition of the BP polymers. The loss modulus curve for each BP composition also reveals only one α -relaxation peak suggesting the presence of a single phase material in these polymer hybrids. In theory, if the two starting materials had undergone phase separation upon copolymerization, two glass transition peaks would be expected, one for each of the starting homopolymer.

The $\tan\delta$ curve of the BA-a/Ph-a polymers at various the Ph-a contents was also depicted in Figure 6.11. Again, only a single $\tan\delta$ peak was observed in each BP polymer in good agreement with the loss modulus result in Figure 6.10. The magnitude of the α -relaxation from $\tan\delta$ peak reflects trend in large scale segmental mobility in the polymer network. In the network, a greater separation between crosslinks permits greater mobility of chain segments while the width of the α -relaxation peak of the $\tan\delta$ curve relates to network homogeneity. From our experiment, the maximum amplitude of the α -relaxation peak was found to increase with increasing the Ph-a resin composition. This behavior suggested the lower crosslinking density of the BP polymers when the Ph-a mass fraction increased thus allowing greater segmental mobility in the polymers. The lower degree of crosslinking of the BP polymers with the amount of the Ph-a content was also confirmed by the lower rubbery plateau modulus of the polymer hybrids with increasing the amount of the Ph-a diluent as shown in Figure 6.9. Moreover, the widths at half height of the α -relaxation peaks are about the same for all Ba-a/Ph-a polymers. This implies that the degree of network homogeneity of the two polymers as well as their hybrids is likely to be similar.

Figure 6.12 shows the flexural moduli of the specimens at different Ph-a contents. From this plot, the flexural moduli of the samples were found to increase with increasing the Ph-a resin. This correlation is in good agreement with the modulus values obtained from our dynamic mechanical analysis in the previous section. The flexural modulus of the poly(BA-a) was calculated to be 5.69 ± 0.14 GPa while that of the poly(Ph-a) was 6.51 ± 0.15 GPa. Furthermore, the flexural modulus values of the BA-a/Ph-a polymers at various Ph-a contents ranging from 0-50% by weight tended to increase with the poly(Ph-a) mass fraction. For instance, BP55 possesses a flexural modulus value of about 6.41 ± 0.28 GPa which is also close to that of poly(Ph-a). The phenomenon was attributed to the ability of the Ph-a diluent to easily react to be a crucial part of the BA-a polymer networks as a result of their similarity in chemical nature. In Figure 6.13, the flexural strength of the poly(Ph-a) was found to be significantly lower than that of the poly(BA-a) i.e. 50 MPa vs. 152 MPa of poly(BA-a). Additionally, the flexural strength of the BA-a/Ph-a polymers was observed to decrease with increasing the Ph-a content in the polymer hybrids from 0 to 50% by weight. The lower degree of crosslinking of the poly(Ph-a) comparing with that of poly(BA-a) might be responsible for the observed characteristics. The phenomenon is also understandable as the Ph-a resin

has functional groups only half of those of BA-a resin. Its ability to crosslink is thus inferior to that of BA-a resin.

6.1.5 Thermal degradation behaviors of BA-a/Ph-a polymers

The TGA thermograms of the poly(BA-a), the poly(Ph-a), and the BA-a/Ph-a polymers were shown in Figure 6.14. Intriguingly, all specimens exhibited an improvement in their degradation temperature at 5% weight loss and char yield over the poly(BA-a) with an addition of the Ph-a diluent. The degradation temperature at 5% weight loss of the poly(BA-a) was determined to be 334°C comparing with the value of 352°C of the poly(Ph-a). In addition, the decomposition temperature of the BA-a/Ph-a polymers was found to gradually increase with increasing the mass fraction of the poly(Ph-a) as shown in the inset of Figure 6.14. This behavior can be explained by the fact that there was no *isopropyl* moiety in the poly(Ph-a) structure. Therefore, the less stable, weaker moieties in the poly(Ph-a) structure were eliminated whereas in poly(BA-a), the *isopropyl* linkages from its bisphenol-A structure had been reported to undergo thermal decomposition at relatively lower temperature [51,76,90].

The study on a bisphenol-A-based polybenzoxazine exposed to ultraviolet radiation had revealed that the *isopropyl* linkage was the reactive site of cleavage and oxidation [91]. Moreover, the substituents of poly(Ph-a) are also different from that of poly(BA-a). Poly(BA-a) has only one unblocked *ortho* position to form the hydroxyl group that is subjected to electrophilic aromatic substitution upon its ring-opening polymerization while the poly(Ph-a) has two unblocked positions, one at the *ortho* and another at the *para* position. The study on polybenzoxazine model dimers had demonstrated that the absence or presence of the substituents had profound effects on thermal decomposition patterns and the char formation of the dimers. Therefore, the absence of *isopropyl* moiety along with the absence of substituents at both *ortho* and *para* positions are likely responsible for the greater thermal stability of the poly(Ph-a) [39,81]. Other possibilities, such as fewer short-chain branches in the poly(Ph-a) structure that could serve as the initiation sites of the degradation process, could also have attributed to the improvement of its thermal stability. As a result, the char yield of the BA-a/Ph-a polymers systematically increased from that of the poly(BA-a) with the increase in the Ph-a content.

Table 6.1 Gelation times of BA-a/Ph-a systems at different temperature

Temperature (°C)	Gelation Time, T_{gel} (min)		
	BP91	BP73	BP55
140	198	185	182
150	152	147	142
160	94	89	82
170	63	62	58



สถาบันวิทยบริการ
จุฬาลงกรณ์มหาวิทยาลัย

Table 6.2 The apparent activation energy values obtained from the rheological tests for the BA-a/Ph-a systems at various Ph-a resin contents.

BP contents	Activation energy (kJ/mol)
BA-a	88*
BP91	61
BP73	59
BP55	62

* E value of benzoxazine resin (BA-a) from Ref.85.



สถาบันวิทยบริการ
จุฬาลงกรณ์มหาวิทยาลัย

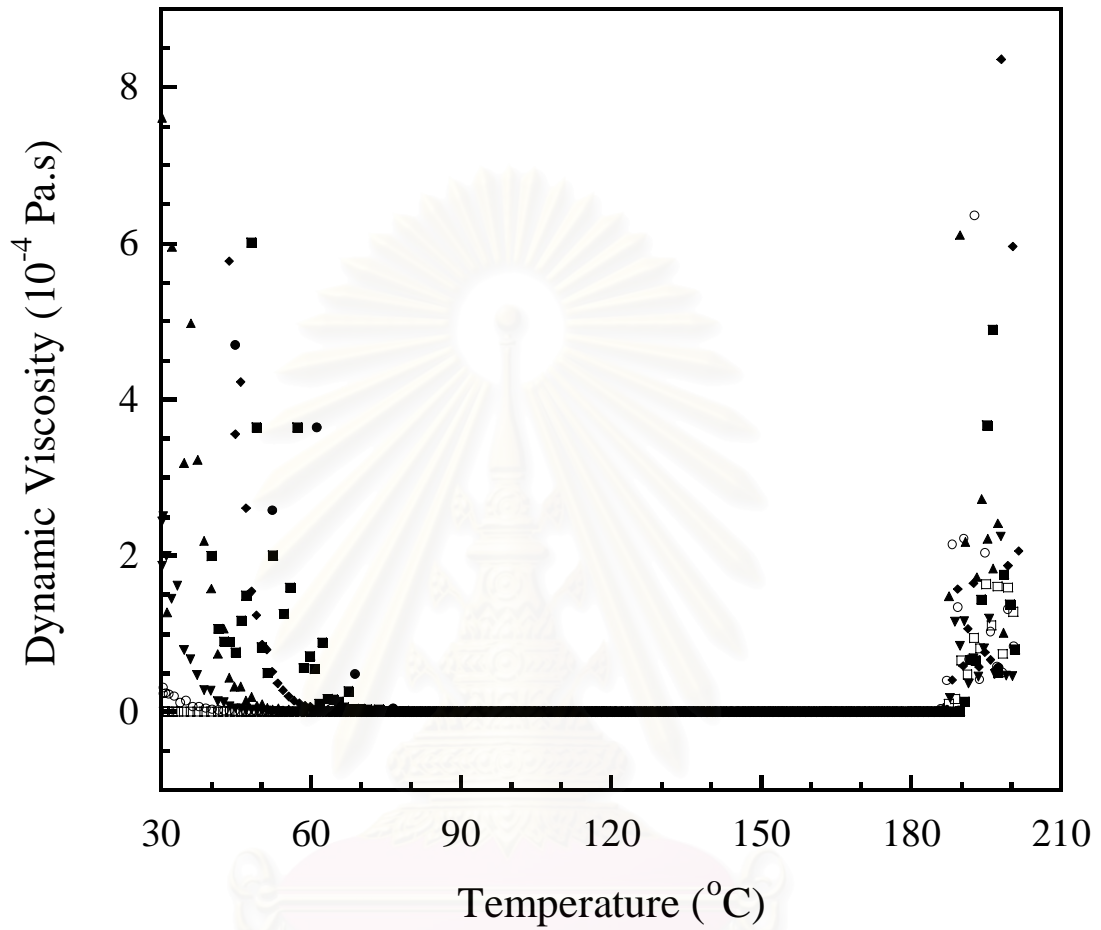


Figure 6.1 Processing window of the BA-a/Ph-a resin mixtures at various Ph-a resin using a heating rate of 2° C/min: (●) BA-a resin, (■) BP91, (◆) BP82, (▲) BP73, (▼) BP64, (○) BP55, (□) Ph-a resin.

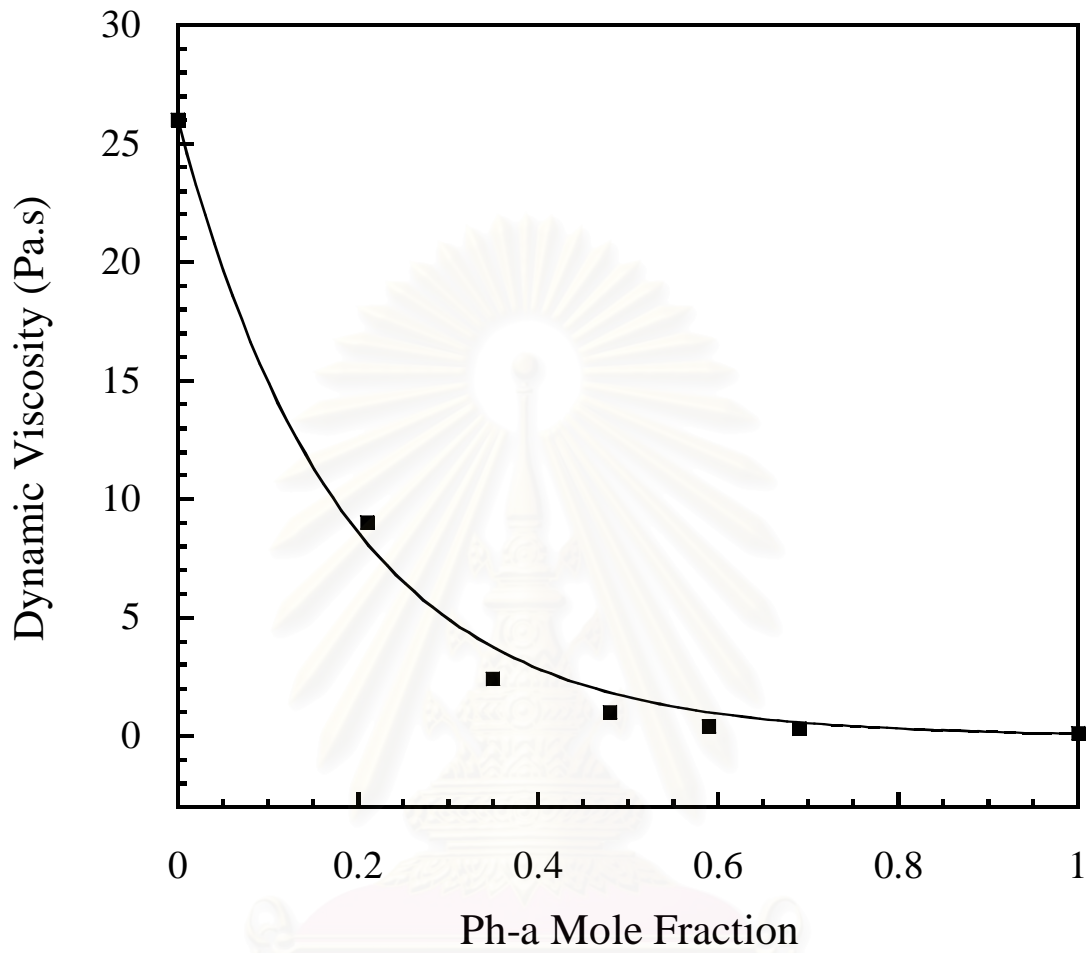


Figure 6.2 Dynamic viscosity at 90°C of the BA-a/Ph-a resin mixtures at various Ph-a mole fractions: Experimental data (symbol), Predicted data with the Grunberg-Nissan equation (solid line).

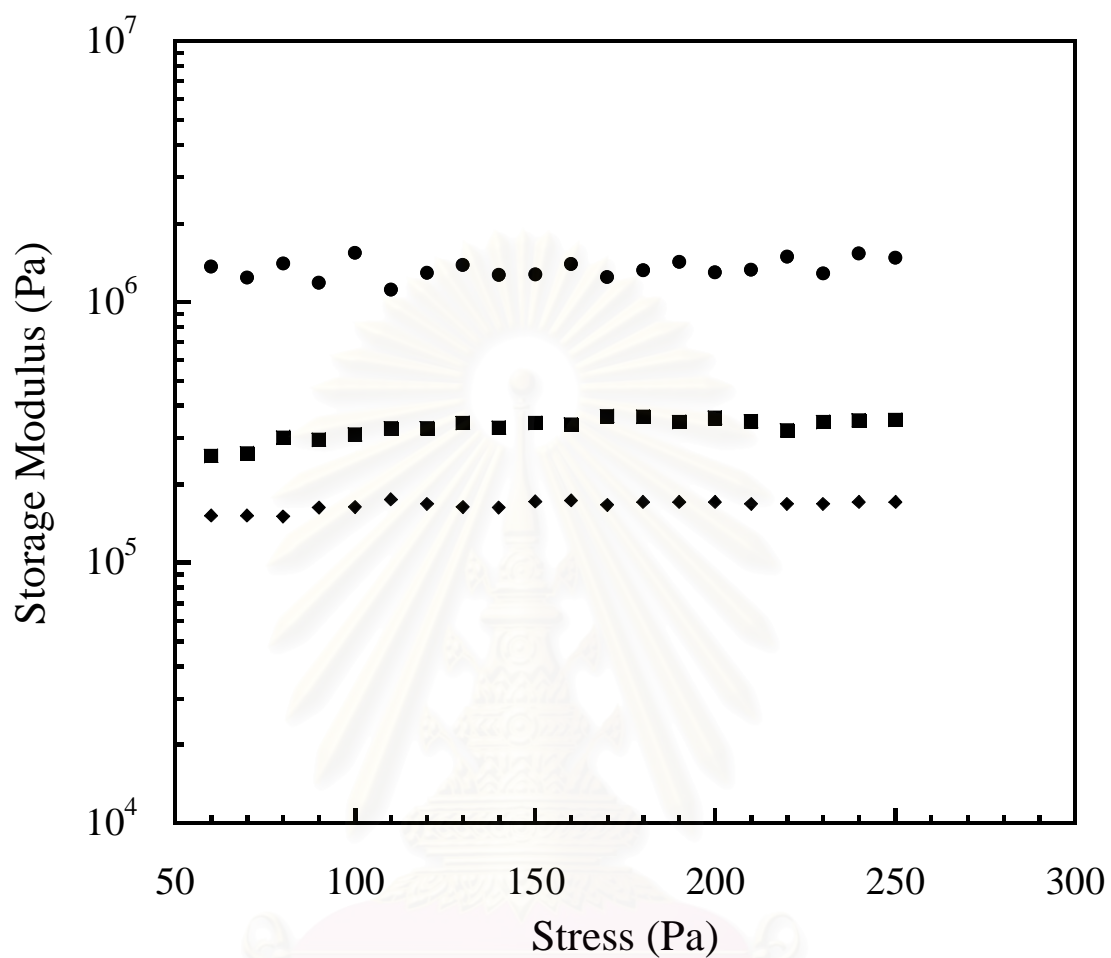


Figure 6.3 Stress sweep experiment at the gel points of BP systems: (●) BP91, (■) BP73, (◆) BP55.

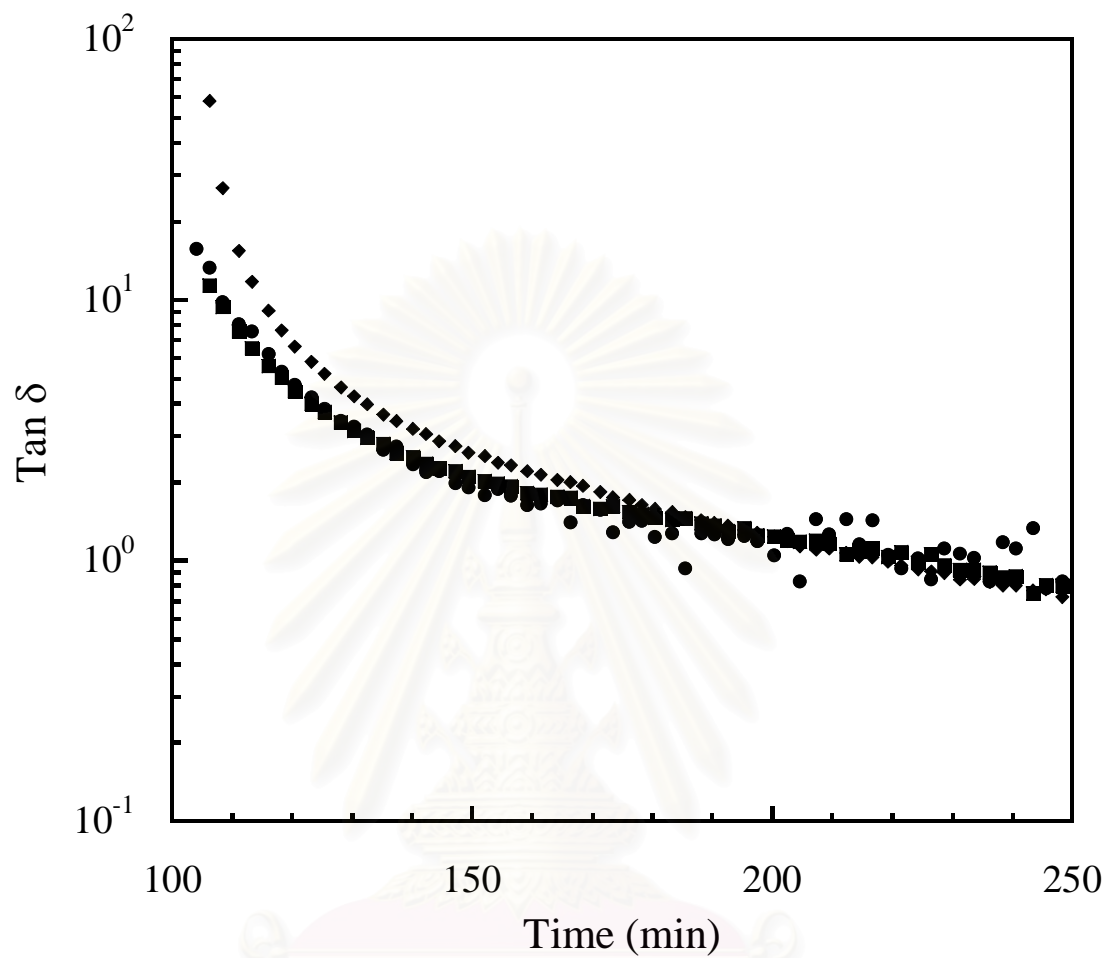


Figure 6.4 Loss tangent at various frequencies as a function of time for BP91 at 140°C :

(●) 10 rad/s, (■) 31 rad/s, (◆) 100 rad/s.

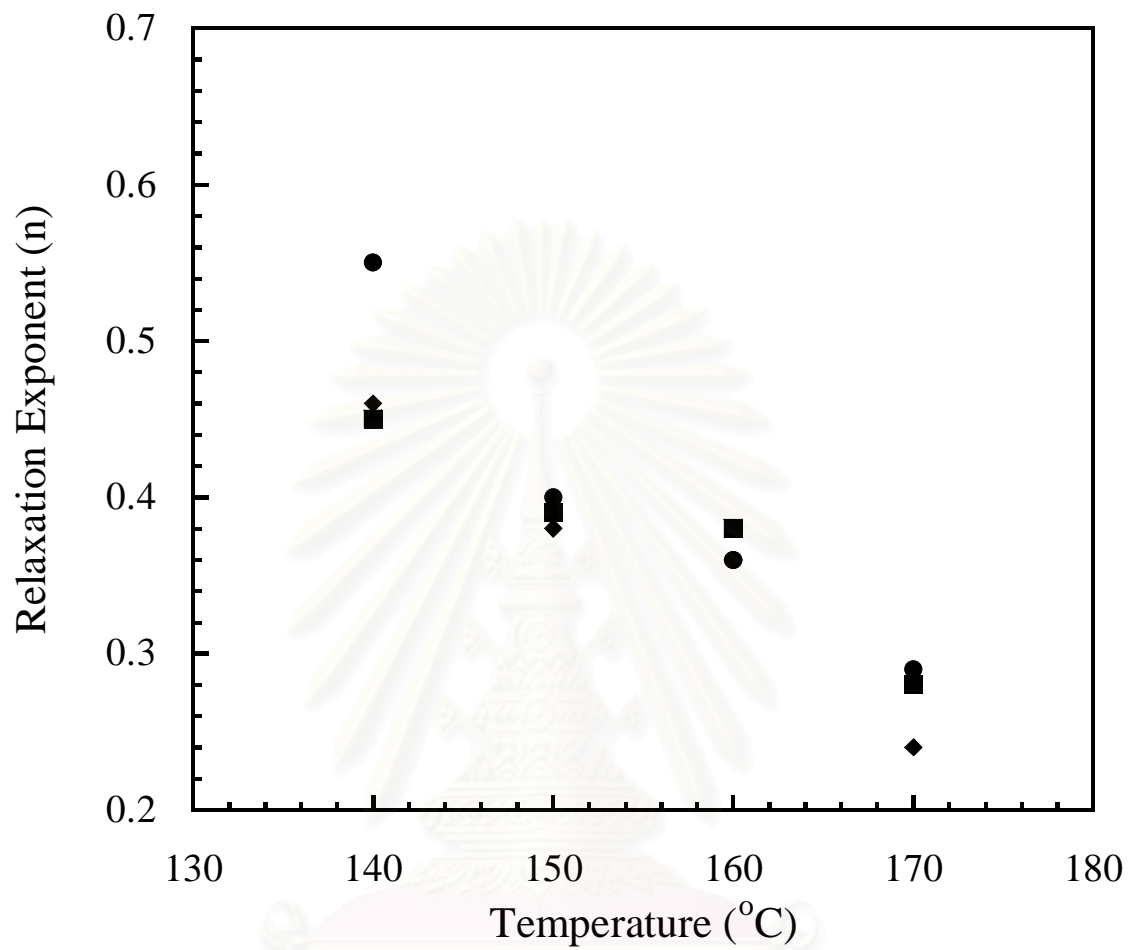


Figure 6.5 The relaxation exponent, n , from gel point as a function of cure temperature at different Ph-a resin content: (●) BP91, (■) BP73, (◆) BP55.

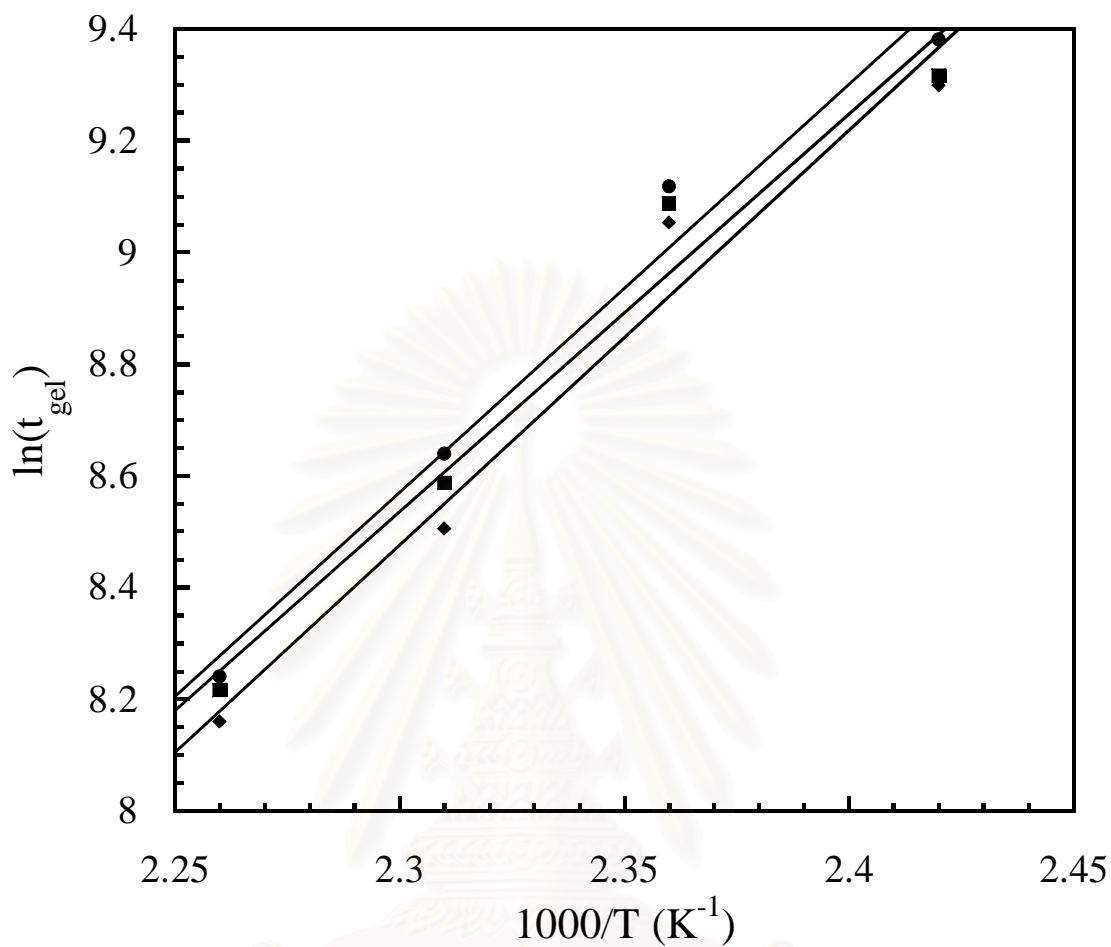


Figure 6.6 Plots of gel times as a function of $1/T$ based on rheology data at various Ph-a mass fractions: (●) BP91, (■) BP73, (◆) BP55.

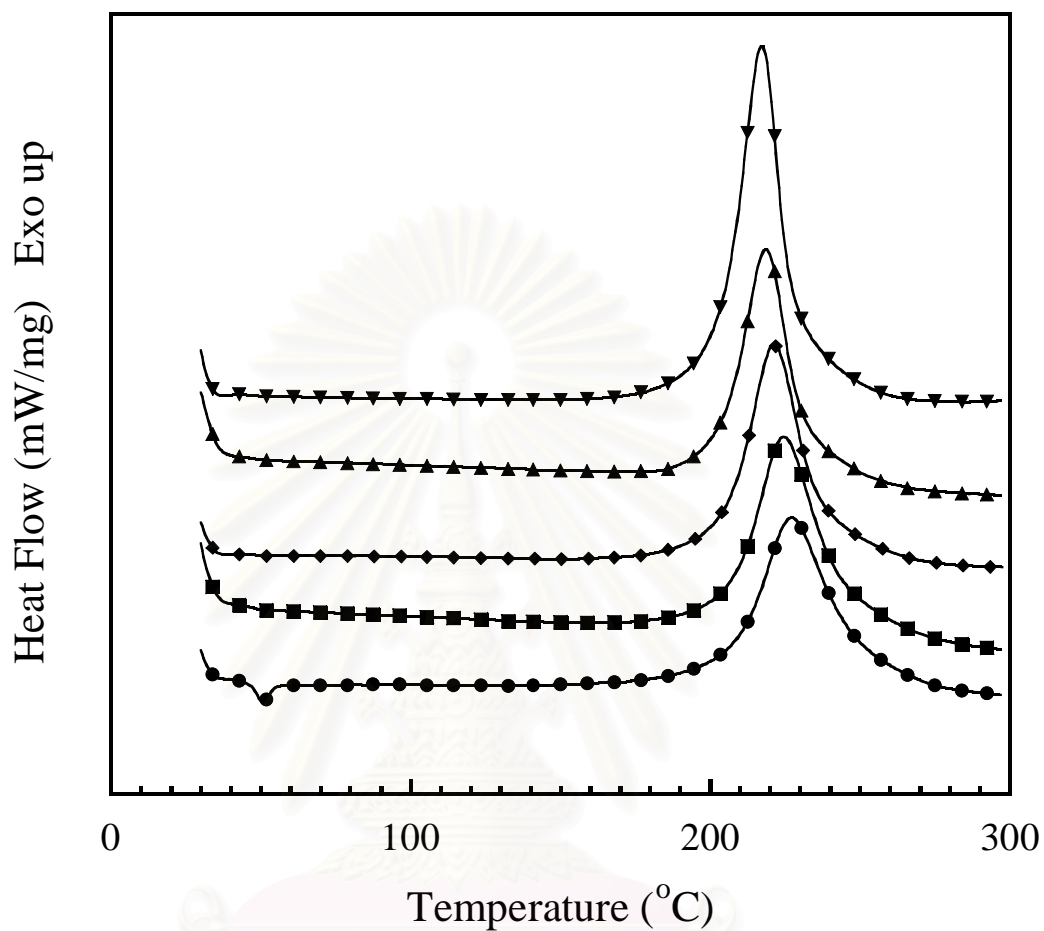


Figure 6.7 DSC thermograms of the BA-a/Ph-a resin mixtures at different Ph-a resin contents: (●) BA-a resin, (■) BP82, (◆) BP55, (▲) BP28, (▼) Ph-a resin.

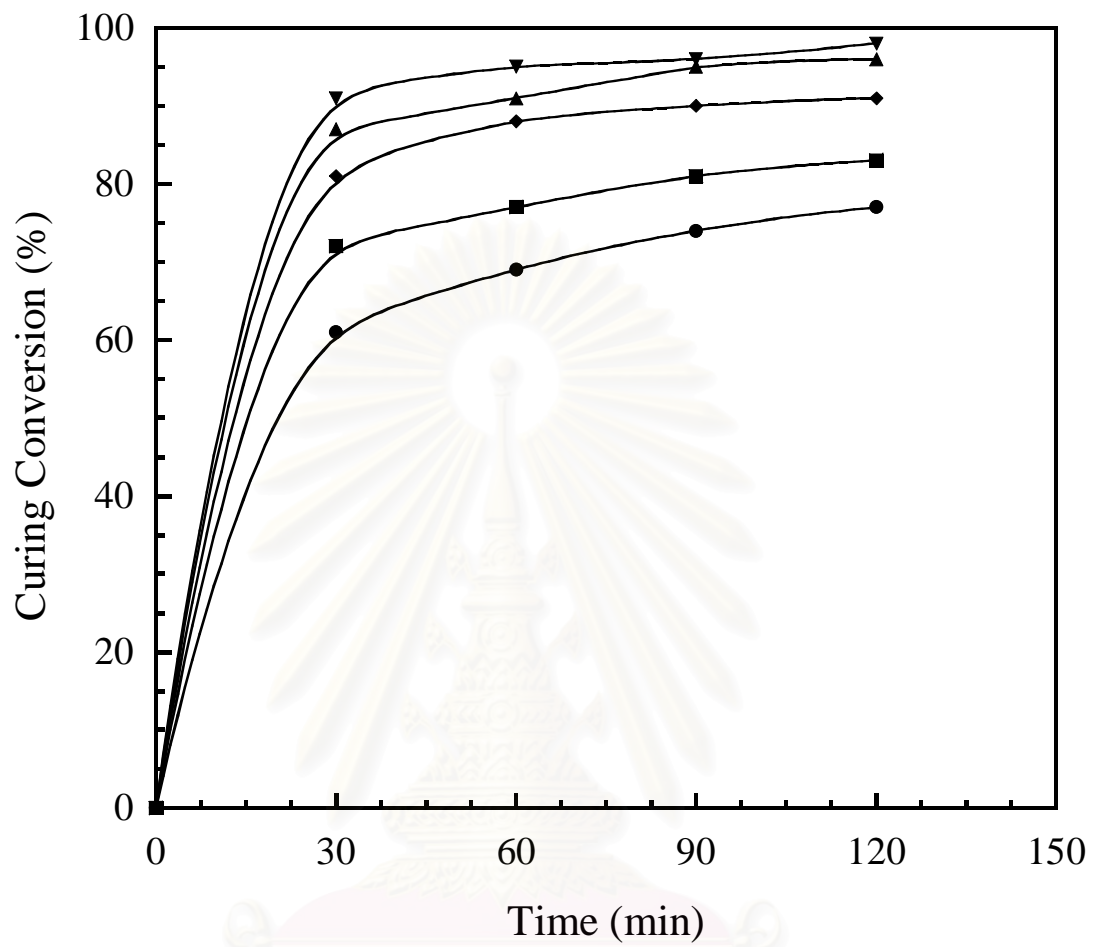


Figure 6.8 Conversion-time curve of thermally cured the BA-a/Ph-a mixtures at 180°C:

(●) BA-a resin, (■) BP82, (◆) BP55, (▲) BP28, (▼) Ph-a resin.

จุฬาลงกรณ์มหาวิทยาลัย

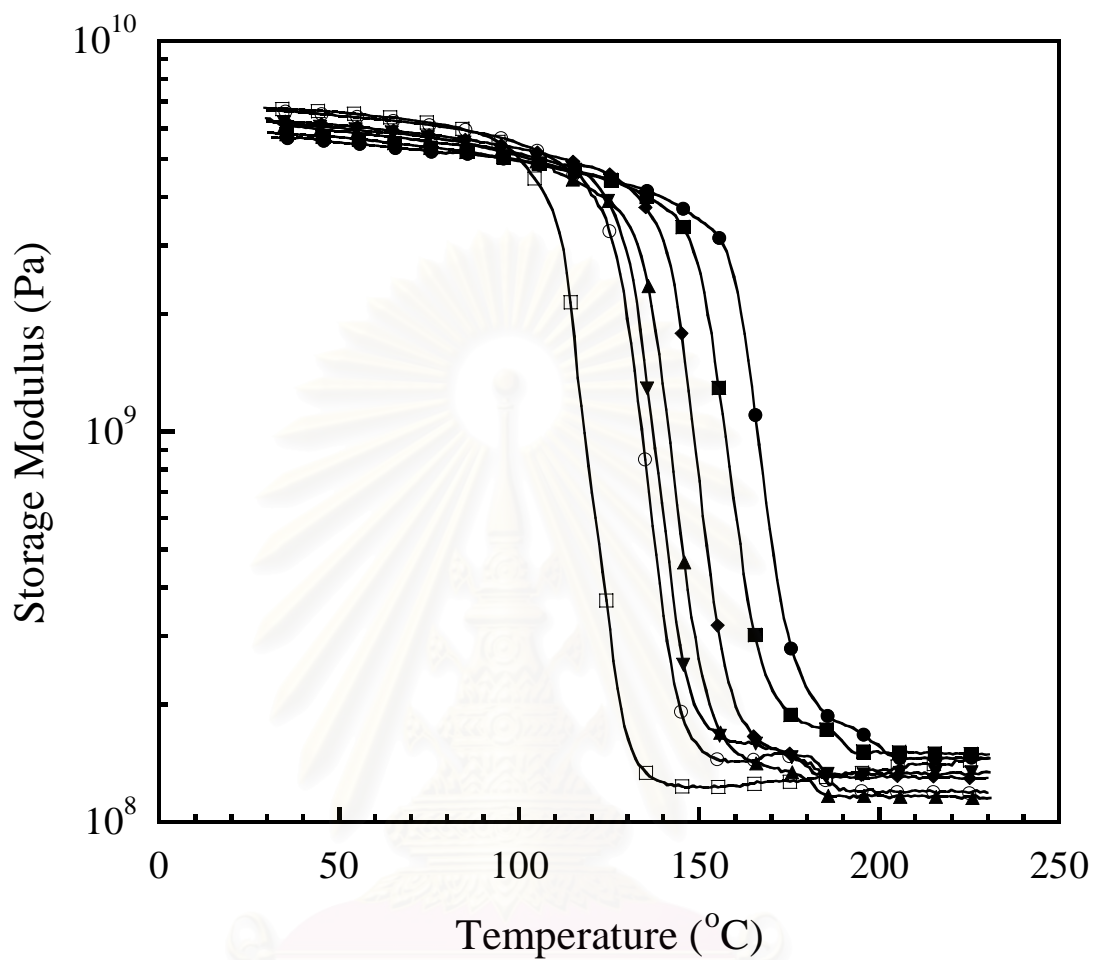


Figure 6.9 Storage modulus of the BA-a/Ph-a polymer as a function of temperature at different Ph-a contents: (●) poly(BA-a), (■) BP91, (◆) BP82, (▲) BP73, (▼) BP64, (○) BP55, (□) poly(Ph-a).

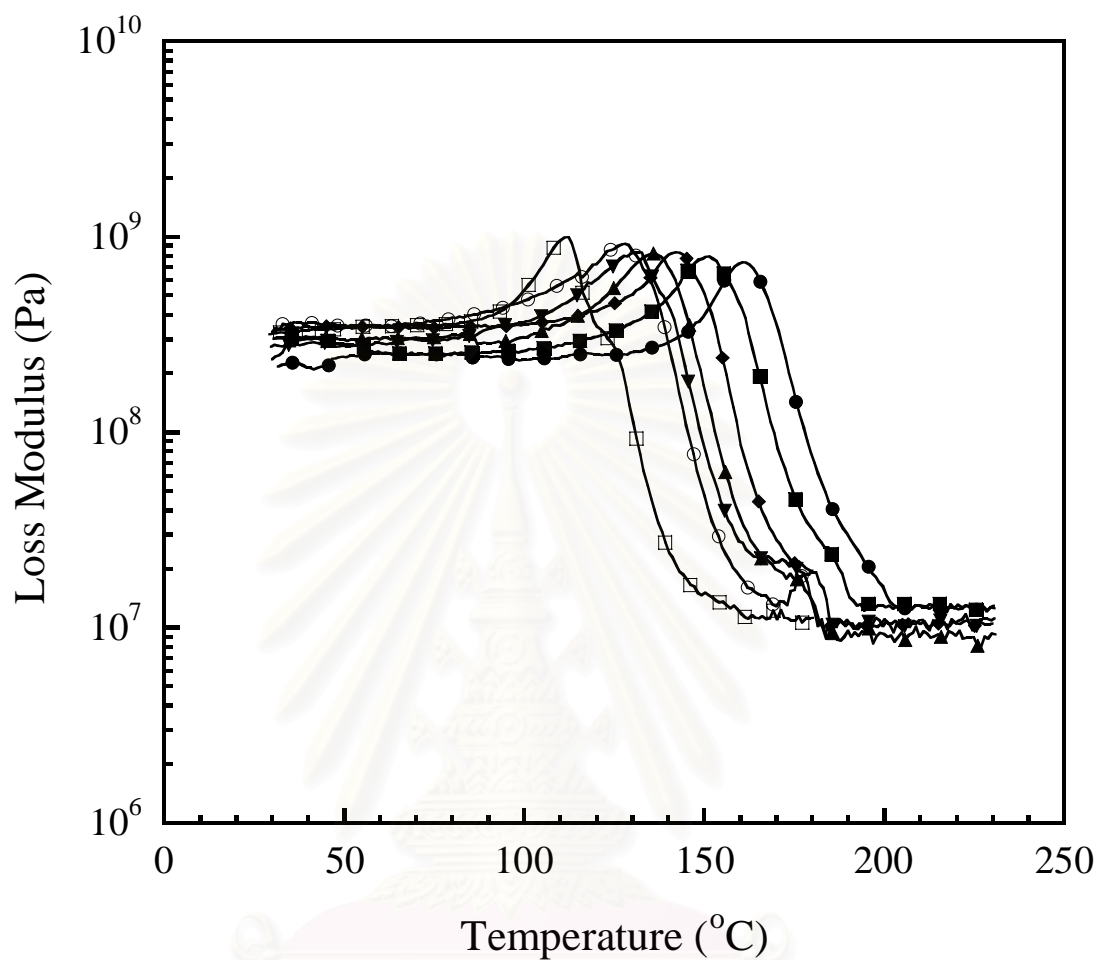


Figure 6.10 Loss modulus of the BA-a/Ph-a polymer as a function of temperature at different Ph-a contents: (●) poly(BA-a), (■) BP91, (◆) BP82, (▲) BP73, (▼) BP64, (○) BP55, (□) poly(Ph-a).

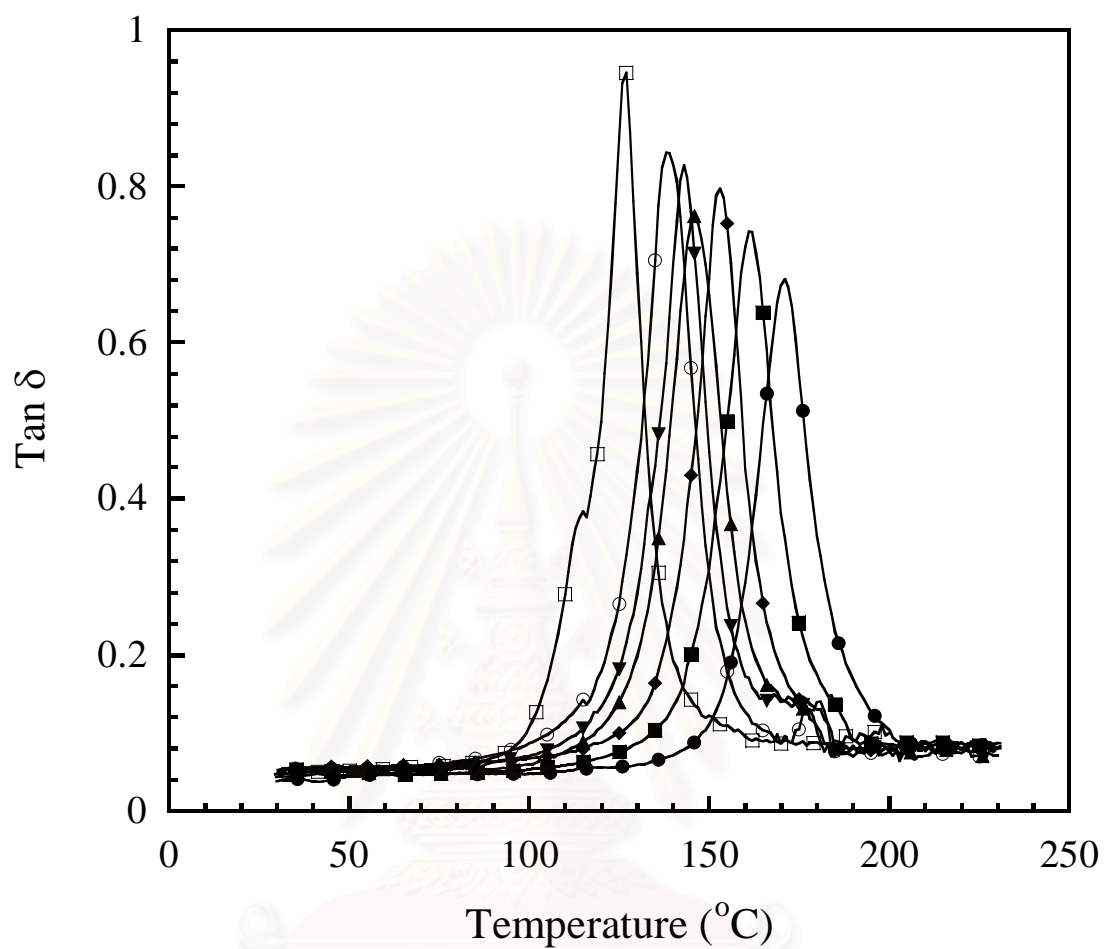


Figure 6.11 Tan δ of the BA-a/Ph-a polymers as a function of temperature at different Ph-a contents: (●) poly(BA-a), (■) BP91, (◆) BP82, (▲) BP73, (▼) BP64, (○) BP55, (□) poly(Ph-a).

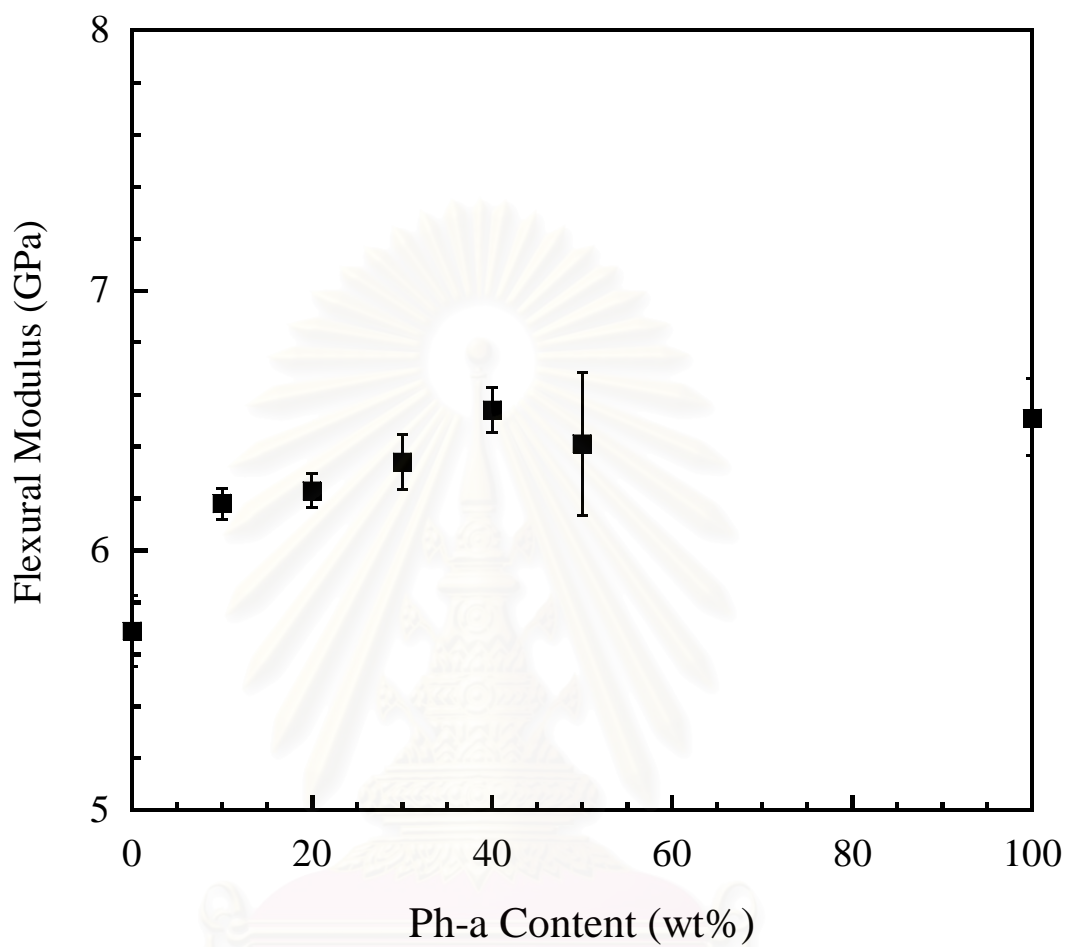


Figure 6.12 Flexural modulus of the BA-a/Ph-a polymers as a function of Ph-a compositions.

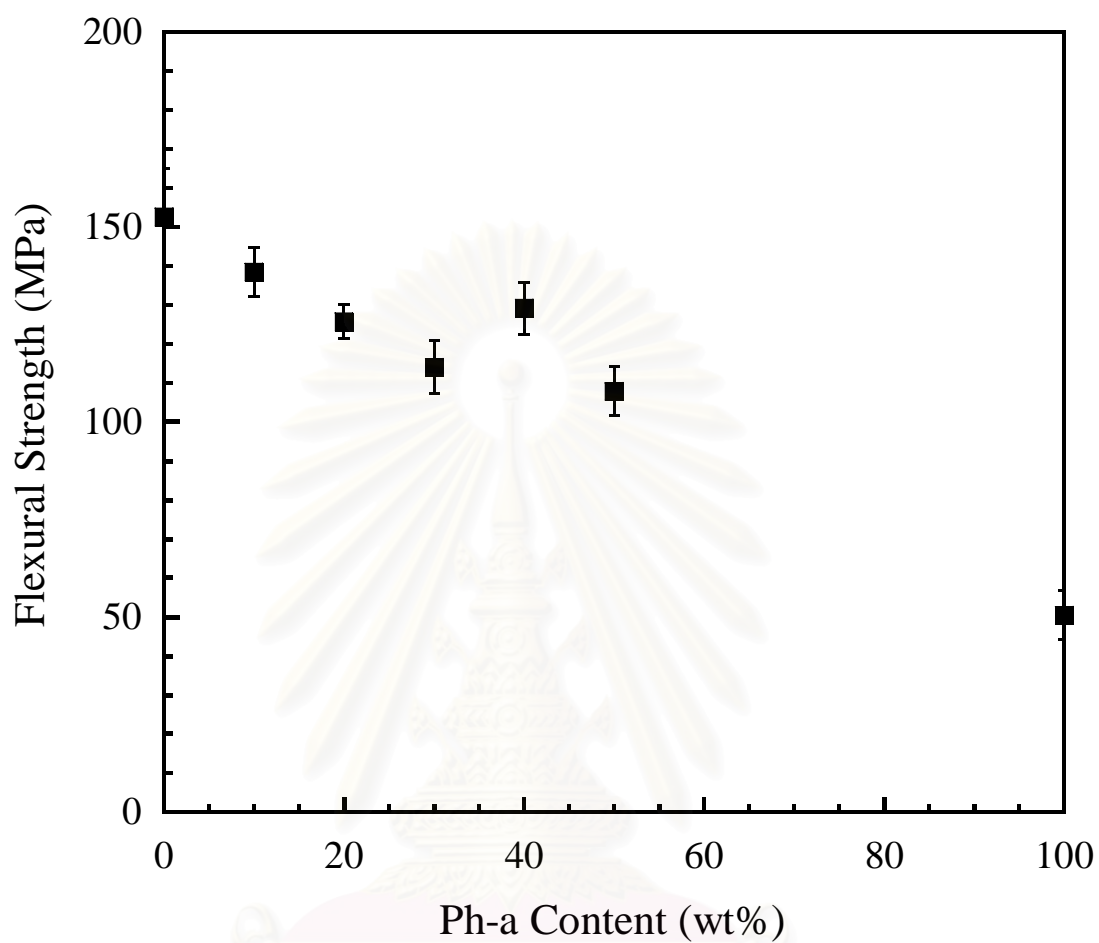


Figure 6.13 Flexural strength of the BA-a/Ph-a polymers as a function of Ph-a compositions.

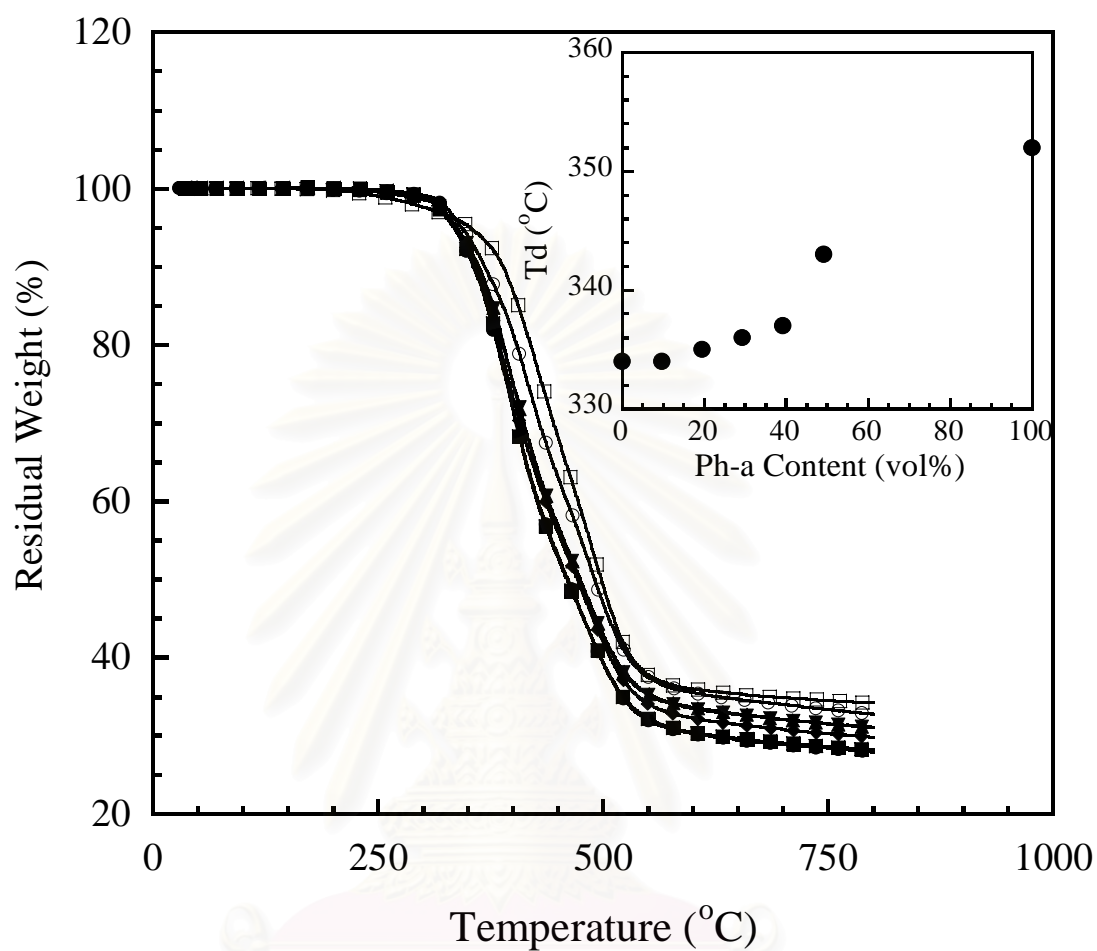


Figure 6.14 TGA thermograms of the BA-a/Ph-a polymers at different Ph-a mass fractions: (●) poly(BA-a), (■) BP91, (◆) BP82, (▲) BP73, (▼) BP64, (○) BP55, (□) Poly(Ph-a).

CHAPTER VII

HIGH PERFORMANCE WOOD COMPOSITES BASED ON BENZOXAZINE-EPOXY ALLOYS

Polymeric matrices reinforced with woodflour filler or natural fiber show a rapid growth recently due to their many advantages such as light weight, reasonable strength, and stiffness. Their processing is flexible, and economical. In addition, the use of waste wood will help solving the severe environmental problem [92,93]. Many researches in recent years have gained much attention in using some thermosetting [94,95] and thermoplastics i.e. polyethylene [96-98], polypropylene [99,100], polystyrene [101], polyvinyl chloride [102,103] as wood composite's matrices due to their promising ability to render improved composite performance from recycled materials [41,104]. However, the main problem encountered in using this type of matrix is its rather poor interfacial adhesion between the polar untreated wood particle and the more hydrophobic characteristics of those polymeric matrices [105,106]. The polar nature of woodflour results in a relatively low composite's strength, poor stiffness and high moisture sorption characteristics. Another major shortcoming of this type of matrix is the relatively low filler content, typically of less than 50-60% by weight, to be added into the matrix [107,108]. One way to achieve greater wood filler content is a modification at the interface between the wood filler and the matrix either using physical or chemical treatments [109,110]. However, the surface treatment of filler normally increases both processing steps and its cost.

As mentioned previously, the mixture of benzoxazine, epoxy, and phenolic novolac resins to form the BEP ternary systems can provide a large variety of resin properties suitable for wide applications, particularly in the highly filled systems. Therefore, the main objective of this study is to investigate the effect of the ternary system composition on their processing ability and their interaction with *Hevea brasiliensis* woodflour. The obtained mechanical and thermal performance of their wood composites will also be evaluated.

7.1 Results and discussion

7.1.1 Chemorheological properties

The complex viscosities of the BEP811, BEP721, BEP631, BEP541 and BEP451 as a function of temperature are shown in Figure 7.1. In the rheograms at low temperatures, all resin mixtures showed a relatively high viscosity due to the solid state nature of these mixtures at room temperature. Upon heating, these uncured mixtures become softened and their viscosity rapidly decreased as the temperature approached their softening points. The next stage was the lowest viscosity range of the BEP mixtures which provided a processing window for the compounding process of each mixture. At the final stage or at higher temperature, gel temperature which is related to the gel point of each resin mixture can also be determined.

As can be seen from the rheograms in Figure 7.1, the complex viscosities compared at the same temperature range of the BEP mixtures at various epoxy resin fractions tended to decrease with an increase in the amount of the epoxy. This could be due to the fact that epoxy resin is liquid while both benzoxazine and phenolic resins are solid at room temperature. The liquefying temperatures of these mixtures, determined from an intersection between the horizontal line of the lowest viscosity region and the slope of the first-stage viscosity, also systematically decreased with increasing epoxy content in the BEP mixtures. From Fig.1, BEP451 exhibited the lowest liquefying temperature of 75°C, while BEP811 showed the highest liquefying temperature of 92°C among the tested mixtures. On the other hand, the gel point of these BEP mixtures tended to decrease with an increase in the amount of the benzoxazine resin in these BEP mixtures. The rheograms reveal that BEP811 mixture had the lowest gel temperature of 162°C, while those of BEP721, BEP631, BEP541, and BEP451 were determined to be 164°C, 166°C, 175°C, and 180°C, respectively. These gelation characteristics are consistent with the results reported [8].

7.1.2 Evaluation of activation energy for gelation of the BEP resin mixtures

The gel times at different temperatures in the range of 135 to 150°C were determined based on the Winter-Chambon criterion and are shown in Table 7.1. From the tabulated data with increasing the gelation temperature, the gel time of each BEP resin i.e. BEP541, BEP631, and BEP721, expectedly decreased. To determine activation energy of gelation of the BEP resins, the Arrhenius plots of the gel time at different temperatures of

the resins obtained following Eq. (6.7) were also shown in Figure 7.2. From the figure, the slopes of the three curves, which are related to the activation energies of the BEP541, BEP631, BEP721, are approximately the same, i.e., 35, 36, and 40 kJ/mol, respectively. That means epoxy content in the BEP resins will not significantly change the kinetics of the gelation process. However, the substantial difference in the figure is the y-axis intercepts at which BEP721 shows the smallest intercept value and BEP541 provides the largest value. That is BEP721 requires lower starting temperature for the gelation process than BEP631 and BEP541.

7.1.3 Effect of epoxy resin content the resulting BEP matrix specimens

Dynamic mechanical analysis, which provides important thermomechanical properties such as storage modulus (E'), and loss modulus (E'') of materials as a function of temperature, was employed to evaluate different compositions of BEP alloys, including, BEP811, BEP721, BEP631, BEP541, and BEP451. Figure 7.3 depicts the storage modulus under dynamic stress at a temperature range of 30 to 300°C, of the BEP alloys. As expected, the storage modulus at a glassy state decreased with increasing epoxy content in the BEP alloys as a result of the softer molecular structure of the epoxy. That is the epoxy molecules contain a number of ether linkages in which the internal movement of the molecules is greater compared with the rigid phenolic structure of the polybenzoxazine and the phenolic novolac. Therefore, increasing epoxy content in the BEP alloys resulted in lower stiffness of the specimens. As illustrated in Figure 7.3, the storage modulus of the BEP alloy series exhibits a value ranging from 5.7 GPa for BEP811 to 4.2 GPa for BEP451.

The glass transition temperatures (T_g) of all BEP alloys were determined using DMA under the same testing conditions since the technique is highly sensitive to even minor transitions or relaxations. The inset in Figure 7.3 presents the T_g s determined from the maximum of the loss modulus curves at various BEP alloy compositions. The incorporation of epoxy resin into the benzoxazine resin has some effect on an increase of the T_g s of the alloys over that of the neat polybenzoxazine (BA-a) which was reported to be approximately 160-165°C [59, 111]. The BEP alloys, which are BEP811 to BEP541, had the T_g values ranging from 172 to 175°C. Beyond the epoxy fraction of 40% by weight, however, the BEP alloys exhibited a decrease in T_g possibly due to an excess amount of epoxy that did not participated in the network formation i.e. BEP451 having T_g

of 165°C. It can also be concluded that epoxy resin affects the BEP alloys in such a way to enhance their crosslink density but to lower their network rigidity [10, 58]

The effects of the epoxy resin on flexural properties determined by a three point bending test of the BEP alloys are illustrated in Figure 7.4. The flexural stress and flexural strain at break were measured for those BEP alloy series. As seen in the figure, the flexural strength of the BEP721 alloy was higher than that of the BEP811 alloy and the flexural strength slightly decreased with the epoxy content of greater than 20% by weight. In addition, the increase of the epoxy content in the BEP alloys also resulted in a systematic increase of flexural strain at breakage. The increasing amount of epoxy in BEP alloys could enhance their flexural strength and flexural strain at break possibly by inhibiting the crack growth, absorbing, and dissipating mechanical energy in the obtained polymer alloys. Furthermore, the area under the curve refers to the energy absorption capability of the alloy materials and the values were tabulated in Table 7.2. It was observed that the maximum area under the curve tended to increase with increasing epoxy content i.e. 58, 117, 108, 121, and 127 MPa for BEP811, BEP721, BEP631, BEP541 and BEP451, respectively. The epoxy, therefore, was observed to significantly improve the toughness of the polymer alloys as clearly indicated by a greater area under the load-displacement curves of Figure 7.4. Additionally, the flexural modulus as a function of the alloy compositions in Table 7.2 showed a behavior almost identical to those of the storage modulus examined by DMA of Figure 7.3. Again, the flexural moduli of the BEP alloy specimens were found to decrease with increasing the epoxy content. The flexural moduli decrease from 5.9 GPa for BEP811 to 4.1 GPa for BEP451 alloys. This could be due to the greater segmental mobility of the epoxy chain compared with that of the polybenzoxazine.

The relationship between the BEP alloy compositions and their degradation temperature under nitrogen atmosphere is plotted in Figure 7.5. From the thermograms, the decomposition temperature reported at 5% weight loss (T_d) of the BEP alloys clearly increased with increasing epoxy content in a linear manner as seen in the inset of Figure 7.5. One significant feature of the thermograms is the high thermal stability of our BEP alloys providing relatively high T_d such as 357°C for BEP811 to 373°C for BEP451, compared with about 332°C of the pure polybenzoxazine [59]. Such increase in the T_d of the alloys with epoxy fraction was attributed to the cross-linked density improvement occurred from the additional crosslinking reaction between the oxazine ring in the benzoxazine resin and the hydroxyl group of the epoxy. In addition, the optimal amount of the phenolic novolac resin presented may be able to further catalyze the benzoxazine

resin and react with the epoxy resin to render a more complete network structure. Another significant feature in the TGA thermograms of Figure 7.5 is that the char yield of the BEP alloys reported at 800°C slightly decreased with increasing the epoxy mass fraction. The char yields of the BEP811 to BEP541 are ranging from 34 to 30% and further decreased to 26% for BEP451 compared with that of the neat polybenzoxazine which has the reported char yield value of about 28% [10, 59].

7.1.4 Investigation of BEP wood composites filled with 70wt% of woodflour

To investigate the effect of the ternary system compositions on the interfacial interaction with the woodflour filler as well as the relevant mechanical and thermal properties of the resulting wood composites, the fixed woodflour content at 70% by weight was used to make wood composites with each BEP alloy. The above filler content is about the maximum packing of the woodflour used because at this content, the observed densities of all BEP wood composites remained equal to their theoretical densities. An example of the density values of BEP811 wood composites as a function of woodflour content was also listed in Table 7.3. These highly filled composite systems can be produced due to the relatively low melt viscosity of the BEP resin systems used. Figure 7.6 illustrates the storage moduli as a function of temperature of the 70% by weight woodflour-filled BEP alloy series. From the plot, it can be seen that all BEP alloys filled with 70% by weight woodflour showed significantly higher storage modulus values than those of their unfilled BEP alloys. The storage moduli at room temperature were found to range from 6.4 GPa for BEP451 composite to 9.6 GPa for BEP811 composite compared with the values of 4.1 GPa of the unfilled BEP451 and 5.9 GPa of the unfilled BEP811. This is likely due to the reinforcing effect of woodflour filler on the BEP alloys implying substantial interfacial bonding between the matrix and the woodflour. Moreover, the storage moduli of the woodflour-filled BEP composites increased with the amount of the benzoxazine content in the specimens. This is possibly due to the effect of the more rigid molecular structure of the polybenzoxazine compared with that of the epoxy used.

The inset of Figure 7.6 depicts a plot of the loss modulus of the 70% by weight woodflour-filled BEP alloy series as a function of temperature. As previously mentioned, the peak positions of the loss moduli were used to indicate the T_g s of the specimens. In this inset, the systematic shifting of the peaks with the content of the polybenzoxazine to higher temperature is related to an increase in T_g s of the BEP wood composites. In the inset, T_g of BEP811 composite was determined to be 172°C whereas the T_g s of BEP721,

BEP631, BEP541, and BEP451 composites were found to be 164, 153, 146, and 136°C, respectively. Therefore, it can be concluded that a more benzoxazine content in the BEP alloy matrices is able to enhance thermal stability of the wood composites probably due to outstanding compatibility between the woodflour and the polybenzoxazine fraction [59]. This makes benzoxazine alloys highly attractive as a binder or matrix for the production of high performance wood composites with highly filled capability.

Figure 7.7 shows the flexural strength and flexural modulus of the BEP wood composites. The flexural strength of the 70% by weight woodflour-filled BEP composites at different epoxy content has a relatively constant value at about 70 MPa. The value is relatively high and comparable to that of the highly filled polybenzoxazine wood composite in our recent work i.e. 60 MPa at 70% by weight of woodflour [59]. In addition, the flexural modulus of the BEP matrix filled with 70% by weight of woodflour at various epoxy content was also shown in the same figure. The flexural modulus values of the wood composites, as expected, were found to increase with increasing benzoxazine content in the BEP matrices. As explained in our previous section in DMA measurement, the behavior was ascribed to the addition the more rigid benzoxazine structure to the BEP alloys.

TGA thermograms of the 70% by weight of woodflour-filled BEP alloys are presented in Figure 7.8. From the thermograms, T_d at 5% weight loss of the woodflour-filled BEP alloys showed similar values of about 280°C which is lower than that of the BEP alloy matrices. The phenomenon could be attributed to the lower degradation temperature of the woodflour filler which was reported to be about 275°C [59]. This consequently caused a decrease in the T_d s of these highly filled wood composites. The char yield, the percent residue at 800°C, of the woodflour-filled BEP composites can also be determined from Figure 7.8. It can be seen in this figure that the char yield of the wood composites clearly increased as the benzoxazine content increased. Char yields of the BEP wood composite specimens using BEP811 was 37% whereas that of BEP451 decreased to about 30%, as compared to that of the woodflour having approximate value of 18% [59]. This might be due to the possible chemical bonding between the woodflour filler and the BEP matrices in which both the benzoxazine and epoxide moieties are known to be able to react with free OH group highly abundant on the woodflour surface. Figure 7.9 revealed substantial adhesion between the woodflour filler and the BEP721 matrix. The woodflour/fiber breakage was observed. The property represents one of the significant load transfers, which contribute to the high modulus values of the wood composite material.

Table 7.1 Gelation time of BEP mixtures at various temperatures.

Temperature (°C)	Gelation Time, T_{gel} (s)		
	BEP721	BEP631	BEP541
135	2256	2406	3534
140	1962	2222	3006
145	1668	1800	2682
150	1566	1578	2436



สถาบันวิทยบริการ
จุฬาลงกรณ์มหาวิทยาลัย

Table 7.2 Flexural properties of BEP alloys

Composition	BEP alloys		
	Flexural strength (MPa)	Flexural modulus (GPa)	Area under curve (MPa)
80/10/10	76 ± 6.0	5.9 ± 0.21	58.15
70/20/10	96 ± 10.6	5.3 ± 0.07	116.92
60/30/10	91 ± 11.7	4.7 ± 0.15	108.05
50/40/10	92 ± 9.2	4.4 ± 0.11	120.76
40/50/10	92 ± 7.5	4.1 ± 0.13	126.91



สถาบันวิทยบริการ
จุฬาลงกรณ์มหาวิทยาลัย

Table 7.3 Maximum packing density of woodflour-filled BEP composites.

Composition wt% (vol%)	Theoretical density g/cm ³	Experimental density g/cm ³
0 (0)	1.19	1.19
40 (35)	1.29	1.29
50 (44)	1.32	1.33
60 (55)	1.35	1.36
70 (65)	1.38	1.38
75 (71)	1.40	1.38



สถาบันวิทยบริการ
จุฬาลงกรณ์มหาวิทยาลัย

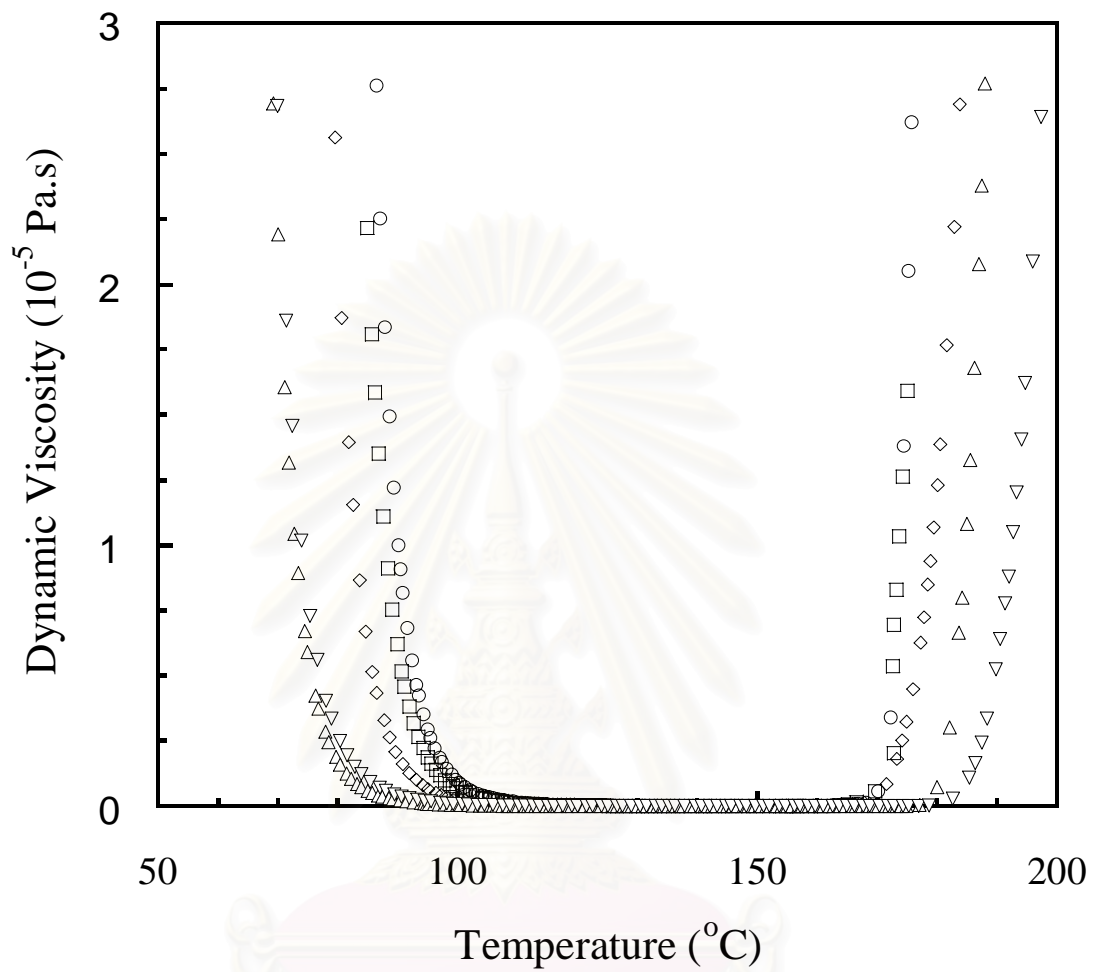


Figure 7.1 Relationship between dynamic viscosity and temperature of BEP mixtures:

(\circ) BEP811, (\square) BEP721, (\diamond) BEP631, (Δ) BEP541, (∇) BEP451.

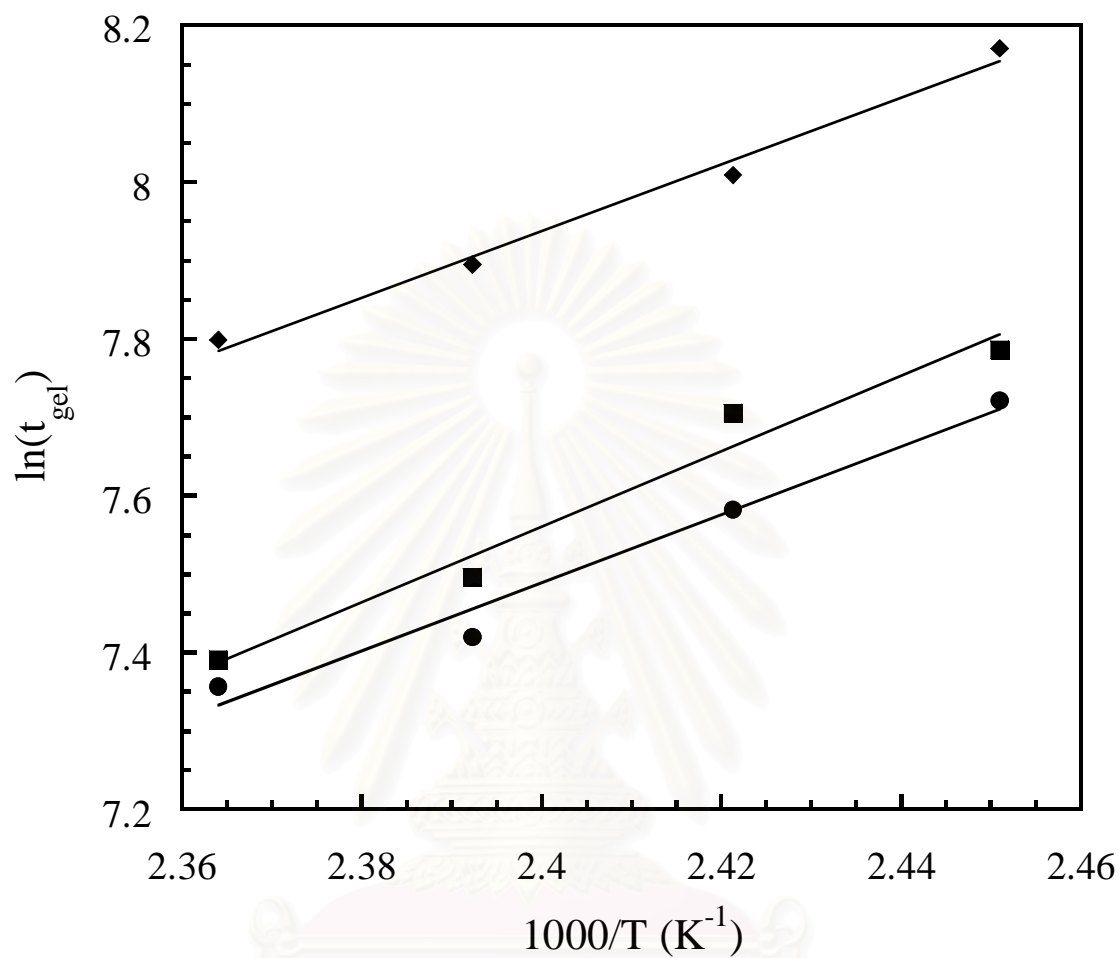


Figure 7.2 Relationship between gel time and temperature based on rheological data as BEP compositions: (●) BEP721, (■) BEP631, (◆) BEP541.

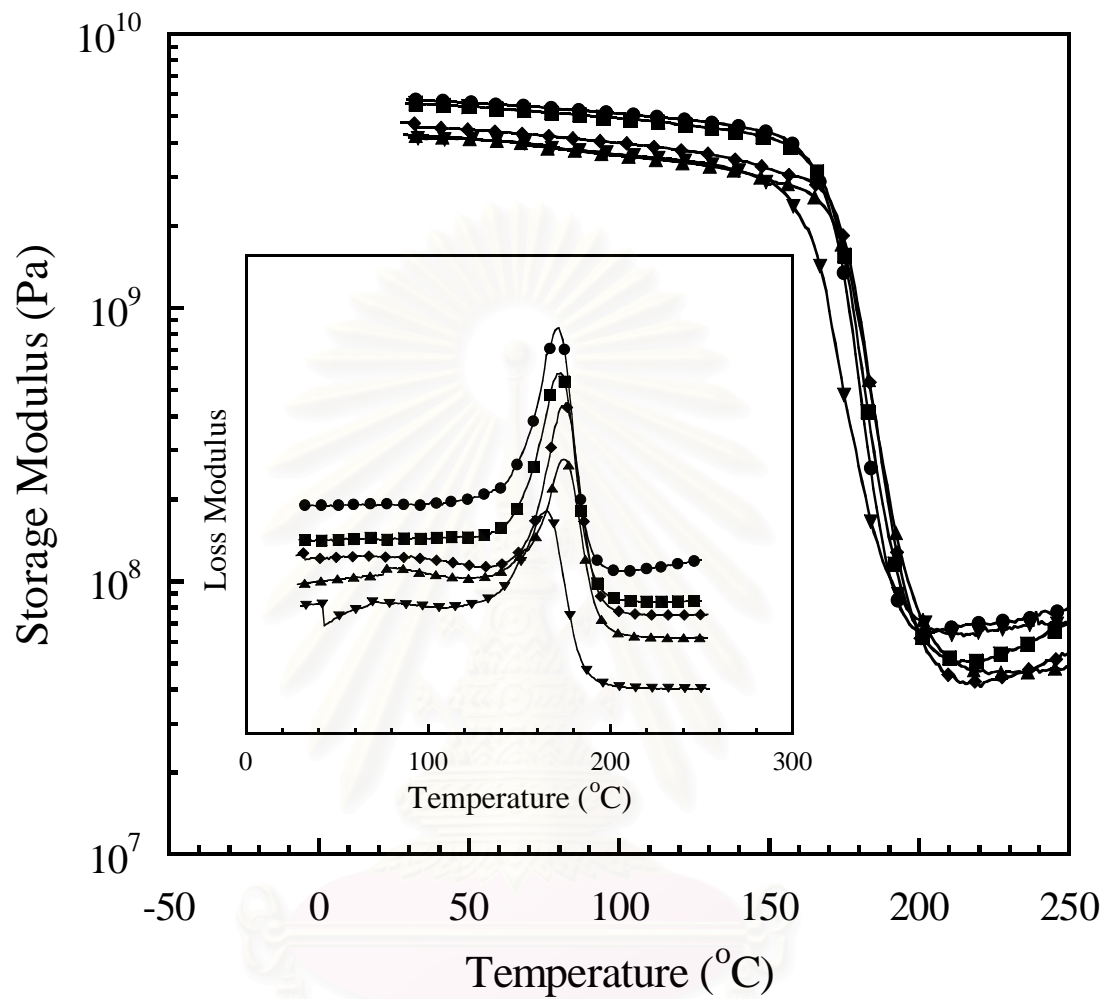


Figure 7.3 Storage and loss modulus of the BEP alloys as function of temperature:

(●) BEP811, (■) BEP721, (◆) BEP631, (▲) BEP541, (▼) BEP451.

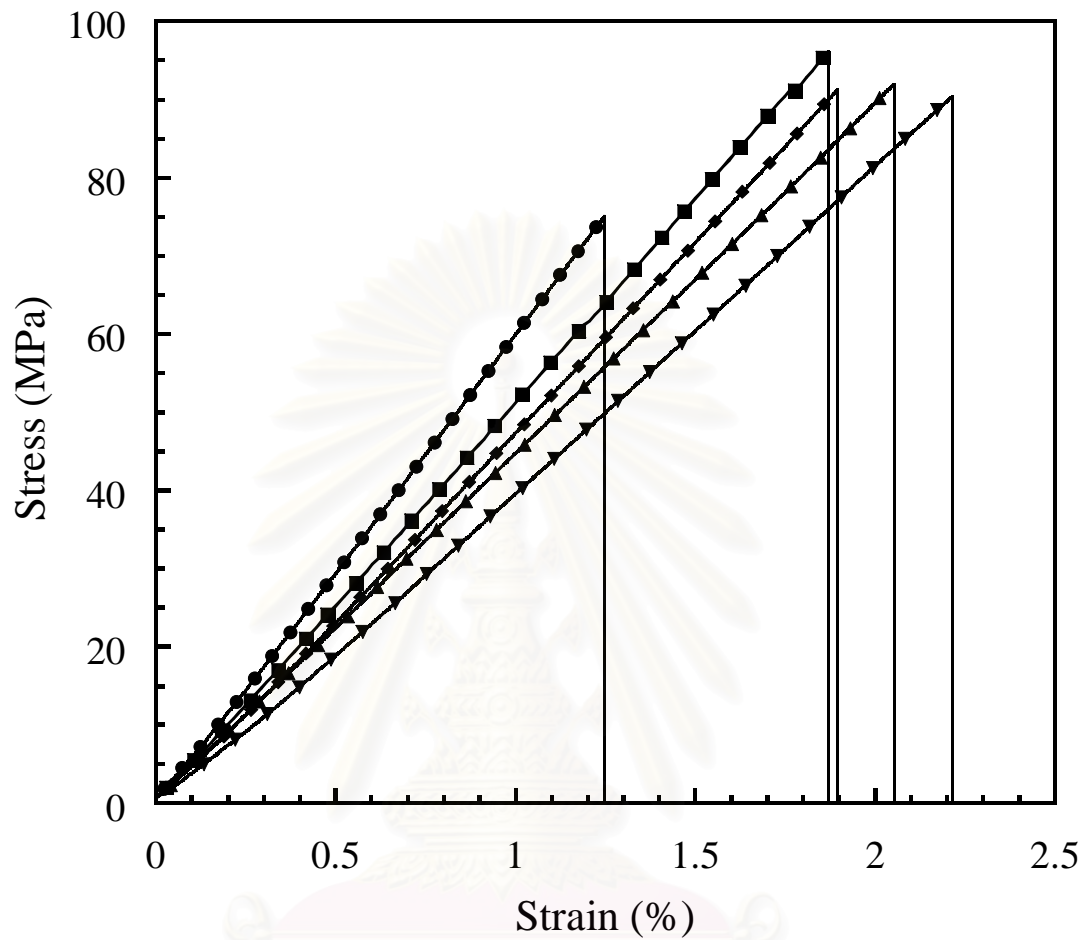


Figure 7.4 Flexural stress and strain relationship of BEP alloys at various compositions:

(●) BEP811, (■) BEP721, (◆) BEP631, (▲) BEP541, (▼) BEP451.

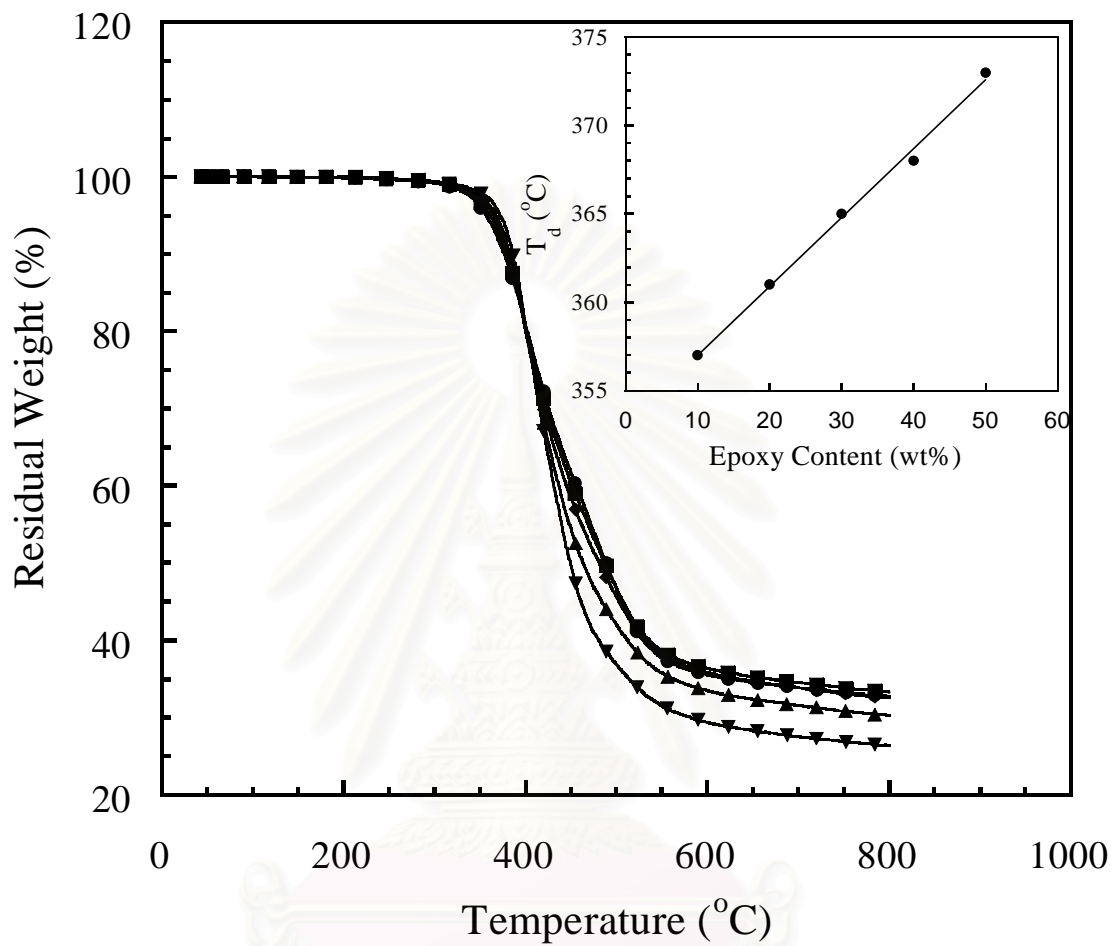


Figure 7.5 TGA thermograms of BEP alloys at different compositions:

(●) BEP811, (■) BEP721, (◆) BEP631, (▲) BEP541, (▼) BEP451.

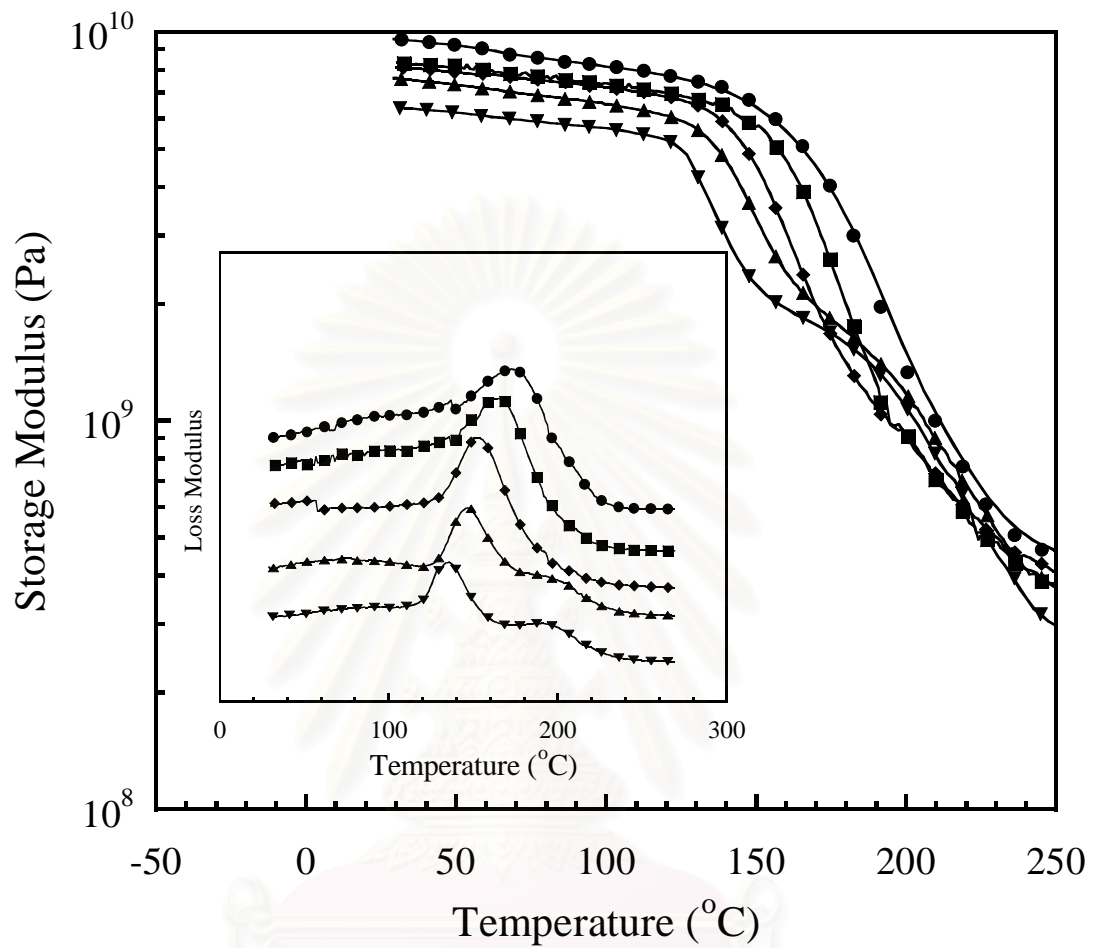


Figure 7.6 Storage and loss modulus of the BEP composites made with 70wt% woodflour as function of temperature: (●) BEP811, (■) BEP721, (◆) BEP631, (▲) BEP541, (▼) BEP451.

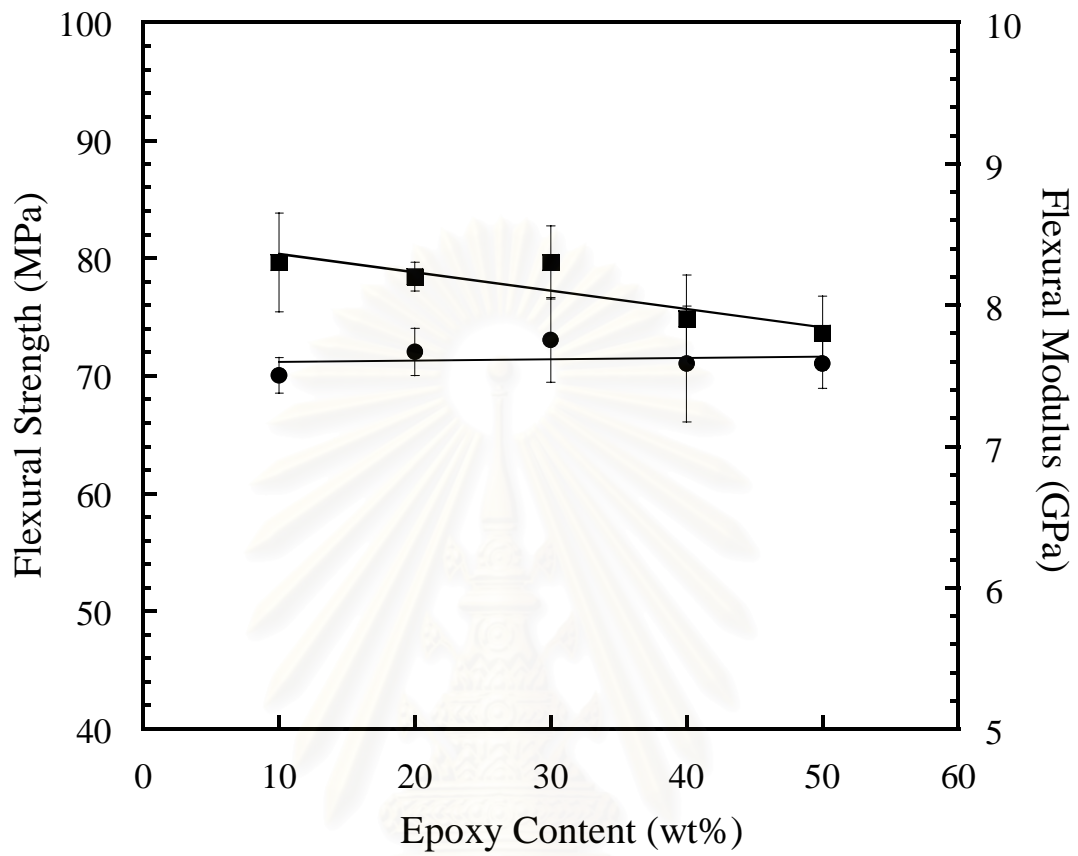


Figure 7.7 Flexural strength and modulus of the BEP composites made with different values epoxy content having 70wt% woodflour. (●) Flexural strength, (■) Flexural modulus.

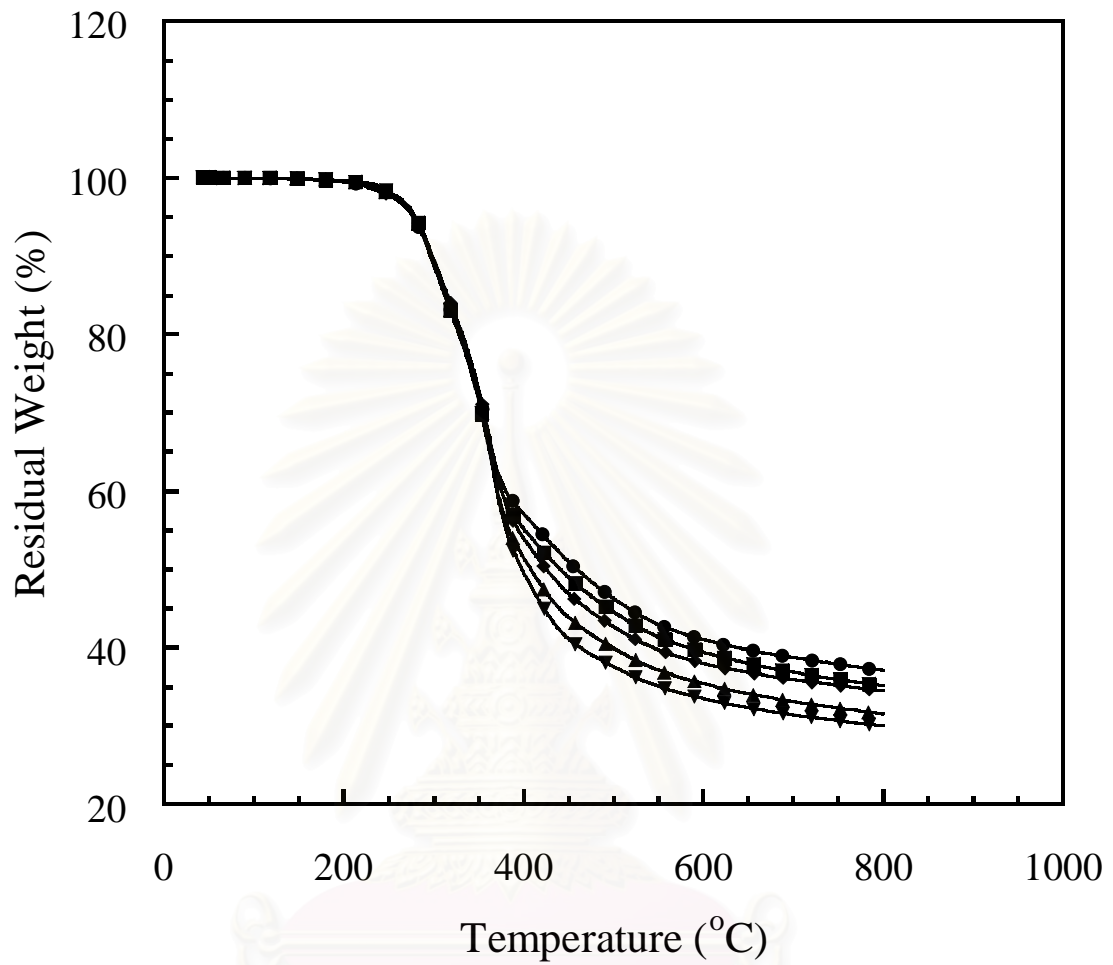


Figure 7.8 TGA thermograms of the BEP composites made with 70wt% woodflour as function of temperature: (●) BEP811, (■) BEP721, (◆) BEP631, (▲) BEP541, (▼) BEP451.

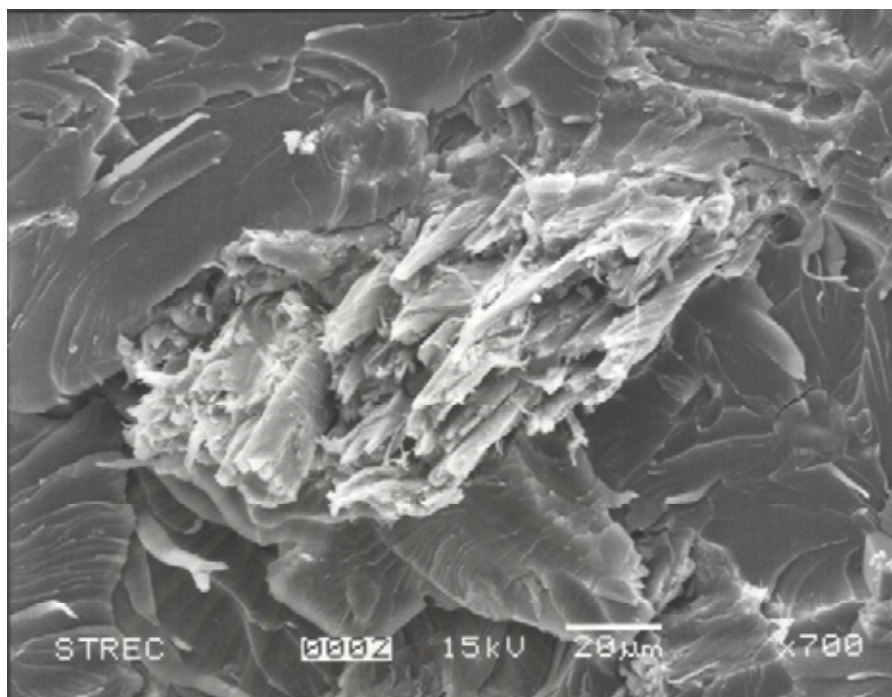


Figure 7.9 SEM micrographs of an interface between woodflour and BEP721 matrix of the woodflour-filled BEP721 fracture surface.

สถาบันวิทยบริการ
จุฬาลงกรณ์มหาวิทยาลัย

CHAPTER VIII

CONCLUSIONS

8.1 Curing Kinetics of Arylamine-based Polyfunctional Benzoxazine Resins by Dynamic Differential Scanning Calorimetry

The curing reaction of polyfunctional benzoxazine resins based on two types of arylamine, aniline and 3,5-xylydine, was studied. It was found that the curing process of BA-a was a single curing reaction, while the curing reaction of BA-35x was composed of two processes (reactions (1) and (2)), as evidenced by the presence of a double peak on the DSC thermograms. By using Kissinger, Ozawa, Flynn–Wall–Ozawa, and Friedman methods approach, the obtained activation energy values of both resins are almost invariable. In addition, the activation energy value of BA-a is close to that of BA-35x (reaction (1)). This indicates the same mechanism of the curing reaction of both exothermic peaks. In the case of BA-35x, the activation energy value at the reaction (1) is much smaller than that of the reaction (2). Therefore, reaction (1) is more sensitive to the temperature than reaction (2). The reaction orders of reactions (1) and (2) are also different. This leads to the fact that there are two different mechanisms involved in the curing reactions. The autocatalytic models are proposed to adequately describe the curing kinetics of the BA-a and BA-35x (reaction (1)) systems while the n th-order model is found to present the curing process of the BA-35x (reaction (2)). Evidently, the kinetic models of the curing reactions of the both resins are in good agreement with non-isothermal DSC results.

8.2 Effect of Novel Benzoxazine Reactive Diluent on Processability and Thermo-mechanical Characteristics of Bi-functional Polybenzoxazine

The monofunctional Ph-a resin can effectively serve as a reactive diluent of the bifunctional BA-a resin to further improve the latter processability. The viscosity and liquefying temperature of the BA-a/Ph-a mixtures were found to significantly decrease with the Ph-a mass fraction. The resin mixture renders miscible, homogeneous, and void-free cured specimen with the properties highly dependent on the composition of the resin mixture.

The relaxation exponent, n , of the BA-a/Ph-a mixtures is dependent on the cure temperature while the activation energy for the gelation process of the BA-a/Ph-a mixtures was found to be a constant and independent on the Ph-a mass fraction. The incorporation of the poly(Ph-a) into the poly(BA-a) helped improve the stiffness as well as the thermal stability (in terms of degradation temperature at 5% weight loss and char yield) of the specimens whereas the T_g and flexural strength of the BA-a/Ph-a polymers were found to increase with the BA-a mass fraction.

8.3 High Performance Wood Composites based on Benzoxazine-Epoxy Alloys

High performance wood composites from highly filled ternary systems of benzoxazine, epoxy, and phenolic resins i.e. BEP resins, were achieved. The woodflour content of 70% by weight can be incorporated into the ternary systems due to the relatively low melt viscosity of the ternary mixtures. The experimental results indicated that the increasing amount of epoxy fraction in the ternary systems enhanced the alloys' flexural strength and toughness. The resulting BEP wood composites showed relatively high flexural modulus value up to 8.3 GPa and flexural strength up to 70 MPa in BEP811 filled system. The increase of polybenzoxazine fraction in the BEP ternary systems was found to effectively enhance the mechanical and thermal characteristics such as the flexural modulus and the glass transition temperature of the resulting wood composites.

REFERENCES

- [1] Rials, T. G.; and Wolcott, M. P. Morphology-property relationships in wood-fiber based polyurethanes. J. Mat. Sci. Let. 17 (1998): 317-319.
- [2] Ghosh, N. N.; Kiskan, B.; and Yagci, Y. Polybenzoxazine-new high performance thermosetting resins: Synthesis and properties. Prog. Polym. Sci. 32 (2007): 1344-1391.
- [3] Rao, B. S.; Reddy, K. R.; Pathak, S. K.; and Pasala, A. R. Benzoxazine-epoxy copolymers: effect of molecular weight and crosslinking on thermal and viscoelastic properties. Polym. Int. 54 (2005): 1371-1376.
- [4] Ishida, H. Process for preparation of benzoxazine compounds in solventless systems. US Patent 5,543,516 (1996).
- [5] He, Y. DSC and DEA studies of underfill curing kinetics. Thermochim. Acta. 367-368 (2001): 101-106.
- [6] Ishida, H.; and Rodriguez, Y. Curing kinetics of a new benzoxazine-based phenolic resin by differential scanning calorimetry. Polymer. 36 (1995): 3151-3158.
- [7] Ishida, H.; and Rodriguez, Y. Catalyzing the curing reaction of a new benzoxazine-based phenolic resin. J. Appl. Polym. Sci. 58 (1995): 1751-1760.
- [8] Rimdusit, S.; and Ishida, H. Gelation study of high processability and high reliability ternary systems based on benzoxazine, epoxy, and phenolic resins for an application as electronic packaging materials. Rheol. Acta. 41 (2002): 1-9.
- [9] Ishida, H.; and Allen, D. J. Mechanical characterization of copolymers based on benzoxazine and epoxy. Polymer. 37 (1996): 4487-4495.
- [10] Rimdusit, S.; and Ishida, H. Development of new class of electronic packaging material based on ternary systems of benzoxazine, epoxy, and phenolic resins, Polymer. 41 (2000): 7941-7949.
- [11] Rimdusit, S.; Jiraprawatthagool, V.; Jubsilp, C.; Tiptipakorn, S.; and Kitano, T. Effect of SiC whisker on benzoxazine-epoxy-phenolic ternary systems: microwave curing and thermomechanical characteristics. J. Appl. Polym. Sci. 105 (2007), 1968-1977.

- [12] Jackson, G. V.; and Orton, M. L. Particulate-filled polymer composites: Filled thermosets. 2nd ed. New York: John Wiley & Sons, 1995.
- [13] Mezzenga, R.; Boogh, L.; and Manso, J. -A. E. A thermodynamic model for thermoset polymer blends with reactive modifier. J. Polym. Sci. Polym. Phys. 38 (2000): 1893-1902.
- [14] Rosu, D.; Cascaval, C. N.; Mustata, F.; and Ciobanu, C. Cure kinetics of epoxy resins studied by non-isothermal DSC data. Thermochim. Acta. 383 (2002): 119-127.
- [15] Su, Y. C.; Yei, D. R.; and Chang, F. C. The kinetics of B-a and P-a type copolybenzoxazine via the ring opening process. J. Appl. Polym. Sci. 95 (2005):730-737.
- [16] Sbirrazzuoli, N.; and Byazovkin, S. Learning about epoxy cure mechanisms from isoconversional analysis of DSC data. Thermochim. Acta. 388 (2002): 289-298.
- [17] Sbirrazzuoli, N.; Vincent, L.; Bouillard, J.; and Elegant, L. Isothermal and nonisothermal kinetics : when mechanistic information available. J. Therm. Anal. 56 (1999): 783-792.
- [18] Sbirrazzuoli, N.; Girault, Y.; and Elegant, L. Simulations for evaluation of kinetic methods in differential scanning calorimetry. Part 3-Peak maximum evolution methods and isoconversional methods. Thermochim. Acta. 293 (1997): 25-37.
- [19] Vyazovkin, S.; and Sbirrazzuoli, N. Mechanism and kinetics of epoxy-amine cure studied by differential scanning calorimetry. Macromolecules. 29 (1996): 1867-1873.
- [20] Sbirrazzuoli, S.; Vyazovkin, S.; Mititelu, A.; Sladic, C.; and Vincent, L. Study of epoxy-amine cure kinetics by combining isoconversional analysis with temperature modulated DSC and dynamic rheometry. Macromol. Chem. Phys. 204 (2003): 1815-1821.
- [21] Vyazovkin, S.; Mititelu, A.; and Sbirrazzuoli, N. Kinetics of epoxy-amine curing accompanied by the formation of liquid crystalline structure. Macromol. Rapid Commun. 24 (2003): 1060-1065.
- [22] Prime, R. B. Thermal characterization of polymeric materials. Turi, E. A. ed. San Diego: Academic Press, 1997.

- [23] Kornpraditsin, P. M.S. Thesis, Reaction kinetics of ternary systems based on benzoxazine, epoxy, and phenolic resins using FT-IR technique. Chulalongkorn University, Bangkok, Thailand, 2002.
- [24] Rimdusit, S. Ph.D. Thesis, Development of high reliability and high processability thermosets for electronic packaging applications based on ternary systems of benzoxazine, epoxy and phenolic resins. Case Western Reserve University, Cleveland, OH, 2000.
- [25] Sun, L.; Pang, S. S.; Sterling, A. M.; Negulescu, I. I.; and Stubblefield, M. A. Dynamic modeling of curing process of epoxy prepreg. J. Appl. Polym. Sci. 86 (2002): 1911-1923.
- [26] Rosu, D.; Mititelu, A.; and Cascaval, C. N. Cure kinetics of a liquid-crystalline epoxy resin studied by non-isothermal data. Polym. Test. 23 (2004): 209-215.
- [27] Montserrat, S.; and Malek, J. A kinetic analysis of the curing reaction of an epoxy resin. Thermochim. Acta. 228 (1993): 47-60.
- [28] Malek, J. A computer program for kinetic analysis of non-isothermal thermoanalytical data. Thermochim. Acta. 138 (1989): 337-346.
- [29] Ozawa, T. Kinetic analysis of derivative curves in thermal analysis. J. Chem. Anal. 2 (1970): 301-310.
- [30] Kessler, M. R.; and White, S. R. Cure kinetics of the ring-opening metathesis polymerization of dicyclopentadiene. J. Polym. Sci. Polym. Chem. 40 (2002): 2373-2383.
- [31] Opfermann, J.; and Kaisersberger, E. An advantageous variant of the Ozawa-Flynn-Wall analysis. Thermochim. Acta. 203 (1992): 167-175.
- [32] Kroschwitz, J. I. ed. High performance polymers and composites: Polymer blends, Encyclopedia Reprint Series. New York: John Wiley & Sons, 1991.
- [33] Fried, J. R. Polymer science & technology: Additives, blends, and composites. 2nd ed. New Jersey: Prentice Hall, 2003.
- [34] Barlow, J. W.; and Paul, D. R. Polymer alloys. Ann. Rev. Mater. Sci. 11 (1981): 299-319.
- [35] Pascault, J. -P.; Verdu, J.; and Williams, R. J. J. Thermosetting polymers: Rheological and dielectric monitoring of network formation. New York: Marcel Dekker, 2000.

- [36] Matejka, L. Rheology of epoxy networks near the gel point. Polym. Bull. 26 (1991): 109-116.
- [37] Tung, C.-Y. M.; and Dynes, P. J. Relationship between viscoelastic. properties and gelation in thermosetting sytems. J. Applied Polym. Sci. 27 (1982): 569-574.
- [38] Chambon, F.; and Winter, H. H. Polym. Bull. 13 (1985): 499-504.
- [39] Reinhart, T. J.; and Clements, L. L. Engineered materials handbook: Introduction to composites. Composite Vol 1. ASM International, 1987.
- [40] Glasser, W. G.; Taib, R.; Jain, R. A.; and Kander, R. Fiber-reinforced cellulosic thermoplastic composites. J. Appl. Polym. Sci. 73 (1999): 1329-1340.
- [41] Bledzki, A. K.; and Gassan, J. Composites reinforced with cellulose based fibers. Prog. Polym. Sci. 24 (1999): 221-274.
- [42] Klyosov, A. A. Wood-plastic composites: Composition of wood-plastic composites: Cellulose and lignocellulose fillers. New Jersey: John Wiley & Sons, 2007.
- [43] Schragar, M. The effect of spherical inclusions on the ultimate strength of polymer composites. J. Appl. Polym. Sci. 22 (1978): 2379-2381.
- [44] Holly, F. W.; and Cope, A. C. Condensation products of aldehydes and ketones with *o*-aminobenzyl alcohol and *o*-hydroxybenzylamine. J. Am. Chem. Soc. 66 (1944): 1875-1879.
- [45] Liu, J.; and Ishida, H. The polymeric materials encyclopedia: A new class of phenolic resins with ring-opening polymerization. Salamone, J. C. ed. Florida: CRC Press, 1996.
- [46] Nair, C. P. R. Advances in addition-cure phenolic resins. Prog. Polym. Sci. 29 (2004): 401-498.
- [47] Burke, W. J. 3,4-dihydro-1,3,2H-benzoxazine. Reaction of *p*-substituted phenols with *N,N*-dimethylolamines. J. Am. Chem. Soc. 71(1949): 609-612.
- [48] Burke, W. J.; Bishop, J. L.; Glennie, E. L. M.; and Bauer, W. N. A new aminoalkylation reaction. Condensation of phenols with dihydro-1,3-aioxazine. J. Org. Chem. 30 (1965): 3423-3427.
- [49] Huang, M. T.; and Ishida, H. Dynamic mechanical analysis of reactive diluent modified benzoxazine-based phenolic resin. Polym. Polym. Comp. 7 (1999): 233-247.

- [50] Hemvichian, K.; Laobuthee, A.; Chirachanchai, S.; and Ishida, H. Thermal decomposition processes in polybenzoxazine model dimers investigated by TGA-FTIR and GC-MS. Polym. Degrad. Stab. 76 (2002): 1-15.
- [51] Ishida, H.; and Sanders, D. P. Improved thermal and mechanical properties of polybenzoxazines based on alkyl-substituted aromatic amines. J. Polym. Sci. Polym. Phys. 8 (2000): 3289-3301.
- [52] Ishida, H.; and Sanders, D. P. Regioselectivity and network Structure of difunctional alkyl-substituted aromatic amine-based polybenzoxazines. Macromolecules. 33 (2000): 8149-8157.
- [53] Billmeyer, Fred W. Textbook of polymer science: Thermosetting resins. 3rd ed. Toronto: John Wiley & Sons, 1984.
- [54] Tyberg, C. S.; Bergeron, K.; Sankarapandian, M.; Shih, P.; Loos, A. C.; Dillard, D. A.; McGrath, J. E.; Riffle, J. S.; and Sorathia, U. Structure-property relationships of void-free phenolic-epoxy matrix materials. Polymer. 41 (2000): 5053-5062.
- [55] Ishida, H.; and Allen, D. J. Physical and mechanical characterization of near-zero shrinkage polybenzoxazine. J. Polym. Sci. Polym. Phys. 34 (1996): 1019-1030.
- [56] Kimura, H.; Matsumoto, A.; Hasegawa, K.; and Fukuda, A. New thermosetting resin from bisphenol A-based benzoxazine and bisoxazoline. J. Appl. Polym. Sci. 72 (1999): 1551-1558.
- [57] Rimdusit, S.; Pirstpindvong, S.; Tanthapanichakoon, W.; and Damrongsakkul, S. Toughening of polybenzoxazine by alloying with urethane prepolymer and flexible epoxy: a comparative study. Polym. Eng. Sci. 45 (2005): 288-296.
- [58] Rimdusit, S.; and Ishida, H. Synergism and multiple mechanical relaxations observed in ternary systems based on benzoxazine, epoxy, and phenolic resins. J. Polym. Sci. Polym. Phys. 38 (2000): 1687-1698.
- [59] Rimdusit, S.; Tanthapanichakoon, W.; and Jubsilp, C. High performance wood composites from highly filled polybenzoxazine. J. Appl. Polym. Sci. 99 (2006): 1240-1253.
- [60] Rimdusit, S.; Kampangsaeree, N.; Tanthapanichakoon, W.; Takeichi, T.; and Suppakarn, N. Development of wood-substituted composites form highly filled polybenzoxazine-phenolic novolac alloys. Polym. Eng. Sci. 47 (2007): 140-149.

- [61] Kim, H. D.; and Ishida, H. A Study of hydrogen bonded network structure of polybenzoxazines. J. Phys. Chem. A 106 (2002): 3271-3280.
- [62] Ishida, H.; and Sander, D. P. Activated Arylamine-based Polybenzoxazines US Patent 6,160,079 (2000).
- [63] Shen, S.B.; and Ishida, H. Development and characterization of. high-performance polybenzoxazine composites. Polym. Compos. 17 (1996): 710-719.
- [64] Ishida, H.; and Chaisuwan, T. Mechanical property improvement of carbon fiber reinforced polybenzoxazine by rubber interlayer. Polym. Compos. 24 (2003): 597-607.
- [65] Ishida, H.; and Rimdusit, S. Very high thermal conductivity. obtained by boron nitride-filled polybenzoxazine. Thermochim. Acta. 320 (2001): 177-186.
- [66] Li, L.H.; Lehmann, S. L.; and Wong, R. S. Curable compositions. US patent pending 20040261660 A1 (2004).
- [67] Takeichi, T.; Zeidam, R.; and Agag, T. Polybenzoxazine/clay hybrid nanocomposites: Influence of preparation method on the curing behavior and properties of polybenzoxazines. Polymer. 43 (2002): 45-53.
- [68] Wang, Y. X.; and Ishida, H. Synthesis and properties of new thermoplastic polymers from substituted 3,4-Dihydro-2*H*-1,3-benzoxazines. Macromolecules. 33 (2000): 2839-2847.
- [69] Zvetkov, V. L. Comparative DSC kinetics of the reaction of DGEBA with aromatic diamines. I. Non-isothermal kinetic study of the reaction of DGEBA with *m*-phenylene diamine. Polymer. 42 (2001):6687-6697.
- [70] Zhao, H.; Gao, J.; Li, Y.; and Shen, S. Curing kinetics and thermal property characterization of bisphenol-F epoxy resin and MeTHPA system. J. Therm. Anal. Calorim. 74 (2003): 227-
- [71] Hsieh, T. H.; and Su, A. C. Cure kinetics of an epoxy-novolac molding compound. J. Appl. Polym. Sci. 41 (1990): 1271
- [72] Kim, W. G.; Lee, J. Y.; and Park, K. Y. Curing reaction of *o*-cresol novolac epoxy resin according to hardener change. J. Polym. Sci. Polym. Chem. 31 (1993): 633-639.
- [73] Chen, L. W.; Fu, S. C.; and Cho, C. S. Kinetics of aryl phosphinate anhydride curing of epoxy resins using differential scanning calorimetry. Polym. Int. 46 (1998): 325-330

- [74] Brzozowski, Z. K.; SZYMANSKA, E; and Bratychak, M. M. New epoxy-unsaturated polyester resin copolymers. React. Funct. Polym. 33 (1997): 217-224.
- [75] Takeichi, T.; Guo, T.; Agag, T. Synthesis and characterization of poly(urethane-benzoxazine) films as novel type of polyurethane/phenolic resin composites. J. Polym. Sci. Polym. Chem. 38 (2000): 4165-4176.
- [76] Wang, Y. X.; and Ishida, H. Development of low-viscosity benzoxazine resins and their polymers. J. Appl. Polym. Sci. 86 (2002): 2953-2966.
- [77] Jubsilp, C.; Damrongsakkul, S.; Takeichi, T.; and Rimdusit, S. Curing kinetics of arylamine-based polyfunctional benzoxazine resins by dynamic differential scanning calorimetry. Thermochim. Acta. 447 (2006): 131-140.
- [78] Grunberg, L.; and Nissan, A. H. Mixture law for viscosity. Nature. 164 (1949):799-800.
- [79] Monnery, W. D.; Svrcek, W. Y.; and Mehrotra, A. K. Viscosity: a critical review of practical predictive and correlative methods. Can. J. Chem. Eng. 73 (1995): 3-40.
- [80] Kjøniksen, A. L.; and Nyström, B. Effects of polymer concentration and cross-linking density on rheology of chemically cross-linked poly(vinyl alcohol). Macromolecules. 29 (1996): 5215-5222.
- [81] Chiou, B. S.; English, R. J.; and Khan, S. A. Rheology and photo-cross-linking of thiol-ene polymers. Macromolecules. 29 (1996): 5368-5374.
- [82] Commereuc, S.; Bonhomme, S.; Verney, V.; and Lacoste, J. Photooxidation of polyoctenamer: viscoelastic assessment of gel formation. Polymer. 41 (2000): 917-923.
- [83] Meng, J.; Hu, X.; C Boey, F. Y.; Li, L. Effect of layered nano-organosilicate on the gel point rheology of bismaleimide/diallylbisphenol A resin. Polymer. 46 (2005): 2766-2776.
- [84] Winter, H. H.; and Mours, M. Rheology of polymers near liquid-solid transitions. Adv. Polym. Sci. 134 (1997): 165-234.
- [85] Ishida, H.; and Allen, D. J. Gelation behavior of near-zero shrinkage polybenzoxazines. J. Appl. Polym. Sci. 79 (2001): 406-417.
- [86] Kwak, G. H.; Park, S. J.; and Lee, J. R. Viscoelastic behavior of anhydride-cured epoxy system initiated by thermal latent catalyst. J. Appl. Polym. Sci. 81 (2001): 646-653.

- [87] Scanlan, J. C.; and Winter, H. H. Composition dependence of the viscoelasticity of end-linked poly (dimethylsiloxane) at the gel point. Macromolecules, 24 (1991): 47-54.
- [88] Winter, H. H.; Morganelli, P.; and Chambon, F. Stoichiometry effects on rheology of model polyurethanes at the gel point. Macromolecules, 21 (1988): 532-535.
- [89] Halley, P. J. A new chemorheological analysis of highly filled thermosets used in integrated circuit packaging. J. Appl. Polym. Sci. 64 (1997): 95-106.
- [90] Hemvichian, K.; Ishida, H. Thermal decomposition processes in aromatic amine-based polybenzoxazines investigated by TGA and GC-MS. Polymer, 43 (2002): 4391-4402.
- [91] Macko, J. A.; Ishida, H. Behavior of a bisphenol-A-based polybenzoxazine exposed to ultraviolet radiation. J. Polym. Sci. Polym. Phys. 38 (2000): 2687-2701.
- [92] Yang, H. -S.; Kim, D. -J.; and Kim, H. -J. Rice straw-wood particle composite for sound absorbing wooden construction materials. Bioresource Technol. 86 (2003): 117-121.
- [93] Ye, X. P.; Julson, J.; Kuo, M.; Womac, A.; and Myers, D. Properties of medium density fiberboards made from renewable biomass. Bioresouce Technol. 98 (2007): 1077-1084.
- [94] Shi, S. Q.; and Gardner, D. J. Hygroscopic thickness swelling rate of compression molded wood fiberboard and wood fiber/polymer composites. Compos. Part A-Appl. S. 37 (2006): 1276-1285.
- [95] Hiziroglu, S.; and Suzuki, S. Evaluation of surface roughness of commercially manufactured particleboard and medium density fiberboard in Japan. J. Mater. Process. Tech. 184 (2007): 436-440.
- [96] Kim, J. -P.; Yoon, T. -H.; Mun, S. -P.; and Rhee, J. -M. Wood-polyethylene composites using ethylene-vinyl alcohol copolymer as adhesion promoter. Bioresource Technol. 97 (2006): 494-499.
- [97] Lei, Y.; Wu, Q.; Yao, F.; and Xu, Y. Preparation and properties of recycled HDPE/natural fiber composites. Compos. Part A-Appl. S. 38 (2007): 1664-1674.

- [98] Lu, J. Z.; and Wu, Q., Negulescu, I. I. Wood-fiber/high-density-polyethylene composites: coupling agent performance. J. Appl. Polym. Sci. 96 (2005): 93-102.
- [99] Mohanty, S.; and Nayak, S. K.. Dynamic and steady state viscoelastic behavior and morphology of MAPP treated PP/sisal composite. Mat. Sci. Eng. A-Struct. 443 (2007): 202-208.
- [100] Ichazo, M. N.; Alabno, C.; Gonzalez, J.; Perera, R.;and Candal, M.V. Polypropylene/wood flour composites: treatments and properties. Compos. Struct. 54 (2001): 207-214.
- [101] Yildiz, Ü. C.; Yildiz, S.; and Gezer, E. D.. Mechanical properties and decay resistance of wood–polymer composites prepared from fast growing species in Turkey. Bioresource Technol. 96 (2005): 1003-1011.
- [102] Maldas, D.; and Kokta, B. V. Studies on the preparation and properties of particle boards made from bagasse and PVC: II. Influence of the addition of coupling agents. Bioresource Technol. 35 (1991): 251-261.
- [103] Ge, X. C.; Li, X. H.; and Meng, Y. Z. Tensile properties, morphology, and thermal behavior of PVC composites containing pine flour and bamboo flour. J. Appl. Polym. Sci. 93 (2004): 1804-1811.
- [104] Farid, S. I.; and Kortschot, M. T. Wood-flour-reinforced polyethylene: viscoelastic behavior and threaded fasteners. J. Appl. Polym. Sci. 42 (2002): 2336-2350.
- [105] Oksman, K.; and Lindberg, H. Influence of thermoplastic elastomers on adhesion polyethylene-wood flour composites. J. Appl. Polym. Sci. 68 (1998): 1845-1855.
- [106] Oksman, K.; Lindberg, H.; and Holmgren, A. The nature and location of SEBS–MA compatibilizer in polyethylene–wood flour composites. J. Appl. Polym. Sci. 69 (1998): 201-209.
- [107] Klason, C.; Kubat, J.; and Gatenholm, P. Wood fiber reinforced composites: Viscoelasticity of Biomaterials. Wolfgang, G.G., Hatakeyama, H. (Eds.), ACS Symposium Series vol. 489, ACS, Washington: 1992, pp. 82–98.
- [108] Geng, Y.; Li, K.; and Simonsen, J. Effects of a new compatibilizer system on the flexural properties of wood-polyethylene composites. J. Appl. Polym. Sci. 91 (2004): 3667-3672.

- [109] Devi, R. R.; Ali, L.; and Maji, T. K. Chemical modification of rubber wood with styrene in combination with a crosslinker: effect on dimensional stability and strength property. Bioresource Technol. 88 (2003): 185-188.
- [110] Keener, T. J.; Stuart, R. K.; and Brown, T. K. Maleated coupling agents for natural fiber composites. Compos. Part A-Appl. S. 35 (2004): 357-362.
- [111] Jubsilp, C.; Takeichi, T.; and Rimdusit, S. Effect of novel benzoxazine reactive diluent on processability and thermomechanical characteristics of bi-functional polybenzoxazine. J. Appl. Polym. Sci. 104 (2007): 2928-2938.



สถาบันวิทยบริการ
จุฬาลงกรณ์มหาวิทยาลัย



APPENDIX

สถาบันวิทยบริการ
จุฬาลงกรณ์มหาวิทยาลัย

APPENDIX

LIST OF PUBLICATIONS

International papers:

- [1] Jubsilp, C.; Damrongsukkul, S.; Takeichi, T.; and Rimdusit, S. Curing kinetics of arylamine-based polyfunctional benzoxazine resins by dynamic differential scanning calorimetry. *Thermochim. Acta.* 447 (2006): 131-140.
- [2] Jubsilp, C.; Takeichi, T.; and Rimdusit, S. Effect of novel benzoxazine reactive diluent on processability and thermomechanical characteristics of bi-functional polybenzoxazine. *J. Appl. Polym. Sci.* 104 (2007): 2928-2938.
- [3] Jubsilp, C.; Takeichi, T.; Hiziroglu, S.; and Rimdusit, S. High performance wood composites based on benzoxazine-epoxy alloys. *Accepted to Bioresource Technology* (2008).
- [4] Rimdusit, S.; Jiraprawatthagool, V.; Jubsilp, C.; Tiptipakorn, S.; and Kitano, T. Effect of SiC whisker on benzoxazine-epoxy-phenolic ternary systems: microwave curing and thermomechanical characteristics. *J. Appl. Polym. Sci.* 105 (2007), 1968-1977.
- [5] Rimdusit, S.; Jongvisuttisun, P.; Jubsilp, C.; and Hiziroglu, S. Highly processable ternary systems based on benzoxazine, epoxy, and phenolic resins for carbon fiber composite fabrication. *Accepted to J. Appl. Polym. Sci.* (2008).

Patent:

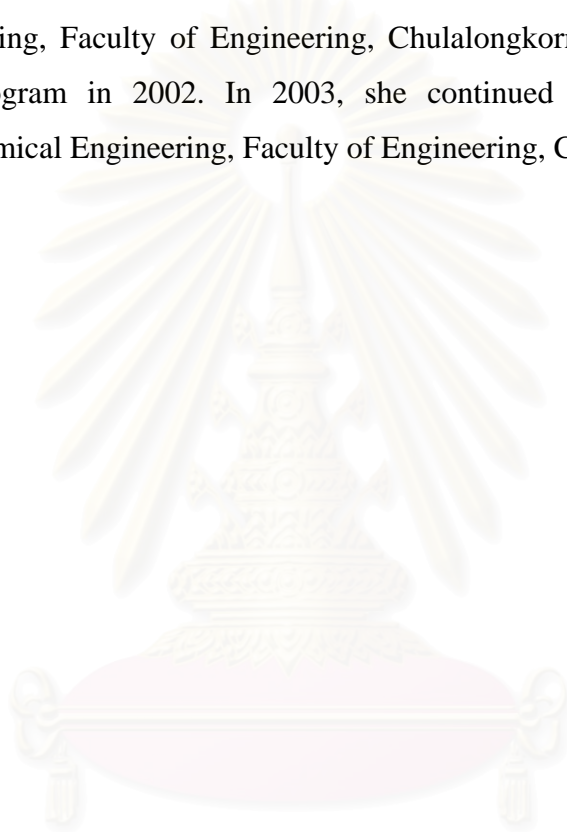
- [1] S. Rimdusit, and C. Jubsilp, "Polymer from Anhydride-Modified Polybenzoxazine," *Thailand Patent pending*, (2007).

International conferences:

- [1] Jubsilp, C.; Takeichi, T.; Tiptipakorn, S.; Tanthapanichakoon, W.; and Rimdusit, S. "Characterization of high performance silicon carbide-filled polybenzoxazine," Proceeding 11th APCChE Congress, Kuala Lumpur, Malaysia, 27-30 August, 2006, p.178.
- [2] Jubsilp, C.; Takeichi, T.; and Rimdusit, S. Kinetic studies of curing reaction of polyfunctional benzoxazine resins by dynamic differential scanning calorimetry methods," Proceeding of 3rd EMSES, Chiangmai, 6-9 April, 2005, p.48.

VITAE

Miss Chanchira Jubsilp was born on October 24th, 1977 in Nakornsrihammarat, Thailand. She received the Bachelor's Degree of Engineering with a major in Chemical Engineering from the Department of Chemical Engineering, Faculty of Engineering, King Mongkut's University of Technology Thonburi in 2000. After graduation, she entered study for a Master's Degree with a major in Chemical Engineering at the Department of Chemical Engineering, Faculty of Engineering, Chulalongkorn University in 2001 and completed the program in 2002. In 2003, she continued her Doctoral Degree in Department of Chemical Engineering, Faculty of Engineering, Chulalongkorn University.



สถาบันวิทยบริการ
จุฬาลงกรณ์มหาวิทยาลัย